EXPERIMENTAL STUDY OF THE EFFECTS OF FLAMEHOLDER GEOMETRY ON
EMISSIONS AND PERFORMANCE OF LEAN PREMIXED COMBUSTORS

By Gerald Roffe and K. S. Venkataramani

REPORT DOCUMENTATION PAGE		READ INSTRUCTIONS BEFORE COMPLETING FORM
1. REPORT NUMBER NASA CR-135424	2. GOVT ACCESSION NO.	3. RECIPIENT'S CATALOG NUMBER
4. TITLE (and Subtitle) Experimental Study of the Effects of Flameholder Geometry on Emissions and Performance of Lean Premixed Combustors		5. TYPE OF REPORT & PERIOD COVERED Contractor Report
		6. PERFORMING ORG. REPORT NUMBER GASL TR 249
7. AUTHOR(s) Gerald Roffe & K. S. Venkataramani		8. CONTRACT OR GRANT NUMBER(s) NAS3-20603
9. PERFORMING ORGANIZATION NAME AND ADDRESS General Applied Science Laboratories, Inc. Merrick and Stewart Avenues Westbury, New York 11590		10. PROGRAM ELEMENT, PROJECT, TASK AREA & WORK UNIT NUMBERS
11. CONTROLLING OFFICE NAME AND ADDRESS NASA, Washington, DC 20546		12. REPORT DATE April 1978
		13. NUMBER OF PAGES 78
14. MONITORING AGENCY NAME & ADDRESS(If different from Controlling Office) Airbreathing Engines Division NASA Lewis Research Center Cleveland, OH 44135		15. SECURITY CLASS. (of this report) Unclassified
		15a. DECLASSIFICATION/DOWNGRADING SCHEDULE

16. DISTRIBUTION STATEMENT (of this Report)

Unclassified - Unlimited STAR Category 07 (Rev.)

17. DISTRIBUTION STATEMENT (of the abstract entered in Block 20, if different from Report)

18. SUPPLEMENTARY NOTES

Final Report, Project Manager, Robert Duerr, Airbreathing Engines Division, NASA Lewis Research Center, Cleveland, OH 44135

19. KEY WORDS (Continue on reverse side if necessary and identify by block number)
Premixing; Combustion; Oxides of Nitrogen, Gas Turbine Combustors, Flameholders, Primary Zones.

20. ABSTRACT (Continue on reverse side if necessary and identify by block number)
Emissions of NO_x, CO and unburned hydrocarbons (UHC) are reported for a lean premixed propane-air system at inlet conditions of 800K and 1MPa using twelve flameholder designs. The flameholders tested represent six design concepts with two values of blockage for each concept. Data were obtained at reference velocities of 35 m/s, 25 m/s and 20 m/s at combustor stations 10 cm and 30 cm downstream of the flameholders. Flameholder pressure drop was found to be a principal determinant of emissions performance. Designs producing larger pressure drops also produced less NO_x, CO and UHC emissions. The lean stability limit

DD FORM 1473 EDITION OF 1 NOV 65 IS OBSOLETE
1 JAN 73

equivalence ratio was found to be approximately 0.35 for all designs. Flashback velocities (axial components in the flameholder passages) varied between 30 m/s and 40 m/s. A perforated plate flameholder was operated with a velocity as low as 23 m/s through the perforations at equivalence ratio 0.7 without producing flashback.

TABLE OF CONTENTS

LIST OF FIGURES

LIST OF FIGURES (Continued)

APPENDIX

Experimental Study of the Effects of Flameholder Geometry
on Emissions and Performance of Lean Premixed Combustors

Gerald Roffe and K. S. Venkataramani

General Applied Science Laboratories, Inc.

SUMMARY

Tests were conducted to determine the effect of flameholder geometry
on the emissions and performance of a lean premixed propane/air combustor.
Six flameholder concepts were evaluated; wire grid, perforated plate, multiple
cone, single cone, vee gutter and swirler. Two blockage values were tested for
each design concept. Emissions of NO_x, CO and unburned hydrocarbons were
measured at combustor entrance conditions of 800K/1MPa and reference velocities
of 35 m/s, 25 m/s and 20 m/s. The lean stability and flashback limits were also
determined.

Emissions measurements at a station 30 cm downstream from the flameholder
showed flameholder pressure drop to be a principal determinant of emissions per-
formance. Increasing pressure drop simultaneously decreased emissions of NO_x,
CO and unbruned hydrocarbons. The details of flameholder geometry appear to be
of second order importance except for their effect on total pressure loss. Emis-
sions measurements at a station 10 cm downstream from the flameholder displayed
greater sensitivity to the details of design geometry. The vee gutter design,
which produced one of the lowest CO and UHC characteristics at the 30 cm station
displayed a large region of incomplete combustion with excessive CO and UHC
species at the 10 cm combustion station. The lean stability limit was found to
correspond to an equivalence ratio of 0.4 for the 800K/1MPa entrance conditions
of this experiment. This condition corresponds to an adiabatic flame temperature
of 1700K. Lean stability limit did not vary significantly with flameholder geom-
etry. The single and multiple cone flameholder designs which were provided with
hollow base cavities suffered burn damage to their downstream surfaces as refer-
ence velocity was reduced. This burnback damage occurred without encountering
flashback. Flashback testing was carried out at equivalence ratio 0.7. All
incidents of flashback occurred at reference velocities producing maximum axial
components of velocity at the flameholder exit station between 30 m/s and 40 m/s.
Two perforated plate flameholders and one wire grid flameholder did not produce
flashback at the lowest velocities (7-9 m/s) at which tests could be conducted.

INTRODUCTION

Lean premixed prevaporized (LPP) combustion is a technique which has demonstrated considerable potential for reducing the production of nitrogen oxides in gas turbine combustors while maintaining high combustion efficiency. An LPP combustor consists of a fuel/air mixture preparation section, a flame stabilization device and a combustion zone. LPP combustion studies carried out to date have dealt principally with the properties and operation of the mixture preparation section and combustion zones. The flameholder, which constitutes an important element of the LPP combustor, has received relatively little attention. This report presents the results of an experimental study of the effects of flameholder geometry on the emissions and performance of lean premixed combustors.

The basic function of the flameholder is to provide a region of increased residence time where a small portion of the combustion gas can react to produce high temperature radical-carrying gases. As these gases diffuse into the premixed fuel/air stream, combustion spreads throughout the remainder of the gas. The flameholder serves a secondary purpose, unique to premixed systems, in that it provides a degree of mixer tube blockage which is sufficient to raise the combustor entrance velocity to a level which will preclude the occurrence of flashback.*

In general, most flameholder designs create a region of flow separation and recirculation in order to produce the required residence time for the system. This can be done using a number of geometric arrangements. For example, if a simple wire grid is placed across the combustor entrance station, each wire element will produce a wake, the near region of which contains a recirculation zone. The gas residence time typical of this recirculation zone is related to its physical extent and thus to the diameter of the wire and the mean flow velocity. In general since the residence time produced by a wire grid is relatively short, one would expect its use to be limited to low combustor entrance velocities or to conditions of relatively short ignition delay time. A somewhat coarser aerodynamic configuration is provided by the

---

*Flashback is defined here as upstream propagation of the flame from the region of stabilized combustion into the mixture preparation section.

perforated plate flameholder employed in many premixed systems. In this case, the array of finite jets issuing from the plate produce locally separated flow in the blocked regions; the associated gas residence time is proportional to the distance between adjacent holes. This type of flameholder would be expected to be best suited to the intermediate range of combustor entrance velocities and ignition delay times. At the coarse end of the spectrum of potential flameholder designs is the single recirculation region produced by a blunt body inserted into the flow at the combustor entrance station. In this case, the near wake of the body contains a region of recirculating flow the size of which is proportional to the body diameter. Since the recirculation zone residence time for this configuration is the highest of any of those yet discussed, one would expect it to be well suited to conditions of high combustor entrance velocity and long ignition delay time where the larger extent of its recirculation region would be helpful in providing adequate radical production. The extent of the recirculation region produced by a single blunt body can be further increased by imparting a swirling motion to the flow. This reduces the axial component of momentum and makes it more difficult for the air entering the combustor to overcome the adverse pressure gradient which results from the sudden expansion into the base region of the flameholder. Swirl is particularly useful under conditions where relatively long residence times are required to initiate combustion and is commonly used in combustion equipment operating at inlet conditions close to ambient.

The geometry of the flameholder can influence the combustion characteristics of the system in a number of ways. The profile drag of the selected geometry influences the degree of pressure drop which the flameholder produces and hence the intensity of the downstream (combustion zone) turbulence. The scale of this turbulence is also influenced by the flameholder geometry. The residence time within the recirculation region can influence the temperature and mixture ratio limits beyond which combustion cannot be sustained. In designs where a significant portion of the total mass flow is entrained within the recirculation region, the residence time can also have a measurable effect on rate controlled parameters such as NO_x emissions. The flameholder geometry also determines the downstream distance required for the flame to propagate completely through the unreacted gas mixture entering the combustor. This effect is particularly significant in that it determines the combustor length necessary to achieve a given level of combustion efficiency.

2

Flameholder designs for lean premixed combustion systems must satisfy six basic requirements. These are:

i) The gas residence time within the recirculation zone produced by the flameholder must be adequate to produce a steady and stable supply of high temperature gas and chemically active species under all conditions at which the flameholder must operate...

ii) The combination of mixer section velocity and flameholder blockage must result in a combustor entrance velocity which is sufficient to preclude flashback under all operating conditions.

iii) The distribution of ignition perimeter across the combustor entrance plane (i.e., the extent of the mixing zone between the reacting recirculation zone and the unreacted zone) must be adequate to assure flame propagation throughout the incoming mixture within a reasonable distance.

iv) The combination of flameholder drag coefficient and total blockage must be such that the total pressure drop produced by the flameholder does not exceed acceptable levels (typically on the order of 5%).

v) In designs where multiple independent areas of flow recirculation are created the flow pattern must be such as to provide ignition interconnection, i.e., to allow flame propagation from one recirculation zone to another during the initial light-up process.

vi) The flameholder must be self cooling, that is, heat transferred to the flameholder by the burning gases in its wake must be radiated and/or conducted to the relatively cooler unreacted gases which flow over its upstream surfaces.

Within the bounds of these constraints there is considerable latitude for design choice. Twelve flameholders were tested in this program representing six design concepts with two values of flow blockage for each concept. The flameholders were tested in a constant diameter (7.9 cm) flametube apparatus in which a well mixed stream of gaseous propane and air was supplied at an inlet

temperature of 300K (1440^OR) and a pressure of 1 MPa (10 atm). The six flame-holder concepts, representing a range of recirculation zone size and ignition perimeter, consisted of wire grid, perforated plate, multiple cone. vee gutter, single cone and swirl flameholders. Emissions of NO_x, CO and unburned hydro-carbons (UHC) were measured as functions of equivalence ratio* at stations 10 cm and 30 cm downstream from the flameholder at reference velocities of 20, 25 and 30 m/s. Flameholder pressure drop, lean stability limit and flash-back limit were also determined.

*Fuel/air ratio divided by stoichiometric fuel/air ratio.

APPARATUS AND PROCEDURES

Flameholder Designs

All flameholders were mounted on support rings with 7.9 cm inside diameters which could be slipped into a holder in the test rig as illustrated in Figure (1). Thus, except for the points of flameholder attachment, the wall of the mixer-combustor assembly is an uninterrupted cylinder of constant diameter. A mixture of hydrogen and air was used in a spark-driven igniter to produce a small jet (0.3 cm dia.) of hot gas to initiate combustion. The ignition jet was fired across the gas stream 0.3 cm downstream of the flameholder face. Wherever possible, the flameholders were designed with one of their support elements aligned with the igniter port to provide a means of ignition interconnection with the main flameholding region.

The pertinent physical characteristics of the twelve flameholders tested are summarized in Table I. Blockage is defined as the ratio of blocked area in the plane normal to the flow direction at the flameholder exit station to total mixer tube area. Blockage depth is defined as the axial distance over which the flameholder increases local velocity. (The blockage depth listed for the swirl flameholders is the length of the swirl passages.) Ignition perimeter is defined as the sum of the perimeters of the individual jets of gas exiting the flameholder. Ignition width is the maximum cross-stream distance over which the flame must propagate (either between adjacent recirculation zones or from a recirculation zone to the combustor wall). For all but the swirl flameholders, the dimension used to characterize wake recirculation region size in Table I is the diameter of the body producing the individual wake. For the case of swirling flow, the characteristic dimension listed is the diameter of the centerbody multiplied by the recirculation zone extension factor (2.0 for the 40° swirler, 3.5 for the 50° swirler).

The details of the two wire grid flameholder designs are presented in Figure (2). Each consisted of a single ply of stainless steel wire mesh (0.42 cm wire spacing): one employed 0.16 cm wire to produce an overall blockage of 60% and the other used 0.20 cm wire to produce 73% blockage. The ignition perimeter is defined as the sum of the perimeters of all jets of gas passing through the open areas of the flameholder and can be used as an indi-

5

Igniter Air Inlet

Igniter H₂ Inlet

Support Ring

Igniter Flame Port

Combustor Liner
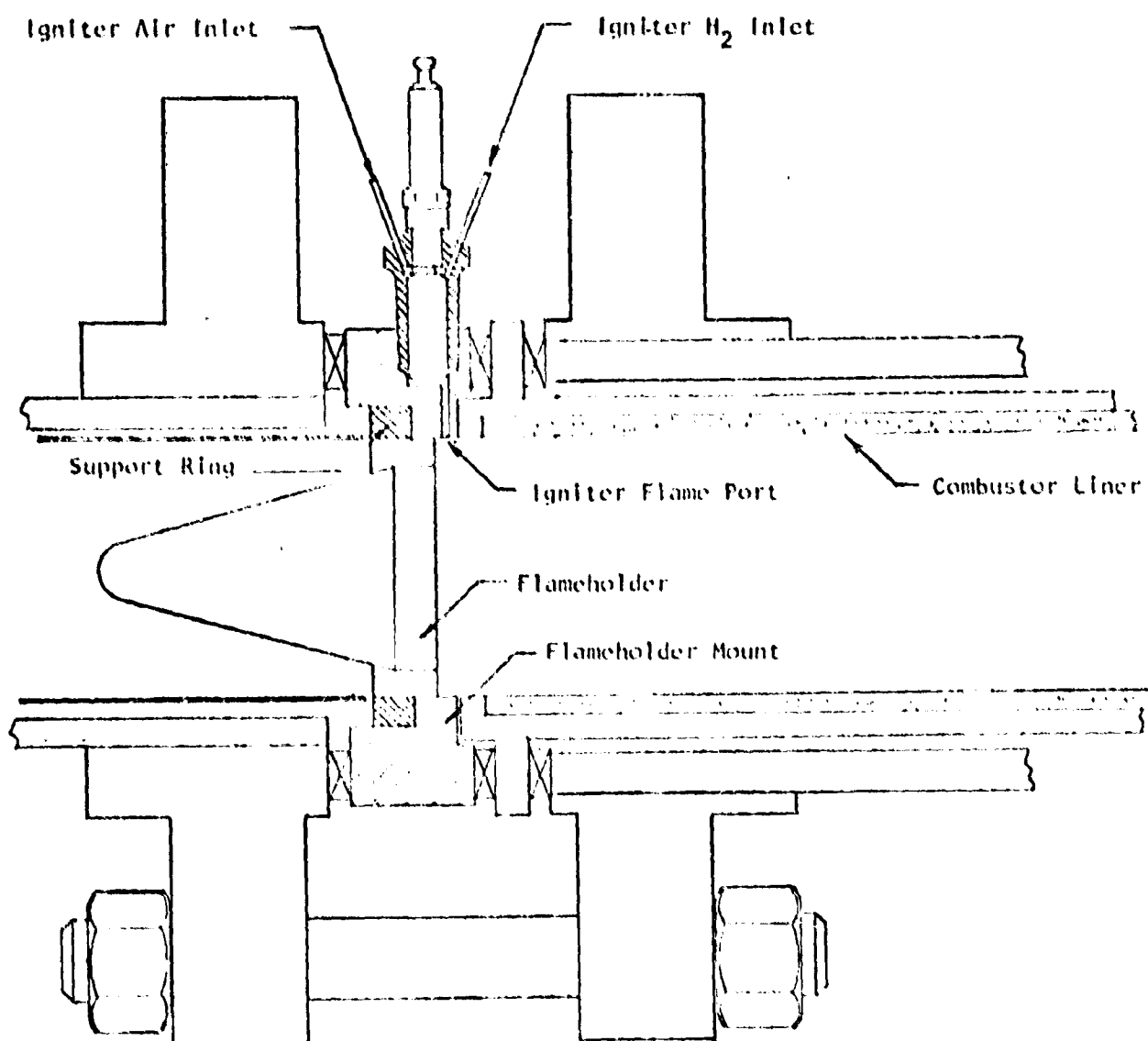
Flameholder

Flameholder Mount

FIGURE 1.   FLAMEHOLDER MOUNTING IN TEST RIG

TABLE I

SUMMARY OF FLAMEHOLDER CHARACTERISTICS

TYPE	BLOCKAGE	BLOCKAGE DEPTH	IGNITION PERIMETER	IGNITION WIDTH	CHAR. WAKE DIMENSION	DESCRIPTION
Wire Grid	60%	0.16cm	300cm	0.27cm	0.16cm	0.16cm dia. wire - 0.42cm wire spacing
	73%	0.20cm	230cm	0.22cm	0.20cm	0.20cm dia. wire - 0.42cm wire spacing
Perforated Plate	70%	0.64cm	83cm	0.71cm	0.84cm	37 holes - 0.71cm dia.
	80%	0.64cm	65cm	0.56cm	0.99cm	37 holes - 0.56cm dia.
Multiple Cone	70%	3.2cm*	71cm	1.03cm	1.9cm	1.9cm base dia. cones - 2.1cm spacing
	80%	3.2cm*	102cm	0.79cm	1.9cm	1.9cm base dia. cones - 1.9cm spacing
Vee Gutter	70%	1.9cm*	33cm	3.05cm	2.1cm	30° half angle - 2.88cm OD annulus
	80%	1.9cm*	32cm	2.54cm	2.5cm	30° half angle - 2.96cm OD annulus
Single Cone	70%	10.5cm*	20cm	0.79cm	6.4cm	15° half angle - 6.35cm dia. hollow base
	80%	11.6cm*	22cm	0.48cm	7.0cm	15° half angle - 7.00cm dia. hollow base
Swirl	73%	1.8cm	18cm	1.07cm	12.0cm	40° turning vanes - hub/tip ratio 0.73
	83%	1.8cm	18cm	1.07cm	20.0cm	50° turning vanes - hub/tip ratio 0.73

*Blockage varies across this distance attaining full value only at exit plane.
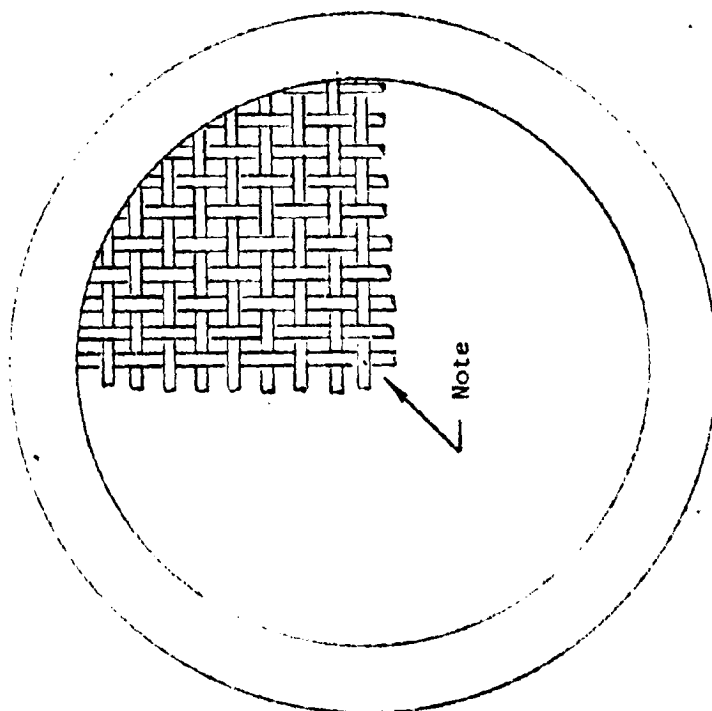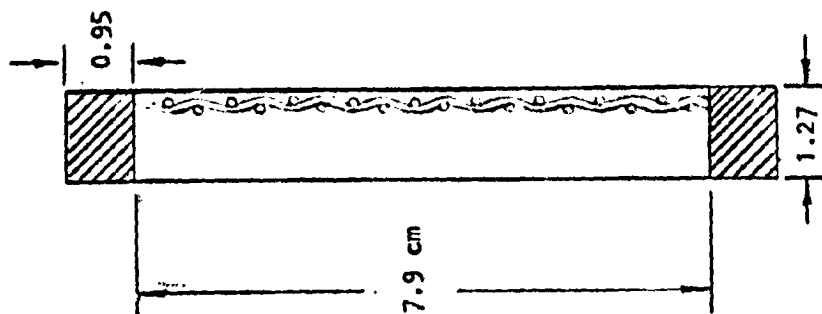
Note: One ply of 0.16 cm (0.20 cm) wire
for 60% (73%) blockage.
Square grid, 0.42 cm center-to-
center spacing

FIGURE 2. WIRE GRID FLAMEHOLDER DETAILS

cator of the flame spreading ability of a given geometry. The ignition perimeter of the lower blockage (60%) design was 300 cm; that of the higher blockage (73%) design was 230 cm. The maximum cross-stream ignition width for these flameholders is the distance between adjacent wires, 0.27 cm and 0.22 cm respectively for the lower and higher blockage designs.
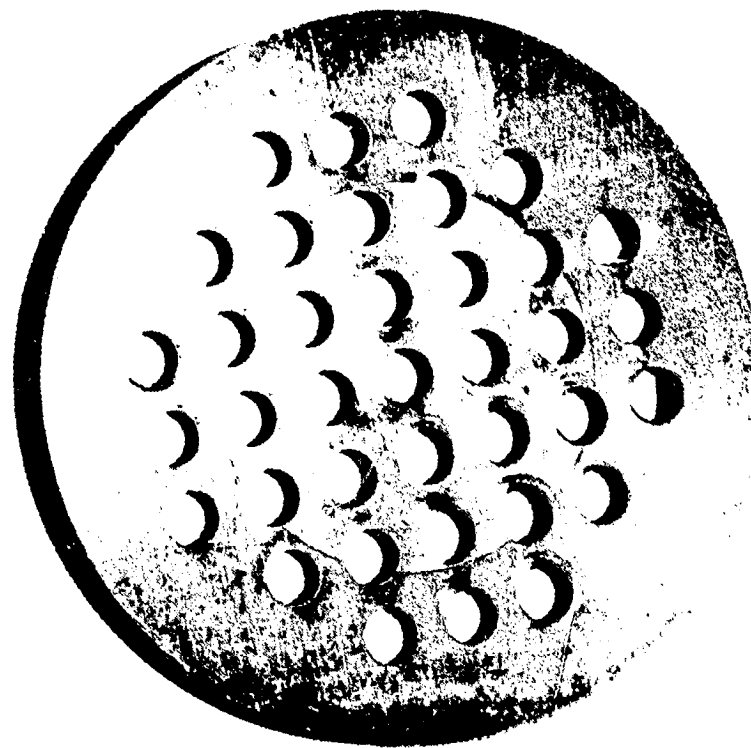
The details of the perforated plate flameholder designs are presented in Figure (3). The flameholders consist of plates 0.63cm thick, mounted within the standard support rings and perforated by square arrays of 37 holes. Two values of blockage, 70% and 80%, were obtained by drilling holes with diameters of 0.71 cm and 0.56 cm respectively. The passages through the plate were rounded on the upstream side to avoid internal flow separation and the possibility of flame stabilization within the passages. The perforated plate flameholders were originally designed with a plate thickness of only 0.32 cm. However, initial testing resulted in localized material failure at the downstream exits of the drilled holes. This difficulty was eliminated by increasing plate thickness to the 0.63 cm indicated in the figure. Figure (4) is a photograph of the 70% blockage perforated plate. The ignition perimeter of this design is 83 cm, approximately one third that of the corresponding wire grid. The characteristic dimension of the blocked areas (and thus the recirculation zones) is 0.84 cm, nearly four times that of the grid. The 80% blockage design has an ignition perimeter of 65 cm, which is smaller than that of the lower blockage plate due to the smaller hole size, and a recirculation zone characteristic dimension of 0.99cm.

The multiple cone flameholder designs are illustrated in Figures (5) and (6). These units employed a square array of strut-supported 10° half angle cones with base diameters of 1.9 cm. The center-to-center spacing of the array was varied to produce flameholders with 70% and 80% blockage. The base regions of the conical elements were hollowed out to a depth of 1.2 cm and ignition interconnection was provided by milling through the solid struts where they intersect the cones. The flameholders were installed in the test rig with the igniter port aligned with one of the conical elements intersecting the support rig. The ignition perimeter of the 70% and 80% blockage designs was 71 cm and 102 cm respectively and is comparable to that of the perforated plate. The characteristic recirculation zone dimension for the two designs is the same; and corresponds to the 1.9 cm base diameter of the conical elements.

9
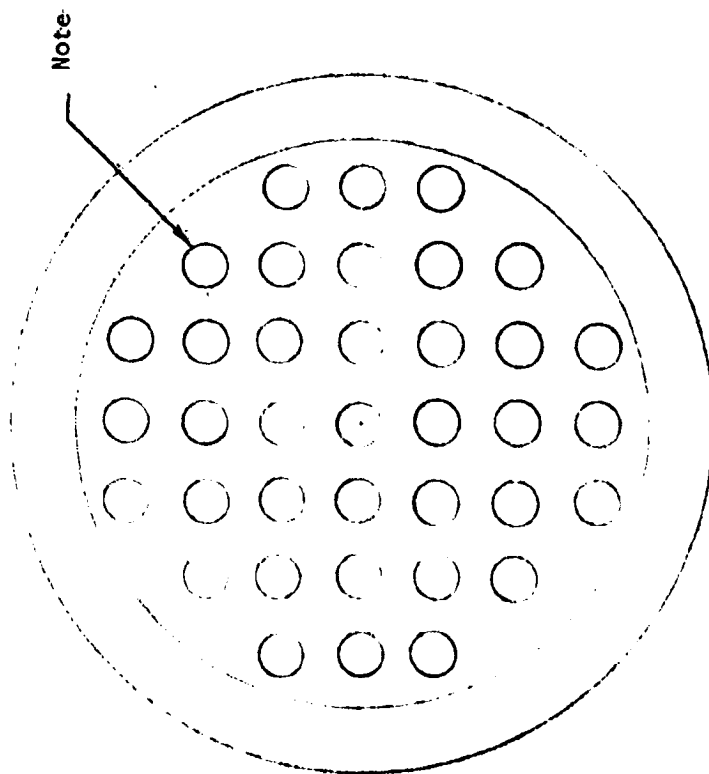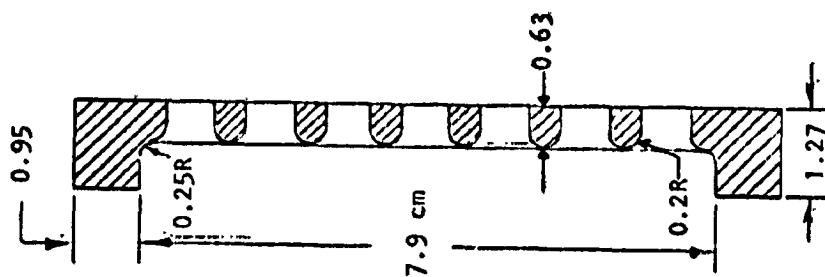
Note: 37 holes on 1.09 × 1.09 grid Hole dia. 0.71 cm for 70% blockage. Hole dia 0.56 cm for 80% blockage

FIGURE 3. PERFORATED PLATE FLAMEHOLDER DETAILS

10

Downstream Side
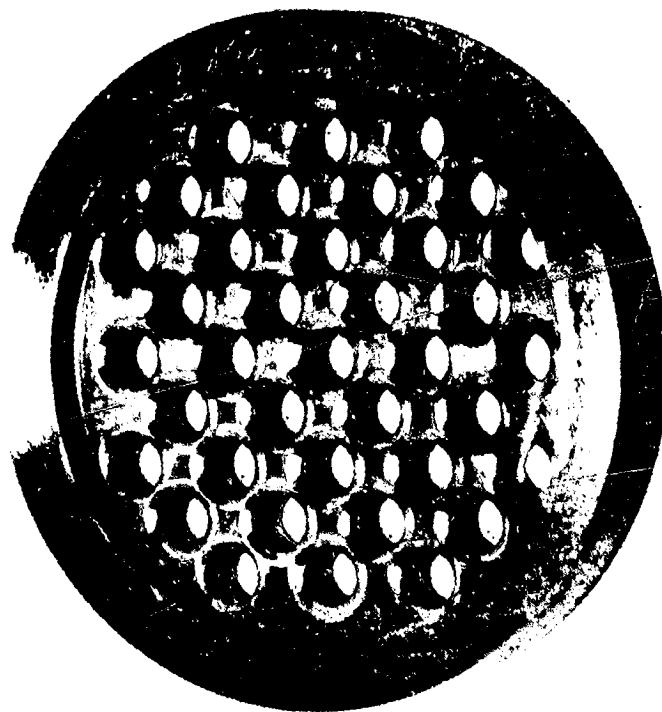
FIGURE 4. PHOTOGRAPH OF PERFORATED PLATE FLAMEHOLDER (FRONT AND BACK VIEWS)

11

0.95

7.9 cm

3.18

1.27

0.48R

Note

0.48
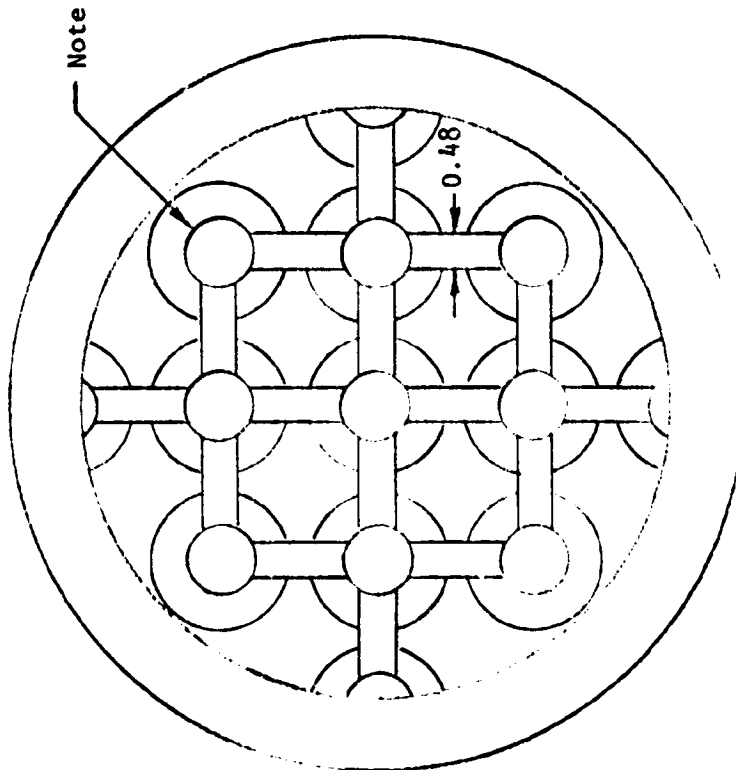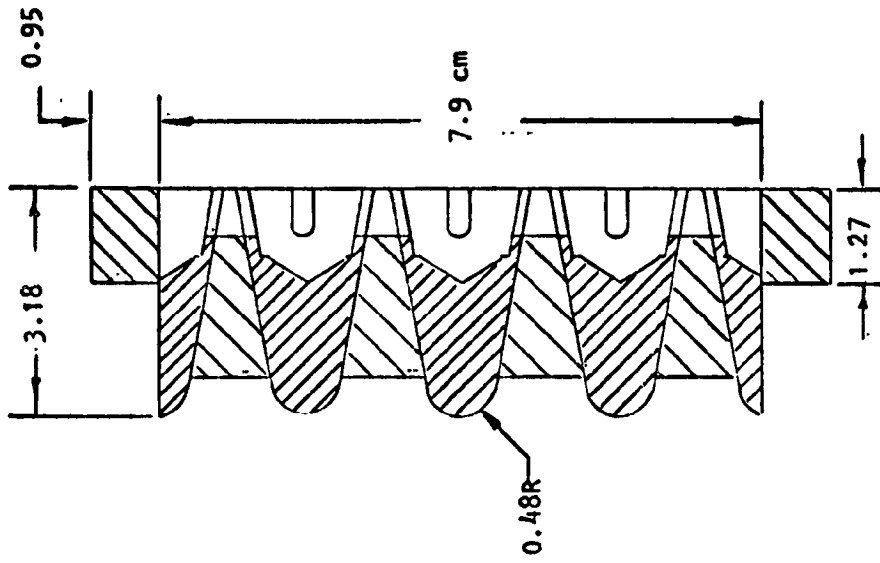
Note: 1.9 cm base diameter,
        10 half-angle cones
        on 2.1 x 2.1 cm grid

FIGURE 5a.   Multiple Cone Flameholder Details   (70% Blockage)
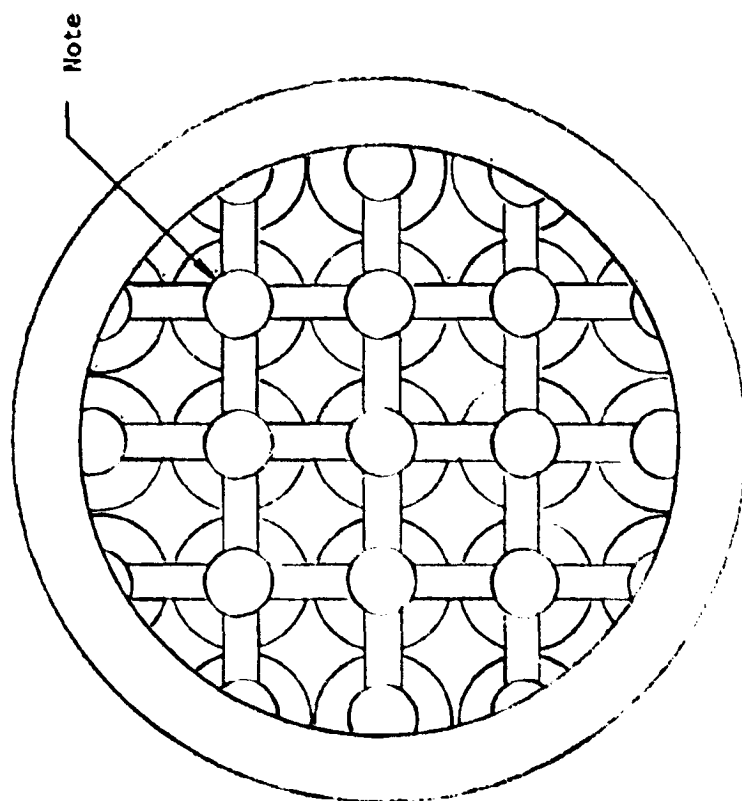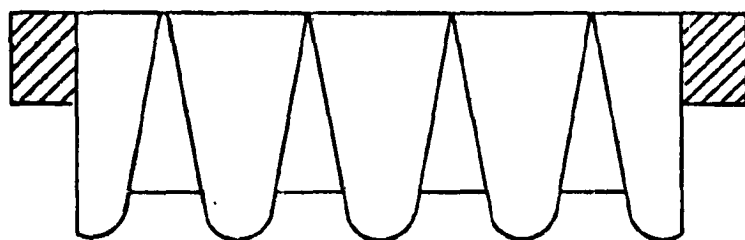
Note: 1.9 cm base diameter
100 half-angle cones
on 1.9 x 1.9 cm grid

FIGURE 5b. MULTIPLE CONE FLAMEHOLDER (80% BLOCKAGE)

13

Downstream Side

FIGURE 6. PHOTOGRAPH OF 70. BLOCKAGE MULTIPLE CONE FLAMEHOLDER (FRONT AND BACK VIEWS)

16

The vee gutter flameholders are illustrated in Figures (7) and (8). These flameholders employ a single hollow gutter element with a 30° wall angle held in place by four solid struts which are welded to the outer support ring. The gutters were sized to produce the desired blockage with an equal division of flow between the central and outer open areas. The ignition perimeter for the vee gutter designs was small; only 33 cm and 32 cm for the 70% and 80% designs. However, the characteristic sizes of the recirculation zones were 2.1 cm and 2.5 cm, more than twice those of the perforated plate. When one considers the two-dimensional nature of the mixing process downstream of the annular ring, its longer residence time and reduced flame spread capability (relative to the previous designs) is accentuated still further. The maximum cross-section ignition width occurs at the center of the annular ring and is 3.05 cm and 2.54 cm for the 70% and 80% designs respectively. This ignition width is larger than that of any other design concept.

The single cone flameholders are illustrated in Figures (9) and (10). Again, two flameholders were constructed; one producing flow blockage of 80% and the other producing 70%. Both flameholders employed a 15° half-angle cone with a hollow base region 3.7 cm deep. The conical centerbody was supported by two struts, 1.2 cm wide. One of these struts was hollowed and the cone wall removed at the point of strut intersection to allow ignition interconnection between the strut and the base region. The flameholders were installed in the test rig with the hollow strut aligned with the igniter port. The base diameter of the conical element varied from 6.4 cm for the 70% blockage flameholder to 7.0 cm for the 80% blockage design and corresponds to ignition perimeters of only 20 cm and 22 cm, respectively. The characteristic recirculation zone dimensions, 6.4 cm and 7.0 cm for the two designs, are on the order of thirty times larger than those for the wire grids and approximately seven times larger than those for the perforated plates. Ignition widths for the two designs are 0.79 cm and 0.48 cm and are comparable to those of the perforated plates.

The swirl flameholders are illustrated in Figures (11) and (12). These flameholders employed a round nosed 20° half-angle conical hub leading to a cylindrical section 1.8 cm in length. A series of 24 thin swirl

15

NOTE B

NOTE A

0.32

30°

1.9

1.27

0.95

7.9 cm

FIGURE 7. VEE GUTTER FLAMEHOLDER DETAILS

Downstream Side

1.27

Note B

7.9 cm Dia.

0.64

1.9

0.95

0.32

1.27

3.81

15°

Note A

NOTES

A. 11.6 cm for 70% Blockage
   10.5 cm for 80% Blockage
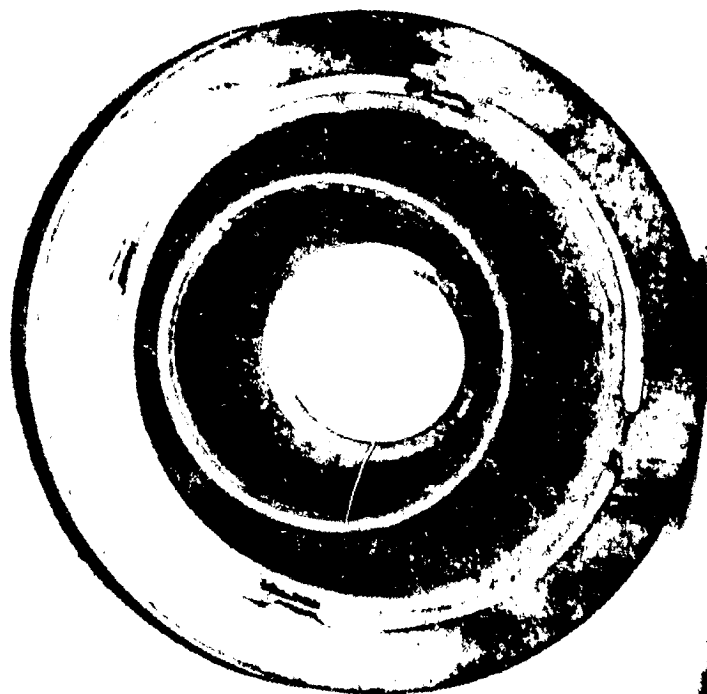
B. 6.35 cm Dia. for 70% Blockage
   7.00 cm Dia. for 80% Blockage
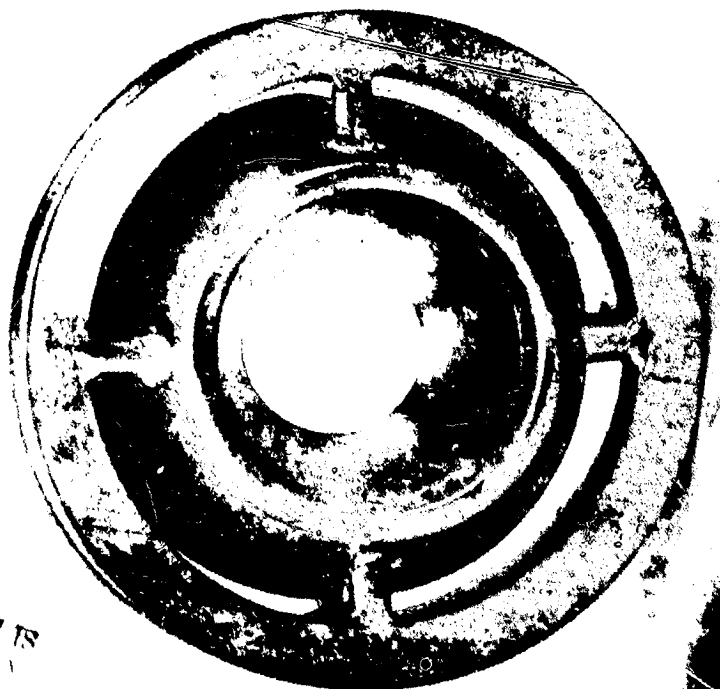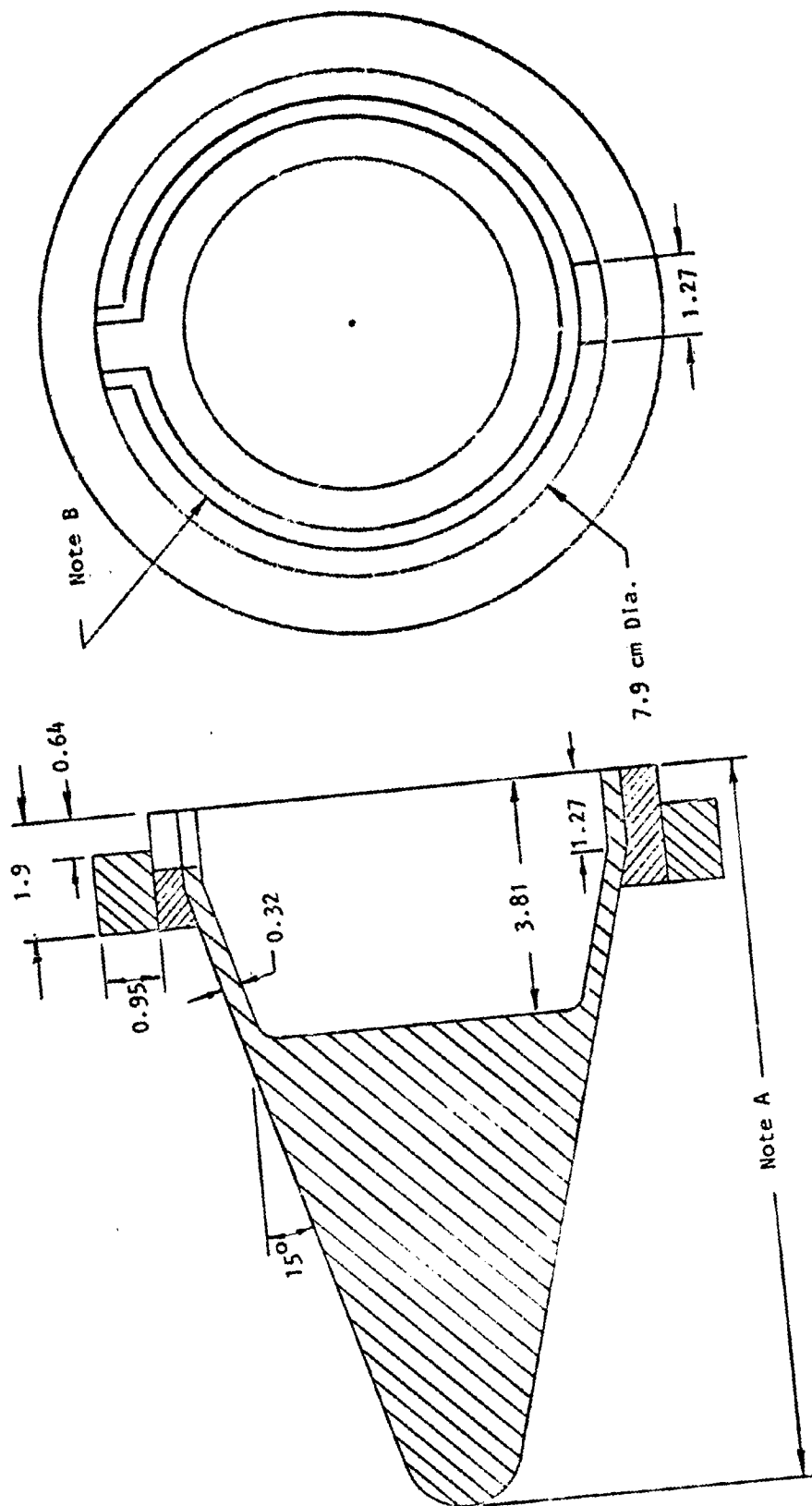
FIGURE 9. SINGLE CONE FLAMEHOLDER DETAILS

18
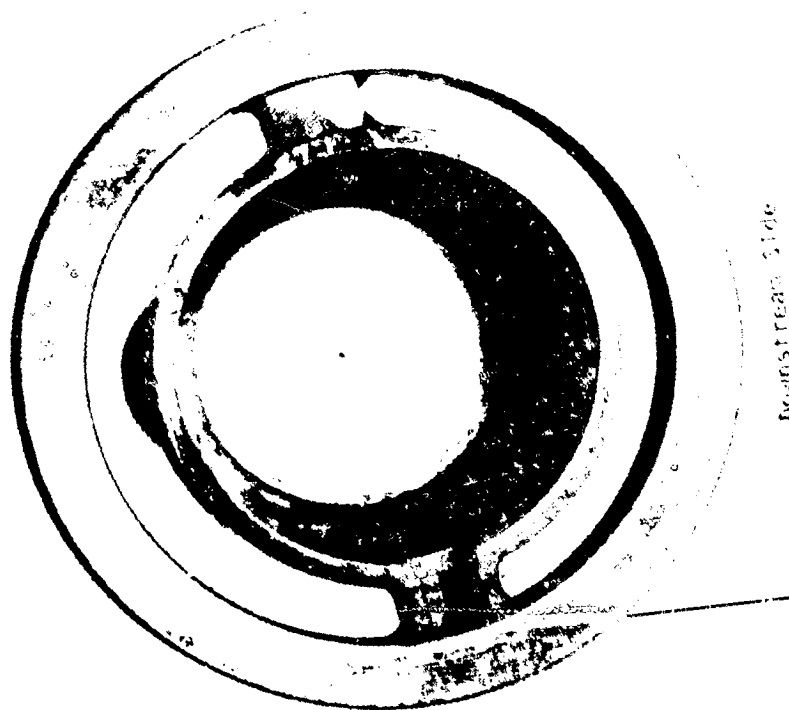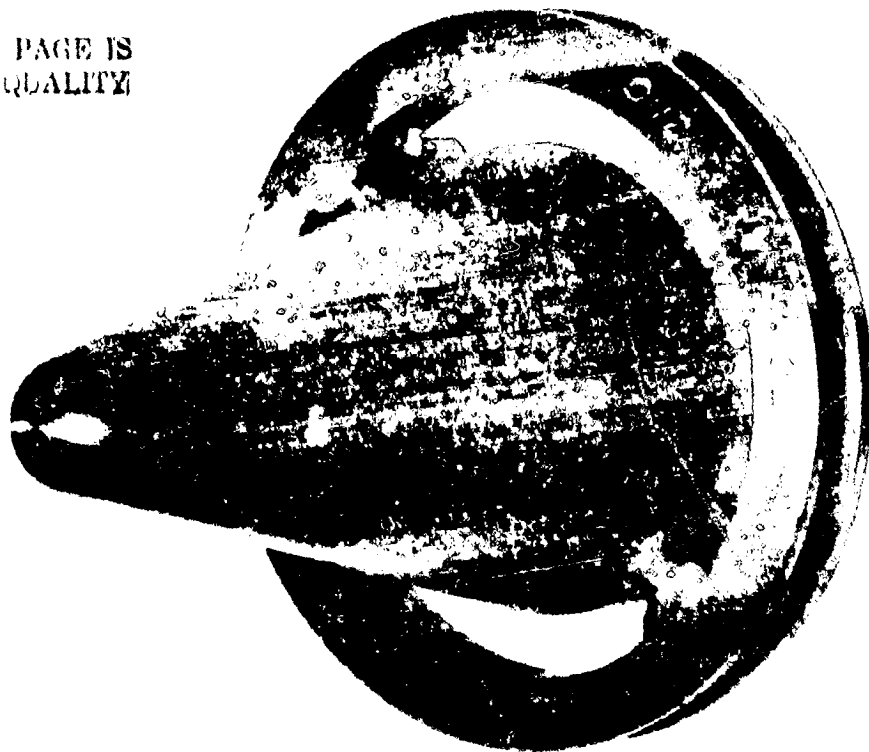
Downstream Side

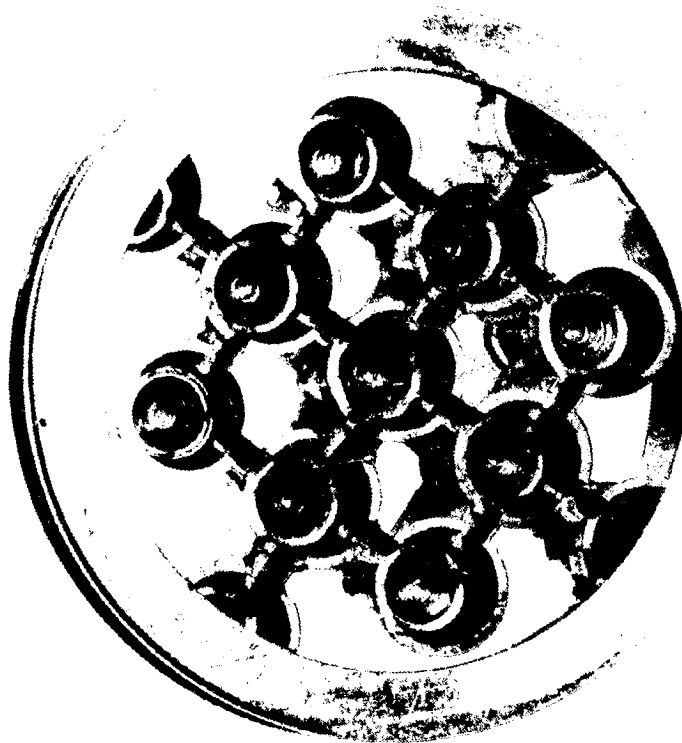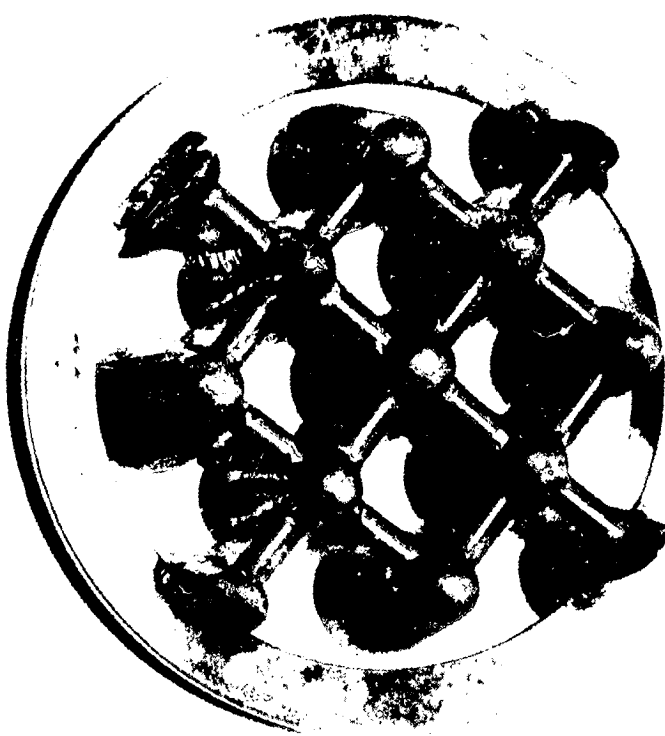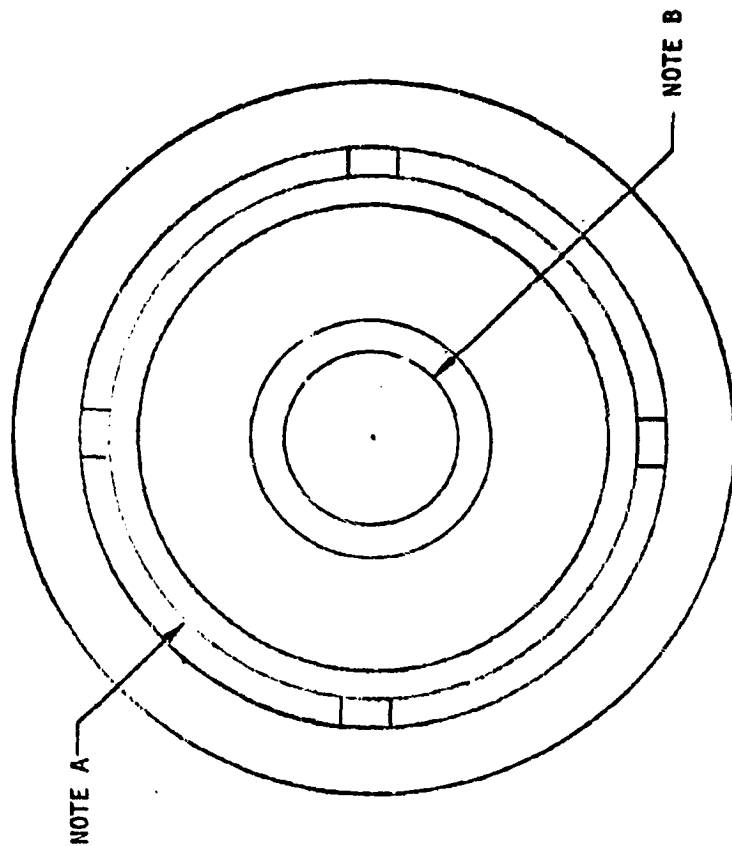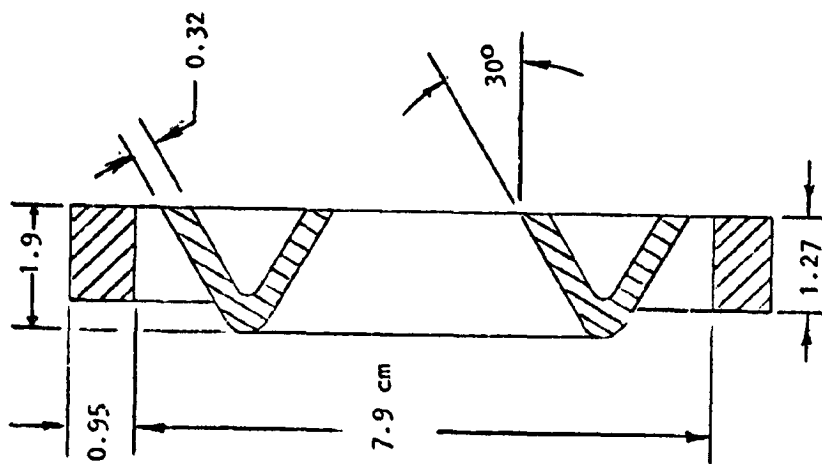FIGURE 10. PHOTOGRAPH OF SINGLE CONE FLAMEHOLDER, FRONT AND BACK VIEWS

19

7.9 cm dia.

5.8 dia.

Note

0.95

1.27

1.59

5.72 cm

2.0°
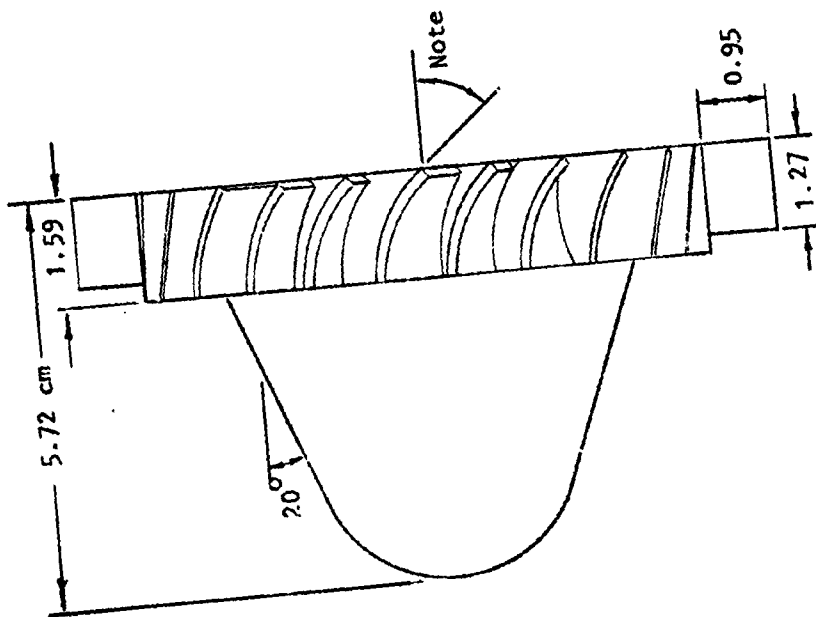
Note: 40° for 73% Blockage
50° for 83% Blockage
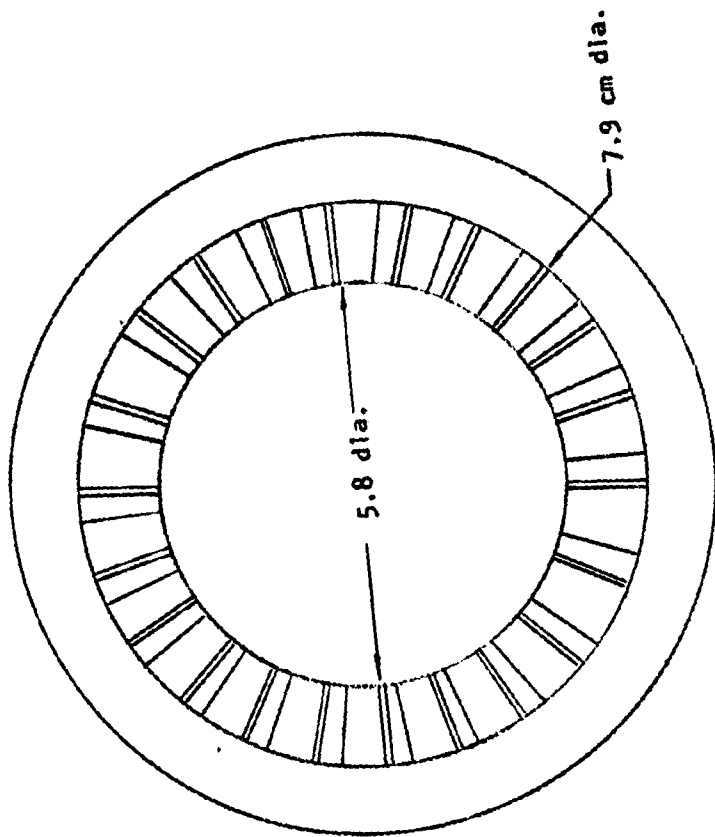
FIGURE 11. SWIRL FLAMEHOLDER DETAILS.

20
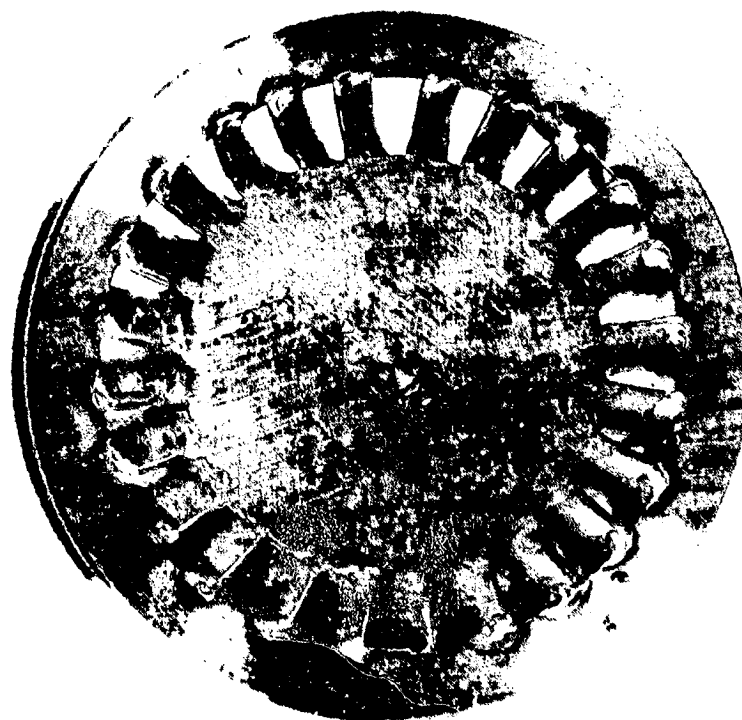
Downstream Side

FIGURE 12. PHOTOGRAPH OF SWIRL FLAMEHOLDER (FRONT AND BACK VIEWS)

21

vanes were welded to this cylindrical section, joining the centerbody and outer support ring. Two versions of the swirl flameholder were constructed; one turning the flow through an angle of 40° and the other through 50°. In both designs, the leading edges of the swirl vanes were aligned with the incoming flow to avoid separation at the entrance to the turning passages with the attendant possibility of ignition and/or internal flame stabilization. The 40° swirl angle design produced a swirl number of 0.7, a value which will approximately double the length of the recirculation zone as compared with that of a centerbody with zero swirl (Reference 1). The 50° design produces a swirl number of 1.0, a value which increases recirculation zone length by a factor of approximately three. The ignition perimeter of the swirl flameholders was 18 cm, the smallest of any design, a characteristic which is intensified by the retarding effect of swirl on mixing rates for the hot gas diffusing outward from the recirculating base flow. However, when one considers the recirculation zone residence time, an increase on the order of one hundred times is anticipated as compared with the wire grid designs. Since the hub diameter and turning vane thickness are the same for the two swirl flameholders, blockage (defined in the plane normal to the exit velocity vector) varies with turning angle and amounts to 73% for the 40° swirl angle and 83% for the 50° swirl angle design.

Test Rig

The combustion test rig is illustrated schematically in Figure (13). Heated dry air enters the apparatus through the bellmouth, passing through an instrumentation spool where the entrance temperature and pitot-static pressure profiles are measured by an imbedded rake. Fuel enters the device by means of a plenum chamber which surrounds the instrumentation spool and feeds fifty-two individual 1.6 mm diameter injection tubes. The tubes extend 7 cm downstream from their entry point and inject fuel in the streamwise direction in order to minimize the possibility of local flow separation. The relatively long and thin injection tubes are supported at their midpoints by a fine (0.05 mm web thickness) honeycomb structure 6 mm in streamwise extent representing a flow blockage of 3%. The fuel injector assembly is shown in Figure (14).

The mixer tube was constructed of a heavy outer pressure wall and a thin stainless steel liner. The two elements were separated by an internally vented air gap to minimize heat loss. Four thermocouples were mounted
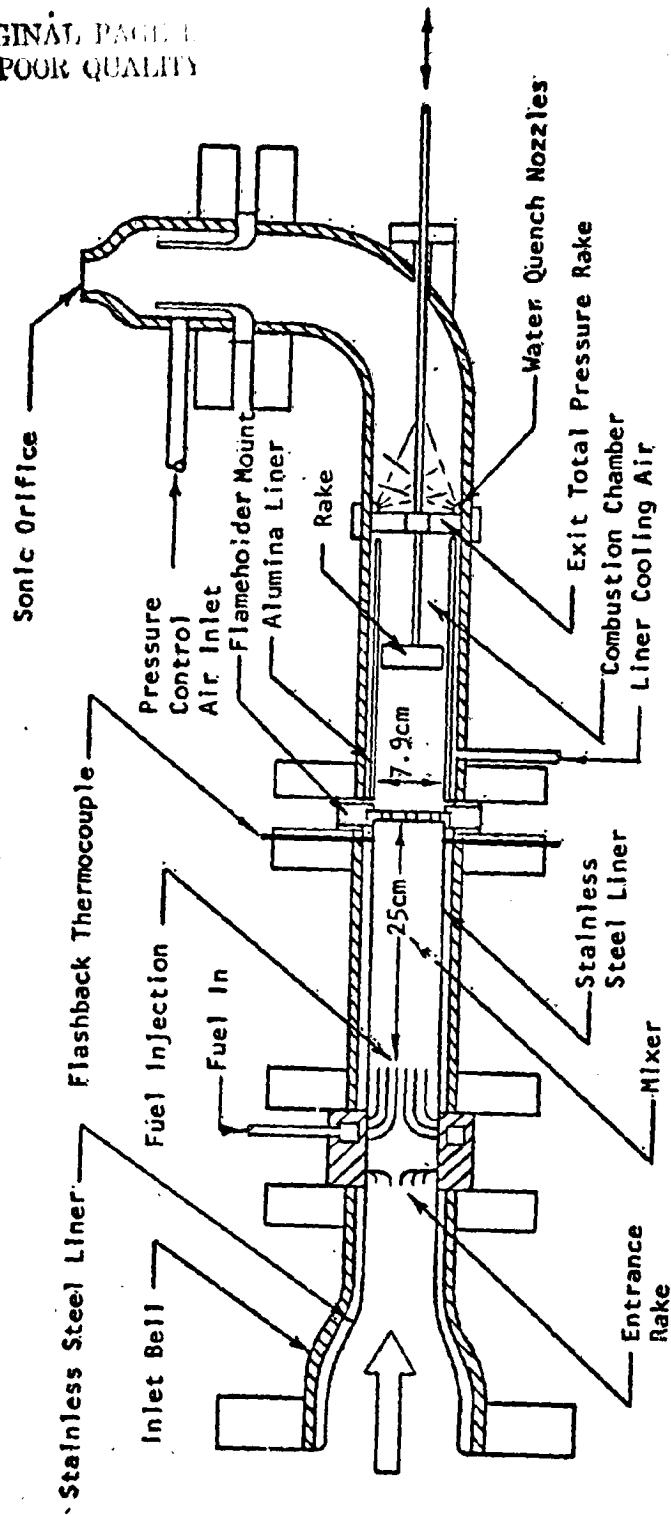
22

FIGURE 13. COMBUSTION TEST RIG.

23

24

Pitot Tube

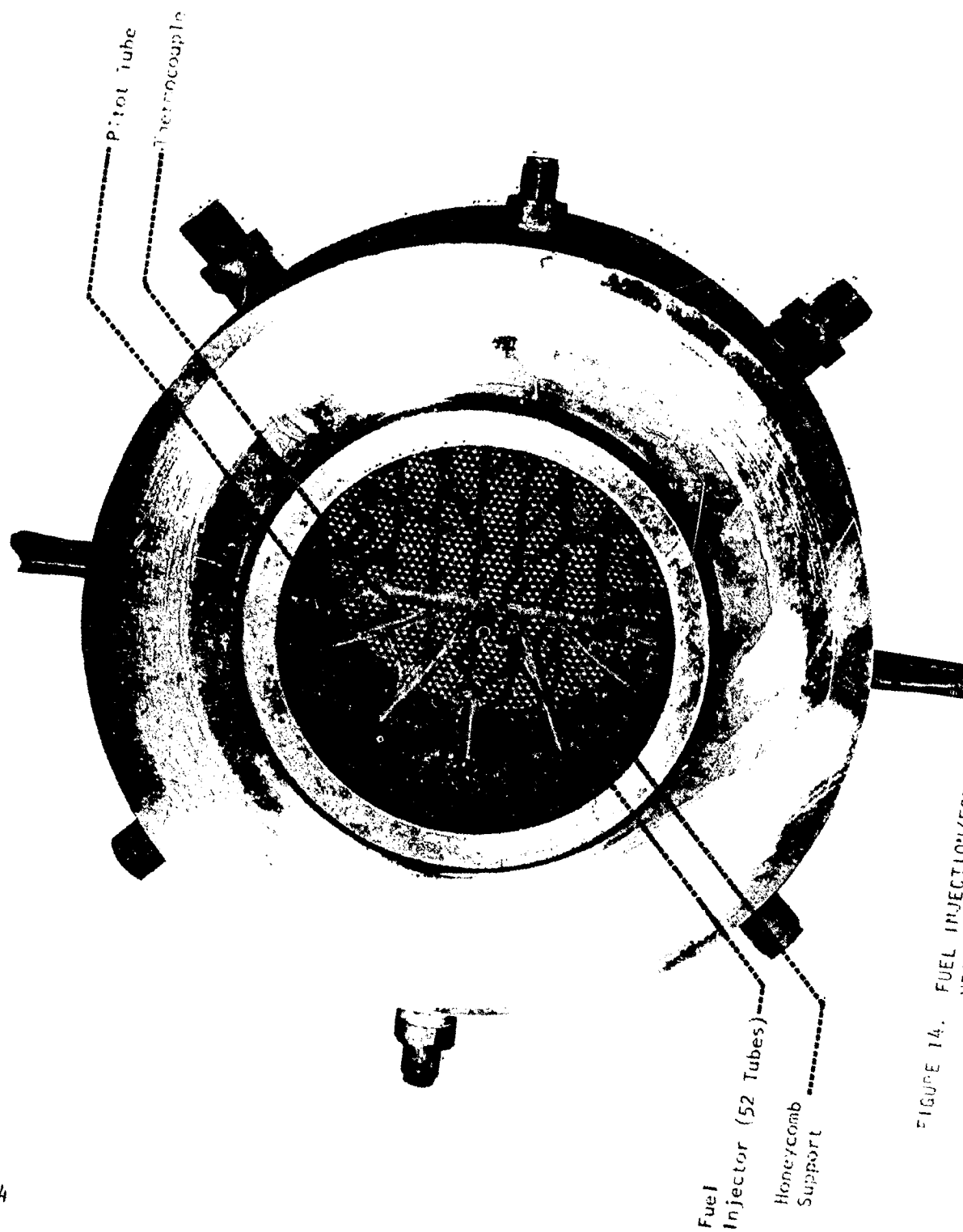Thermocouple

Fuel
Injector (52 Tubes)

Honeycomb
Support

FIGURE 14. FUEL INJECTION/FORWARD INSTRUMENT SPOOL ASSEMBLY VIEWED FROM
UPSTREAM SIDE)

90° apart 2.5 cm from the downstream end of the mixer and placed so that their tips were flush with the inner surface of the liner. The thermocouples served as indicators of autoignition in the mixer or flashback through the flameholder.

The combustor assembly also employed a double wall design to protect the heavy outer pressure wall. However, here the air gap between the combustor liner and the outer wall was kept cool by injecting a small amount of cold air. In addition, an alumina tube was mounted inside the stainless steel liner to provide an uncooled refractory combustor wall, minimizing convective and radiation losses from the gas.

A dome-loaded pressure regulator was used to supply cold air to an annular injection section just upstream of the rig exit orifice. By loading the regulator to the pressure desired for the test, the appropriate amount of cold air is added automatically to produce the correct total pressure in the test rig. This method of pressure control offers the dual advantages of automatic compensation for varying combustor exit temperature and thermal protection for the choked exit orifice.

Instrumentation

During emissions testing, gas samples were withdrawn from the combustor using the sampling rake illustrated in Figure (15). The rake contained seven 1.6 mm diameter sampling tubes supported within a water-cooled body with the sample entrance ports located at the centers of equal flow areas. Water entered the rake through the hollow stem flowing forward to the head where it was exhausted through a number of 0.20 cm diameter holes into the narrow gap between the head and the two deflector plates. The exhausted water was thus used to convectively cool the deflector plates and film cool the rake head. A small portion of the cooling water was exhausted through a set of 0.76 mm diameter holes in the hollow stem near the head junction to fill the space between the stem and a deflection collar, film cooling the upstream portion of the stem. The sample lines were manifolded after exiting the test rig and brought to the gas analysis system through a single stainless steel line heated to 175°C to prevent condensation. The details of the gas analysis system

FIGURE 15. GAS SAMPLING RAKE DETAILS

Deflecting Collar

1.27 cm

6 Holes - 0.76mm dia

14 Holes - 0.20 cm dia.

Deflector Plate

7.6 cm

Note

1.6
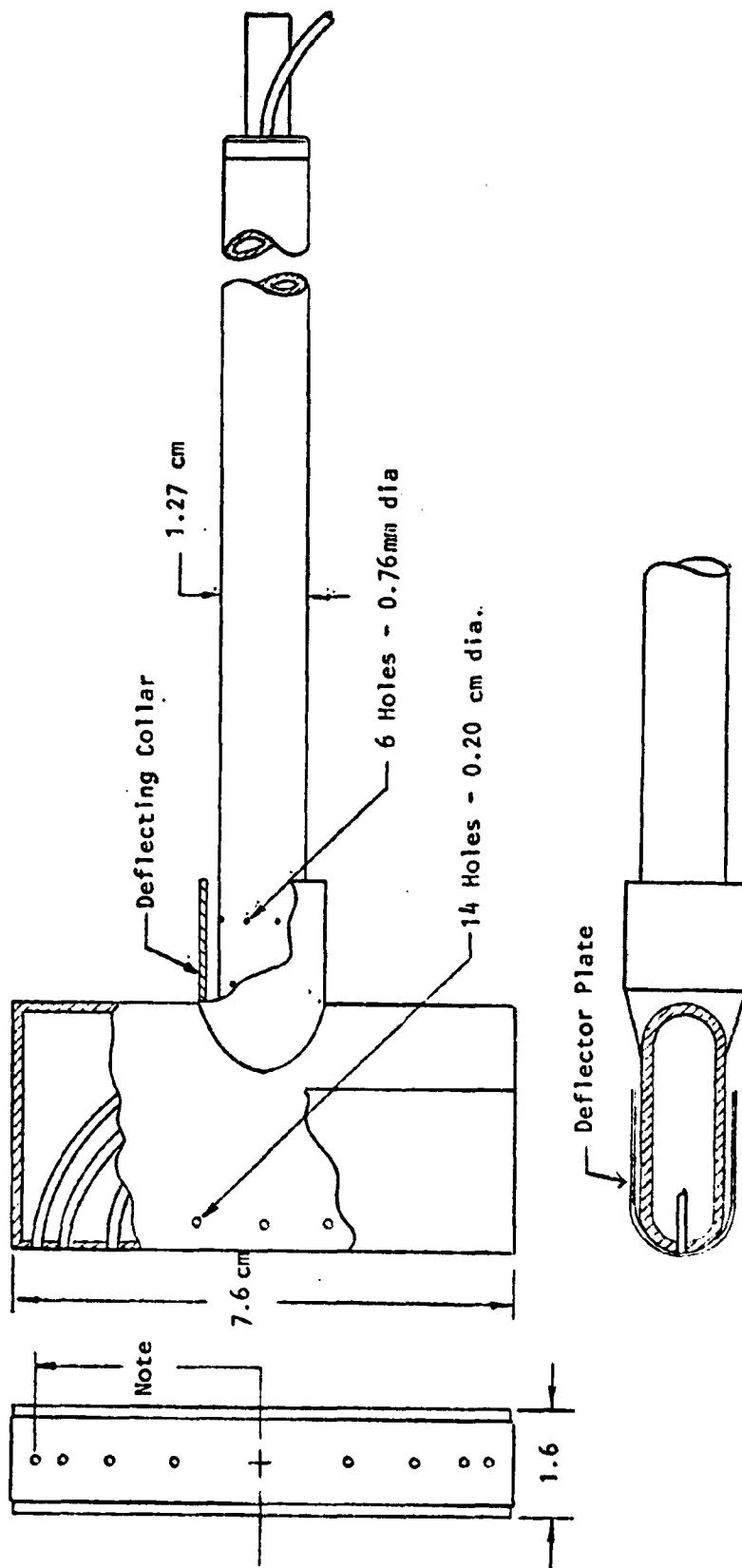
Note: Radii to sampling ports
are 1.4, 2.3, 3.0 and
3.6 cm

and the data reduction equations (in conformance with SAE ARP 1256) are presented in the Appendix. The sampling rake was positioned 10 cm from the flameholder exit station for tests of reference velocities of 20 m/s and 25 m/s and 30 cm downstream for tests at 25 m/s and 35 m/s reference velocity.

Air inlet conditions were monitored using an array of four pitot tubes and four chromel-alumel thermocouples mounted in the inlet instrumentation spool which also contained two static pressure taps spaced 180° apart. A water-cooled strut at the combustor exit station served the dual purpose of supporting the sampling rake stem and housing four pitot pressure tubes. Flameholder pressure drop was measured by a differential pressure transducer connected between corresponding total pressure taps on the entrance and exit survey rakes.

Fuel System and Properties

The fuel supply system is illustrated in Figure (16). Liquid propane is stored in a tank pressurized with nitrogen. The liquid is withdrawn from the lower section of the supply tank, passing through a turbine flowmeter and pressure regulator before entering a cavitating venturi which provides a constant fuel mass flow rate independent of downstream pressure fluctuations. Fuel flow rate is controlled during a test by adjusting the regulated pressure on the upstream side of the cavitating venturi. The propane is heated to a temperature of 380°K (10 degrees above its critical temperature) in a pressurized water bath and passed through a heated line to a metering venturi before being delivered to the injection plenum. An analysis of the commercial grade propane used in these experiments is presented in Table II.

Test Procedure

In operation, the air flow through the rig was first established at a temperature of 800°K and a mass flow rate corresponding to the desired reference velocity. The rig pressure was then brought up the 100N/cm² operating value by injection of an appropriate amount of cold air at the exit orifice. The gas igniter was turned on, fuel flow was initiated and slowly increased until ignition was achieved. The rig equivalence ratio was brought to the highest level desired during the particular test

27
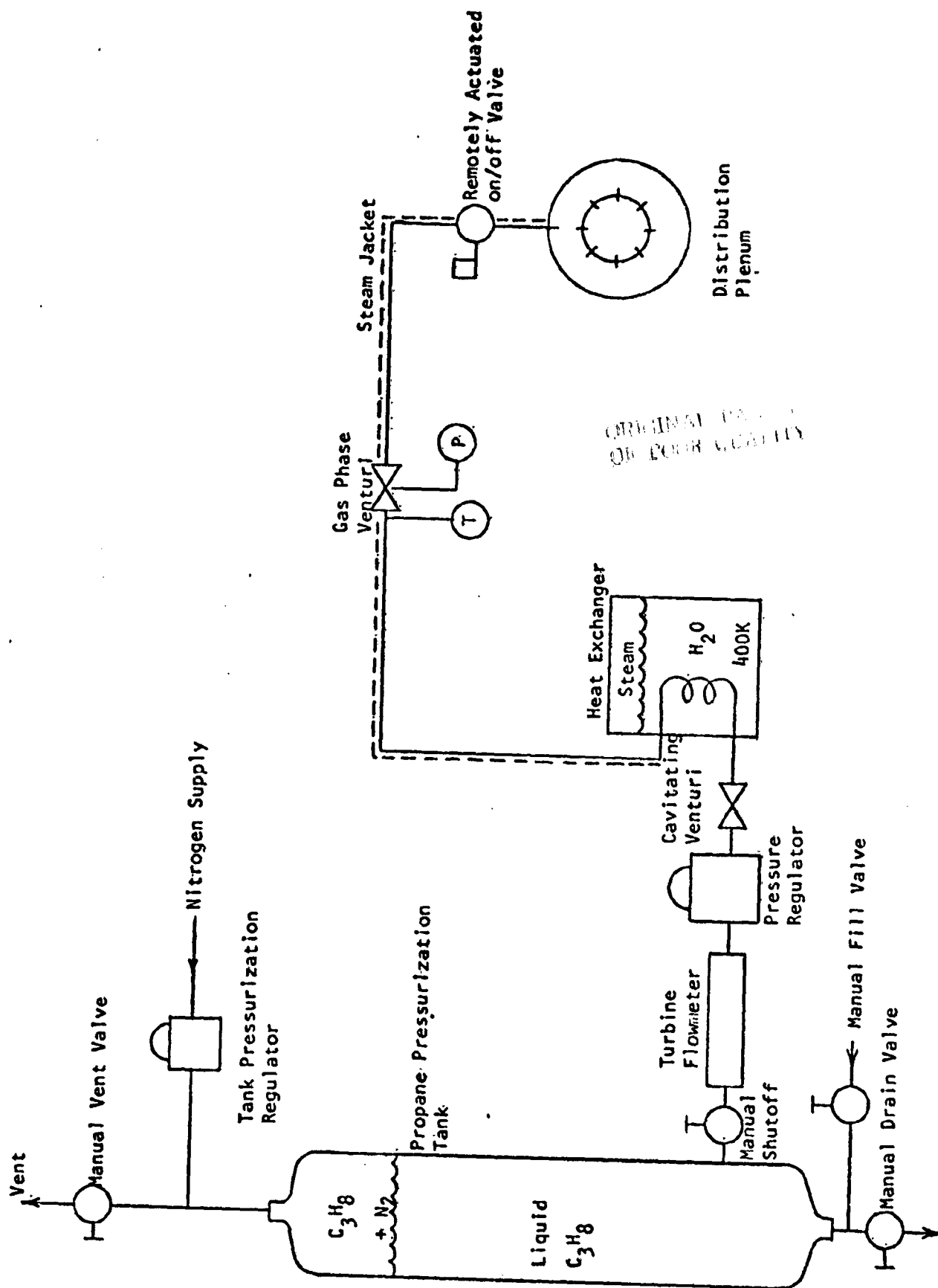
FIGURE 16. PROPANE STORAGE AND DELIVERY SYSTEM SCHEMATIC

28

TABLE II

ANALYSIS OF COMMERCIAL GRADE PROPANE USED IN TEST PROGRAM

Property	Value
% Propane	90
% Butane	0.084
% Ethylene and Ethane	0.034
% Propylene	9.2
% Volatile Sulfur	0.0073
Specific Gravity (air $\equiv$ 1.0)	1.541
Vapor Pressure, N/cm^2	50.3
Hydrogen/Carbon Atom Ratio	2.597

sequence (generally 0.7), the gas igniter shut off and the rig operated for several minutes to assure steady conditions before withdrawing gas samples. The equivalence ratio was then lowered and the procedure repeated. Continuing to lower the equivalence ratio eventually caused the flame to blow out. Conditions at this point were defined as those corresponding to the lean stability limit.

Flashback tests were conducted by bringing the rig to steady state operation at an equivalence ratio of 0.7 and reference velocity of 20 m/s. The fuel flow was then lowered until the equivalence ratio dropped by approximately 5%. At that point, the air flow rate was reduced, lowering the reference velocity, until the equivalence ratio returned to 0.7. Thus, the reference velocity was brought down in steps of approximately 1 m/s at an equivalence ratio which varied only slightly from 0.7. The procedure was repeated until the flashback thermocouples indicated a temperature increase at the mixer exit station or evidence of flameholder damage appeared.

30

RESULTS

Flameholder Pressure Drop

The loss of total pressure which results from sudden contractions and
expansions in flow area can be conveniently represented by a resistance co-
efficient. By definition, the total pressure loss for any flow condition
is given by the expression

$$\Delta p = k \left(\frac{\rho V_{max}^2}{2}\right)$$

where ρ is the gas density, V_{max} is the highest velocity achieved in the
contraction and k is the resistance coefficient, which is solely a function
of the geometry of the system. Total pressure drop was measured for all
flameholders at each of the three reference velocities at which tests were
conducted. Calculated values of resistance coefficient were found (within
a small margin of scatter) to be independent of reference velocity and are
summarized in Table III. The table also presents corresponding values of
total pressure loss for 25 m/s reference velocity. Total pressure losses
for other reference velocities or blockage values are obtained by using the
tabulated resistance coefficients and noting that

$$V_{max} = \frac{V_{ref}}{1-B/100}$$

where B is the flameholder blockage (in percent). It should be noted that
the flameholder resistance coefficient was found to be constant, independent
of blockage, for each geometric configuration. In the case of the two swirl
flameholders, where varying swirl angle changes the relative size of the
recirculation zone and thereby affects the effective geometry of the flowfield,
resistance coefficient is not the same for the two designs.

The vee gutter flameholder (resistance coefficient 2.2) produces by far
the highest total pressure drop of any design tested, a result which very
likely stems from the relatively large flow deflection angle (30°) at its
exit plane. Although the 80% blockage version of this flameholder exceeds
the 5% total pressure drop (at V_{ref} = 25 m/s) guideline set forth earlier,

31

TABLE III

FLAMEHOLDER PRESSURE DROP SUMMARY

GEOMETRY	BLOCKAGE (%)	RESISTANCE COEFFICIENT k	$\frac{\Delta p}{P_T}$(% at V_{ref}= 25 m/s)
Wire Grid	60		0.8
Wire Grid	73	1.0	2.1
Perforated Plate	70		2.5
Perforated Plate	80	1.6	5.8
Multiple Cone	70		2.3
Multiple Cone	80	1.5	5.4
Vee Gutter	70		3.3
Vee Gutter	80	2.2	7.1
Single Cone	70		2.3
Single Cone	80	1.5	5.4
40° Swirl	73	1.8	3.4
50° Swirl	83	0.9	4.8

the results obtained with this design are sufficiently interesting to justify its inclusion in the study. The 40° swirler, perforated plate, multiple cone and single cone designs constitute an intermediate pressure drop group with resistance coefficients ranging from 1.5 to 1.8. The wire grid and 50° swirl flameholders produce very low pressure drops with resistance coefficients of only 1.0 and 0.9, respectively. The low pressure drop potential of the wire grid designs combined with the fact that the blockage of these designs was lower than that of all other concepts (a factor dictated by the use of commercially available screens) resulted in absolute pressure drops for the grid flameholders which were lower than those for any other designs, amounting to only 0.8% for the 60% blockage design at the 25 m/s reference velocity.

Emissions

The emissions performance of the perforated plate flameholders is presented in Figures (17 through 20). At 35 m/s, the highest reference velocity, the perforated plate displays little sensitivity to blockage, with the 80% blockage design differing from the 70% design only in that it fails to produce equilibrium CO levels at high equivalence ratio. At 25 m/s, there are significant differences in the emissions characteristics of the lower and higher blockage designs, differences which are evident at both the 30 cm and 10 cm combustor stations. Here, the higher blockage design produces less NO_x, CO and HC. The data taken at the 10 cm combustor station at 20 m/s reference velocity shows NO_x levels again lower for the higher blockage design but CO and HC levels here are slightly elevated.

The measured emissions performance of the wire grid flameholders is presented in Figures (21 through 24). At the 35 m/s reference velocity condition, NO_x level again is only slightly influenced by flameholder blockage. However, both CO and UHC emissions are decreased by increasing flameholder blockage. The emissions performance of the perforated plate flameholders has been included on these figures as a reference. It can be seen that the NO_x emissions of the wire grid and perforated plate are virtually identical at the 35 m/s condition. However, both CO and UHC emissions for the wire grid flameholder are considerably higher than those obtained

33
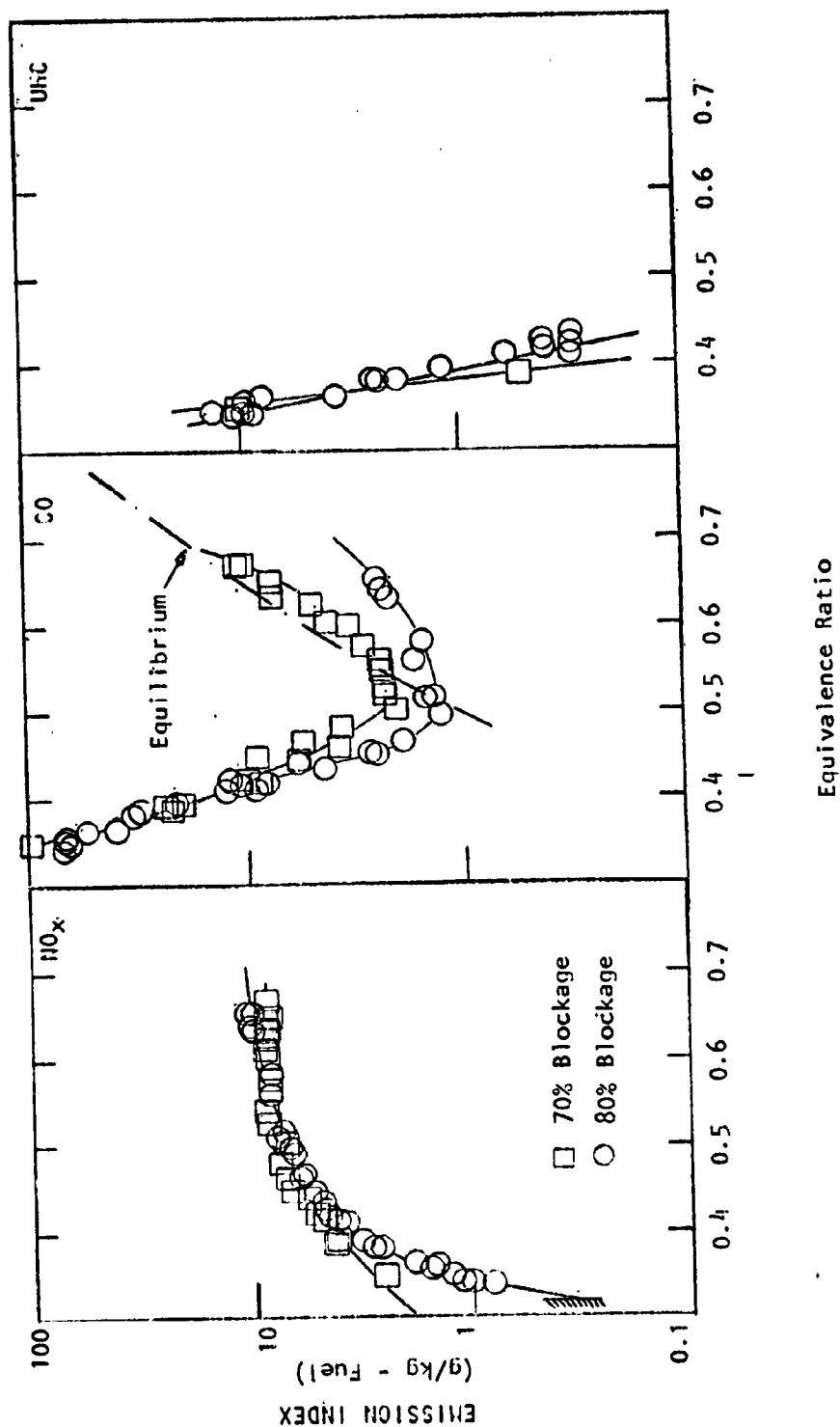
FIGURE 17. PERFORATED PLATE FLAMEHOLDER EMISSIONS (V_{ref} = 35 m/s; x = 30 cm)

Equivalence Ratio

EMISSION INDEX (g/kg - Fuel)

□ 70% Blockage
○ 80% Blockage

NO_x

CO

Equilibrium

UHC

34
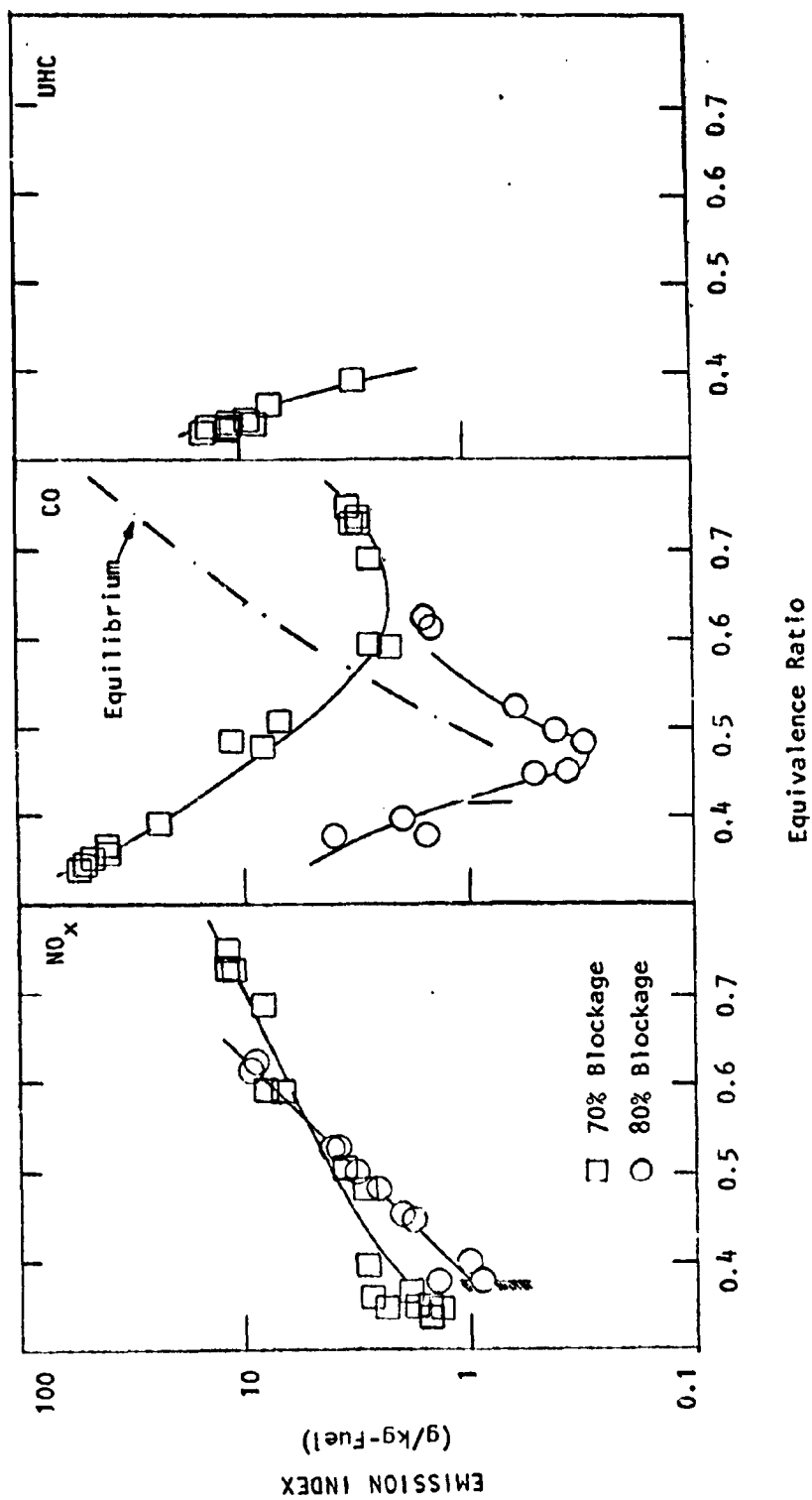
FIGURE 18. PERFORATED PLATE FLAMEHOLDER EMISSIONS (V_{ref} = 25 m/s; x = 30 cm)

35
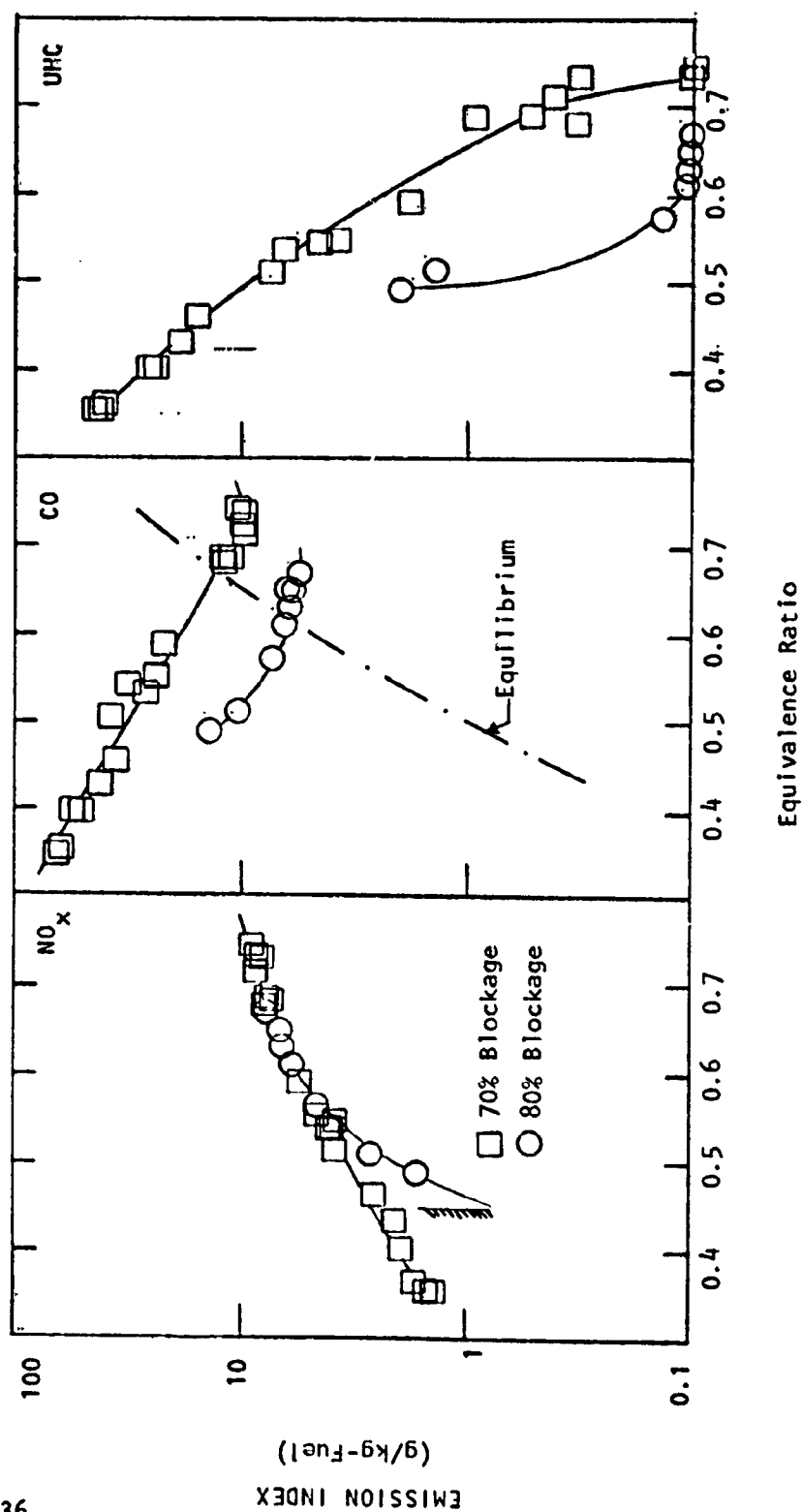
FIGURE 19. PERFORATED PLATE FLAMEHOLDER EMISSIONS ($V_{ref} = 25$ m/s; $x = 10$ cm)
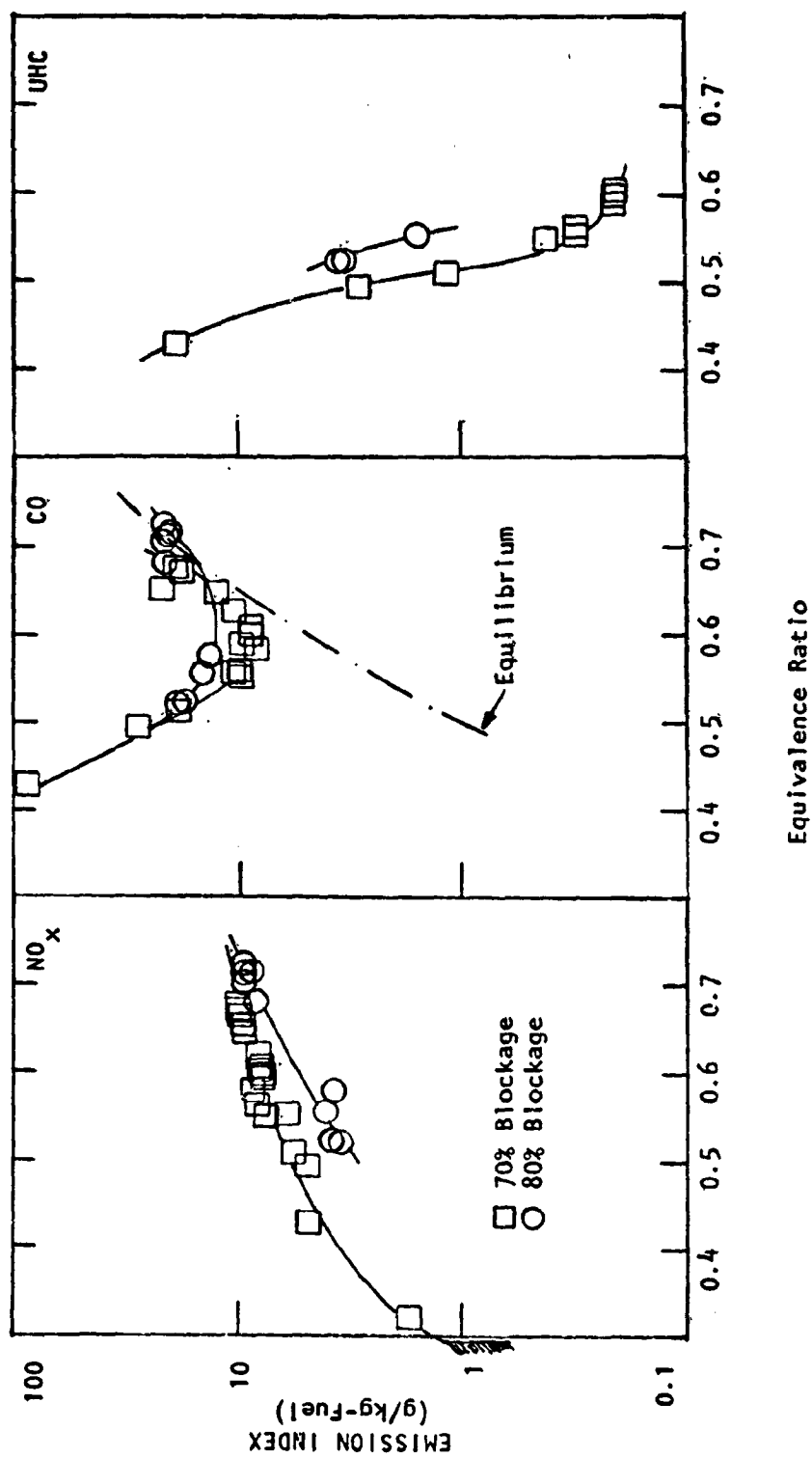
FIGURE 20. PERFORATED PLATE FLAMEHOLDER EMISSIONS (V_{ref} = 20 m/s; x = 10 cm)

37
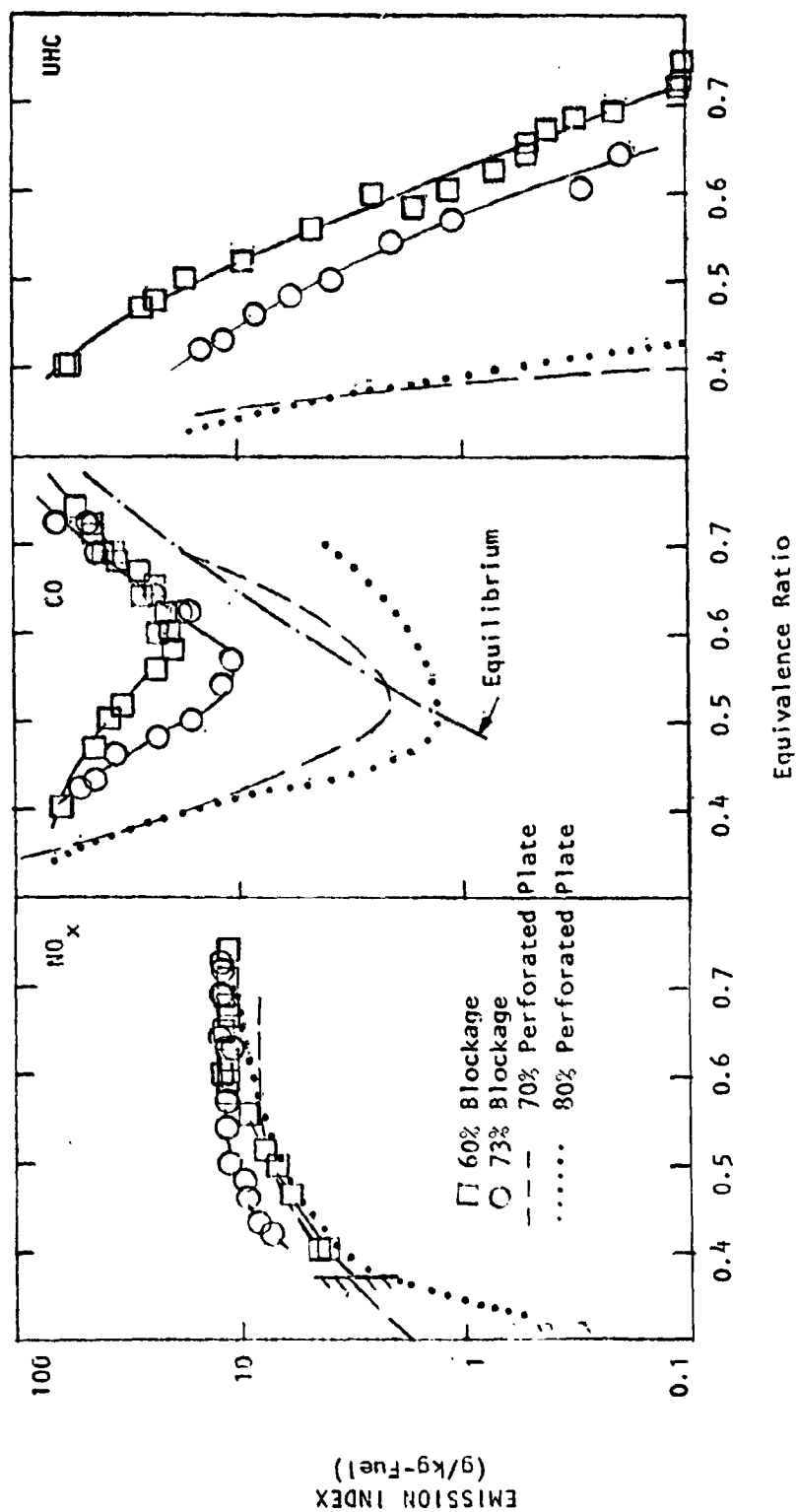
FIGURE 21. WIRE GRID FLAMEHOLDER EMISSIONS (V_{ref} = 35 m/s; x = 30 cm)

FIGURE 22. WIRE GRID FLAMEHOLDER EMISSIONS (V_{ref} = 25 m/s; x = 30 cm)
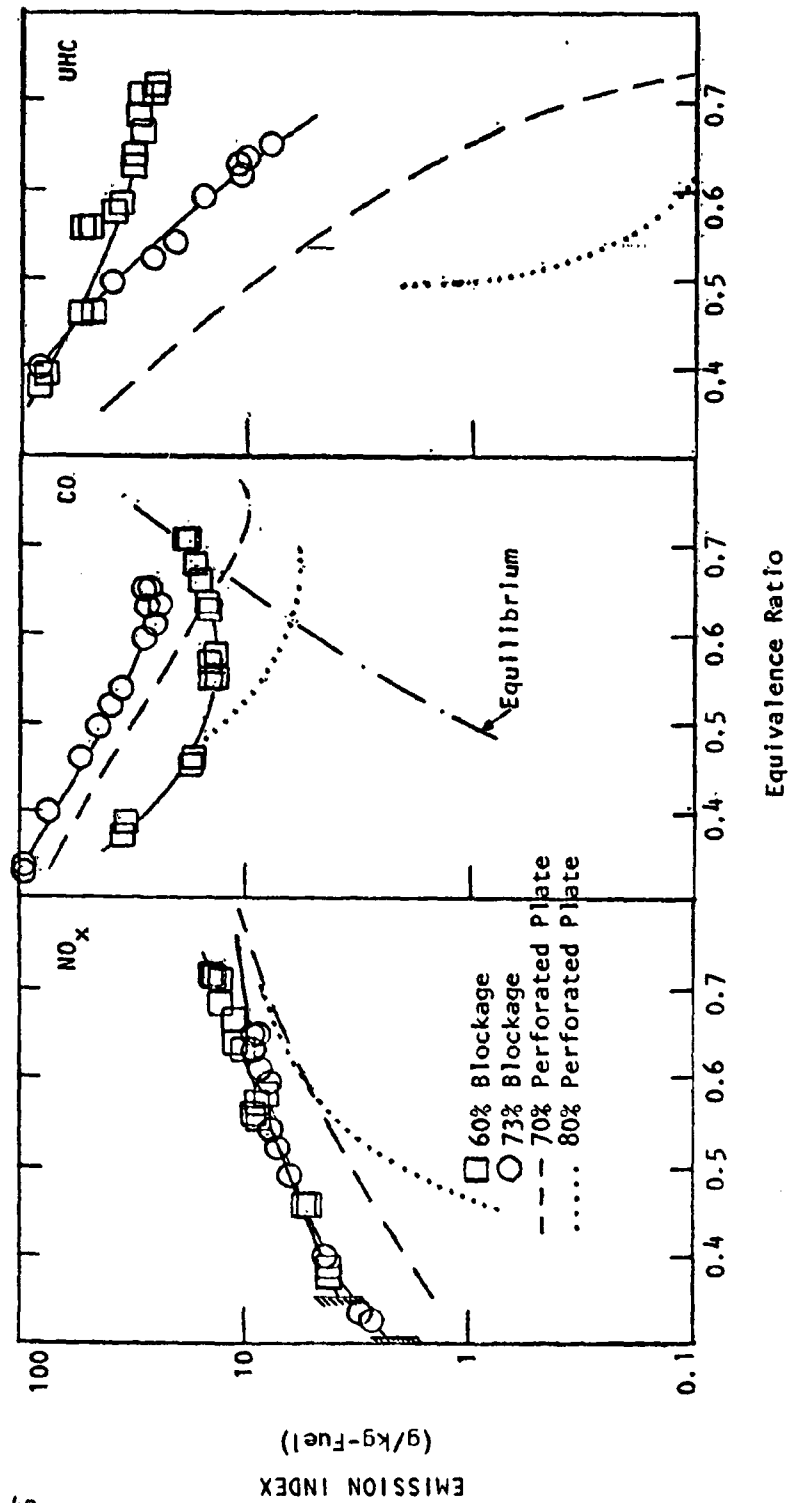
FIGURE 23. WIRE GRID FLAMEHOLDER EMISSIONS. (V_{ref} = 25 m/s; x = 10 cm)

EMISSION INDEX
(g/kg-Fuel)

Equivalence Ratio

60% Blockage
73% Blockage
70% Perforated Plate
80% Perforated Plate

NO$_x$ CO UHC

Equilibrium

40
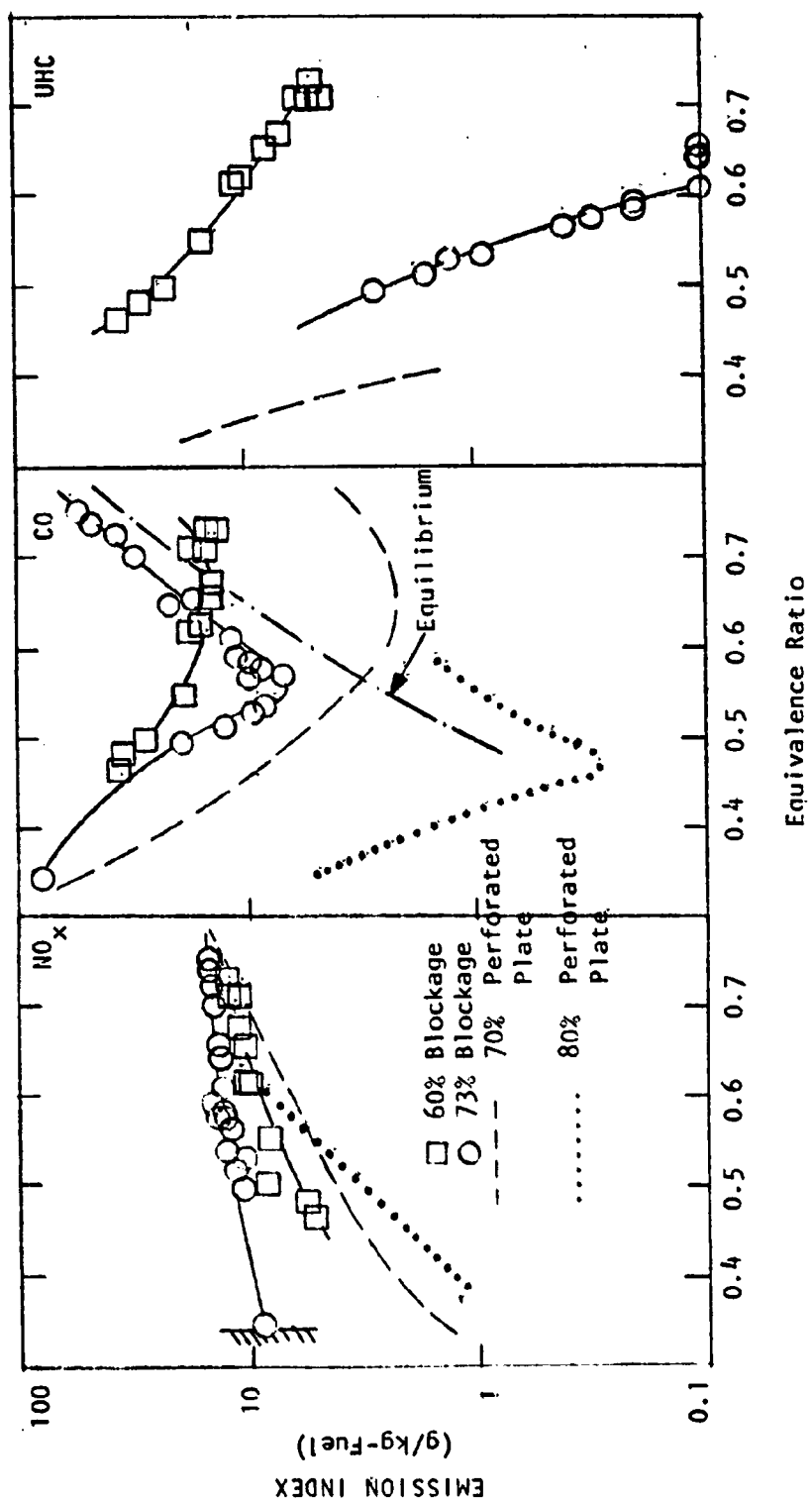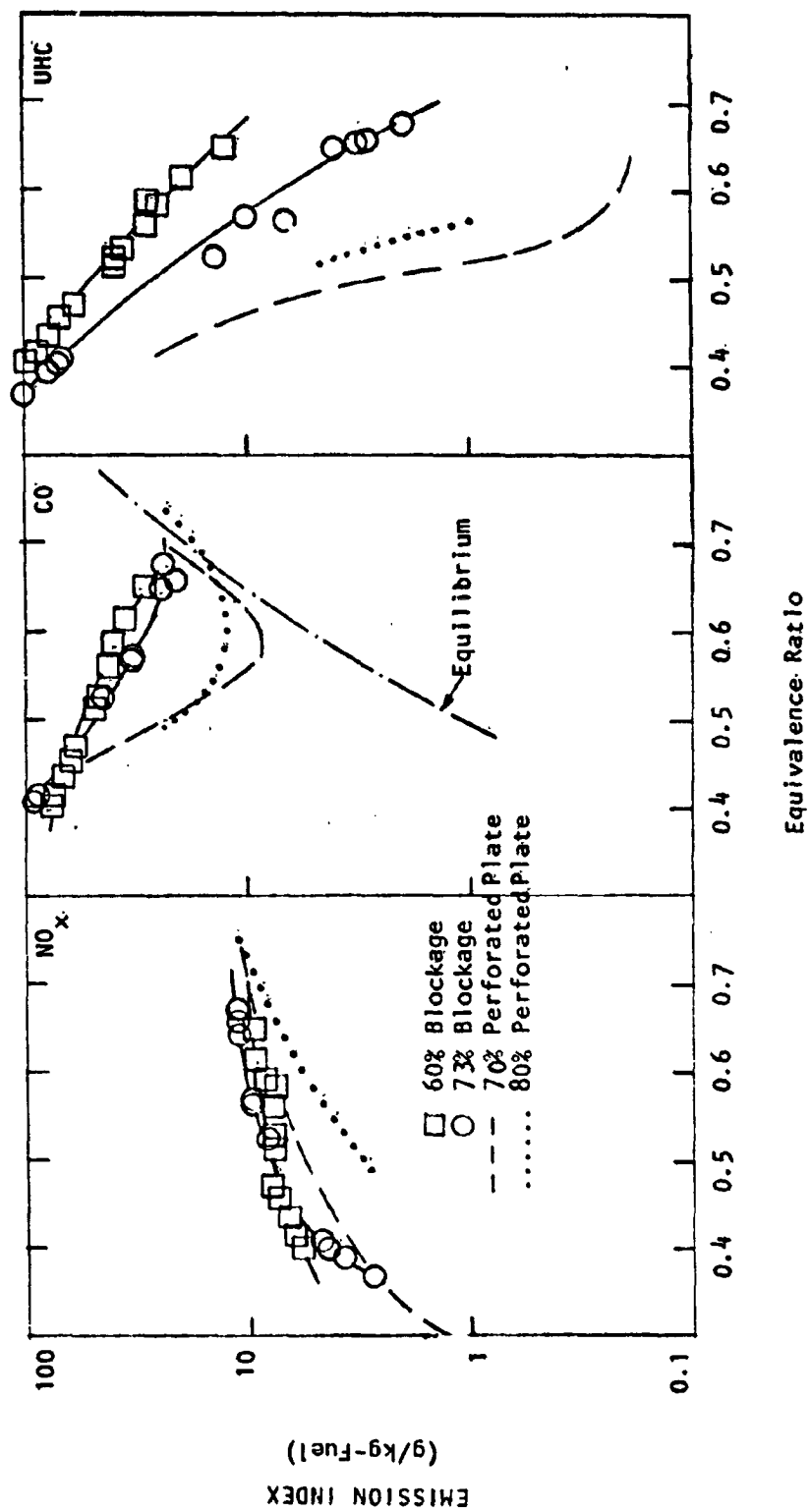
FIGURE 24. WIRE GRID FLAMEHOLDER EMISSIONS (V_{ref} = 20 m/s; x = 10 cm)

41

using the perforated plate. Lowering the reference velocity to 25 m/s again increases the sensitivity of NO_x emissions to blockage. However, contrary to the results obtained for the perforated plate designs, increasing the blockage of the wire grid flameholders increases the production of NO_x. As before, both CO and UHC emissions are reduced by increasing flameholder blockage, although emission levels are considerably higher than those for the perforated plate. It is interesting to note that the CO emissions of the 73% wire grid appear to follow the equilibrium curve for equivalence ratios above 0.55 while those of the corresponding perforated plate are considerably below equilibrium. NO_x levels observed with the wire grid flameholders at the 10 cm combustor position are insensitive to flameholder blockage but show a slight increase with lower reference velocity at low equivalence ratio. NO_x levels at higher equivalence ratios are insensitive to blockage, reference velocity, and combustor position, reaching a limiting value on the order of 10 g/kg-fuel.

The emissions measurements for the multiple cone flameholders are presented in Figures (25 through 28). This design displays increased sensitivity to blockage with significant differences existing under all test conditions. As with the perforated plate designs, increasing the blockage of the multiple cone flameholder decreases not only NO_x emissions but those of CO and UHC as well. As before, lowering the reference velocity from 35 m/s to 25 m/s increases the sensitivity of emissions to blockage. Comparing the emissions for the multiple cone designs with those of the perforated plate reveals a slight decrease in NO_x level for the higher blockage design and a moderate increase in NO_x for the lower blockage design. CO and UHC emissions performance for the multiple cone and perforated plate flameholders appears to be quite similar.

- The measured emission levels for the vee gutter flameholders are presented in Figures (29 through 32), again along with the corresponding performance of the perforated plate. At the 35 m/s reference velocity, NO_x levels are seen to be substantially lower than those obtained using the perforated plate, while CO and UHC emissions are generally comparable. As noted for earlier designs, increasing the blockage of the vee gutter results in a simultaneous decrease of NO_x, CO and UHC, although the general

42
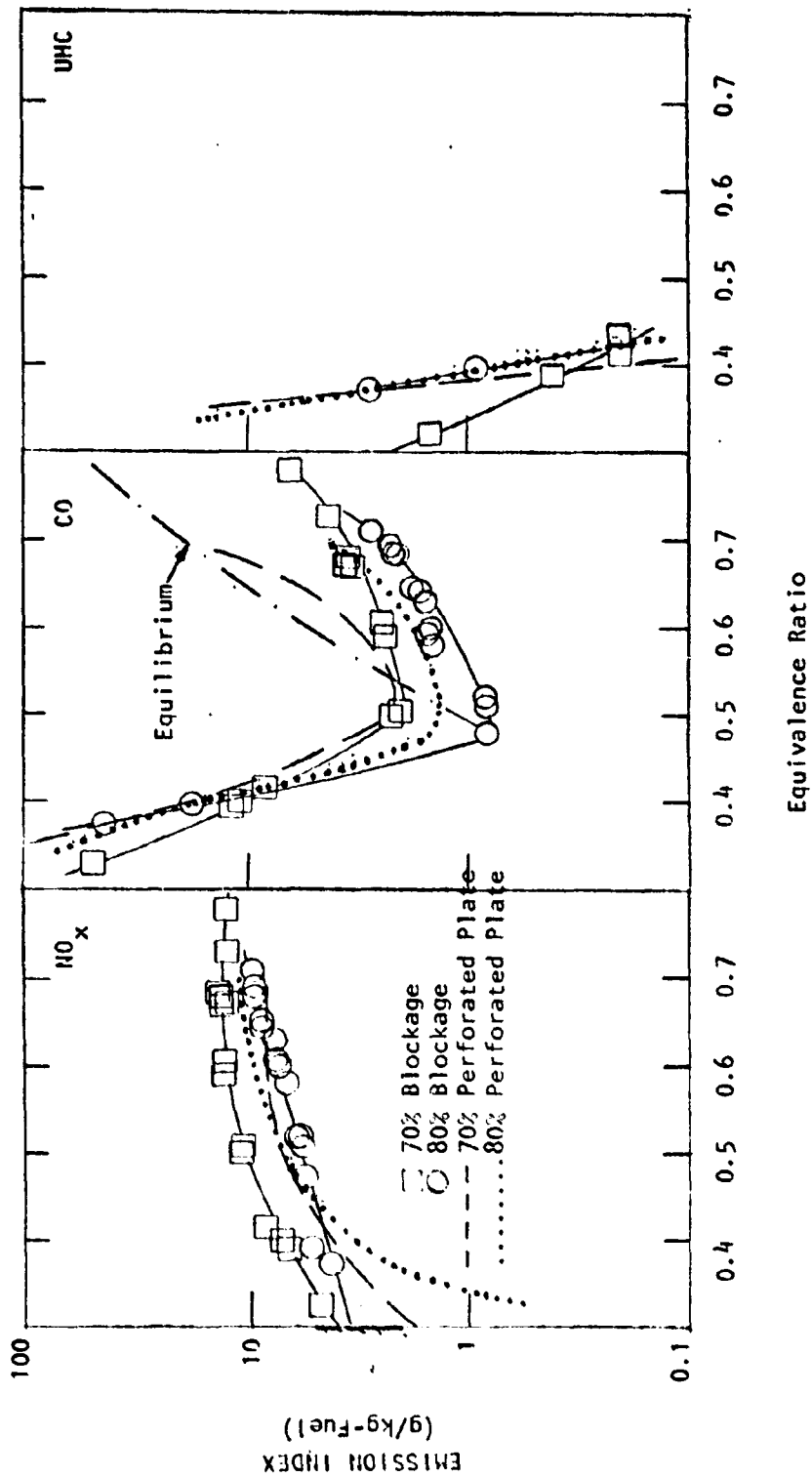
FIGURE 25. MULTIPLE CONE FLAMEHOLDER EMISSIONS (V_{ref} = 35 m/s; x = 30 cm)

43
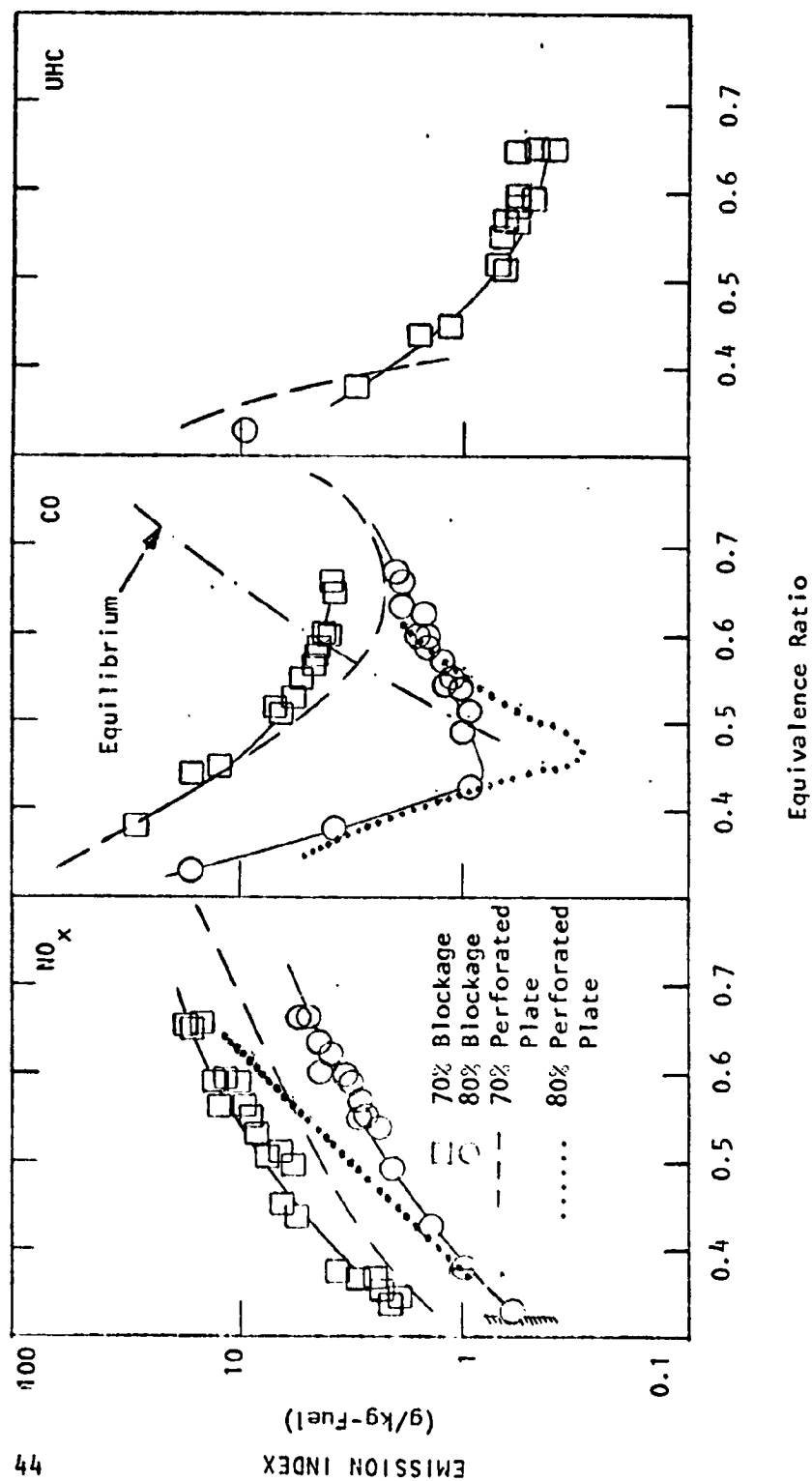
FIGURE 26. MULTIPLE CONE FLAMEHOLDER EMISSIONS (V_{ref} = 25 m/s; x = 30 cm)

44

EMISSION INDEX (g/kg-fuel)

NO_x

CO

UHC

Equivalence Ratio

Equilibrium

Equilibrium

70% Blockage
80% Blockage
70% Perforated Plate
80% Perforated Plate

100
10
1
0.1

0.4 0.5 0.6 0.7
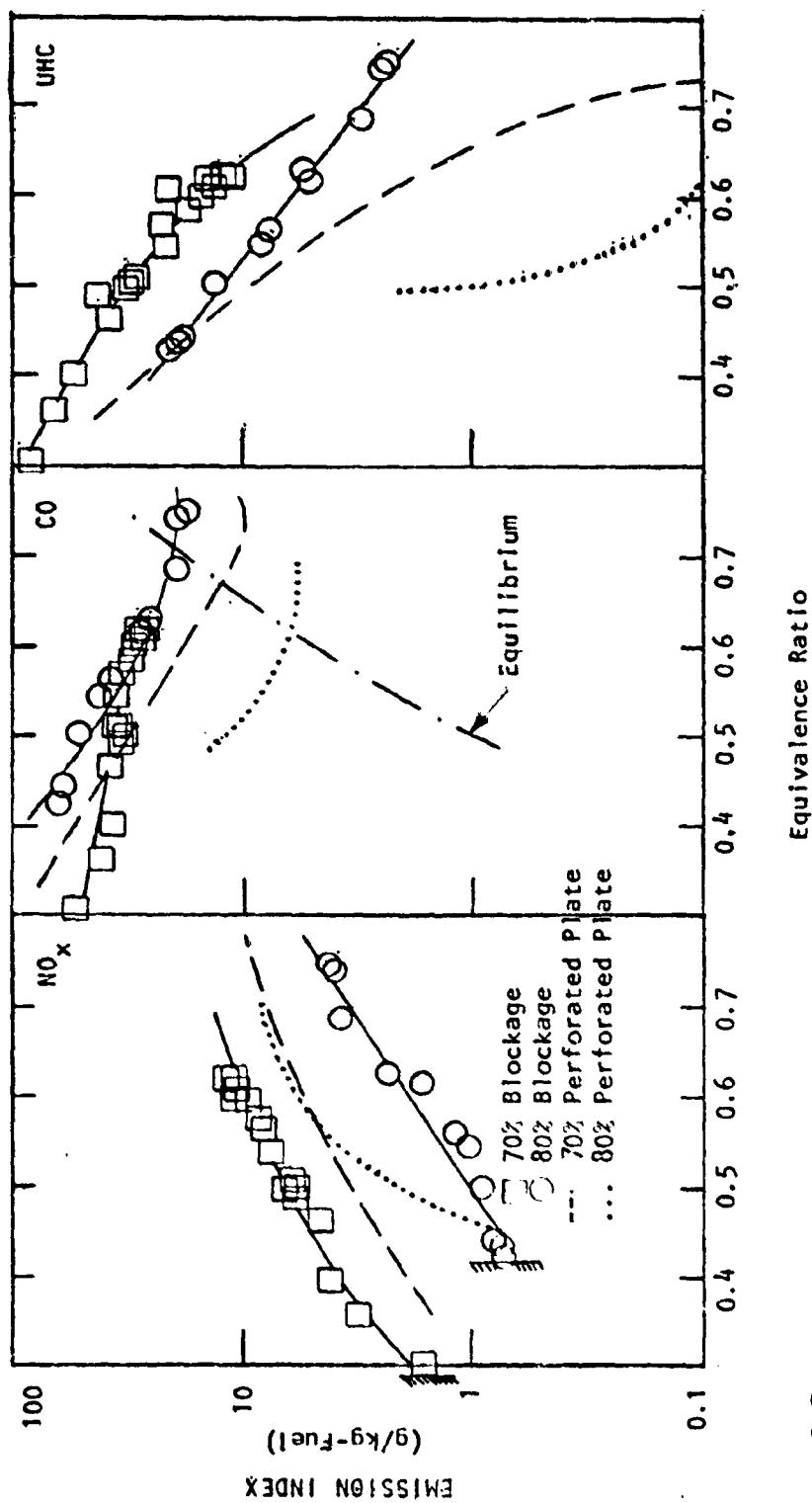
FIGURE 27. MULTIPLE CONE FLAMEHOLDER EMISSIONS (V_{ref} = 25 m/s; x = 10 cm)

45
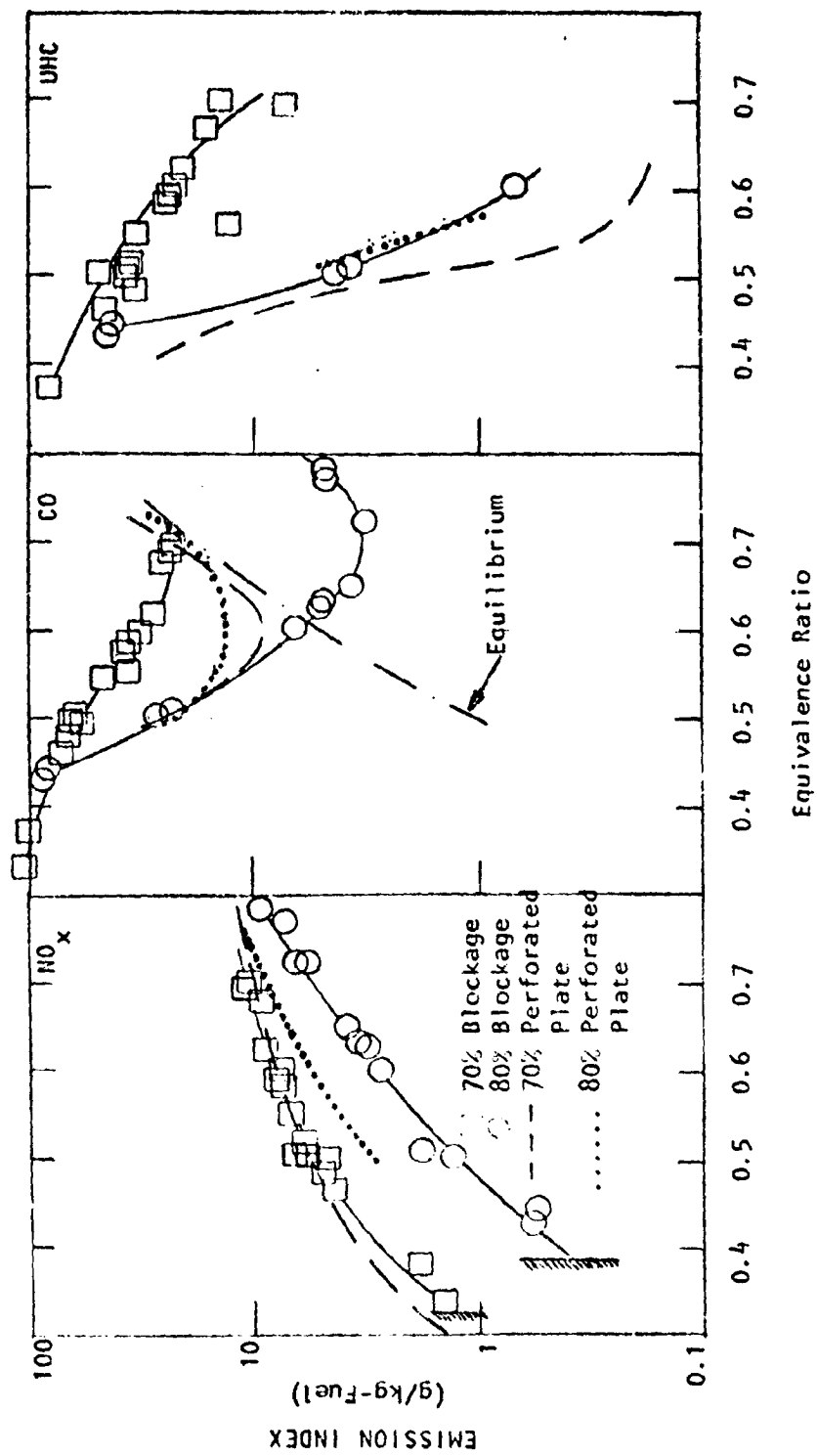
FIGURE 28.   MULTIPLE CONE FLAMEHOLDER EMISSIONS (V_{ref} = 20 m/s;   x = 10 cm)

46

FIGURE 29. VEE GUTTER FLAMEHOLDER EMISSIONS (V_{ref} = 25 m/s; x = 30 cm)

FIGURE 30. VEE GUTTER FLAMEHOLDER EMISSIONS (V_{ref} = 25 m/s; x = 30 cm)

FIGURE 31. VEE GUTTER FLAMEHOLDER EMISSIONS ($V_{ref} = 25$ m/s; $x = 10$ cm)

EMISSION INDEX
(g/kg - Fuel)

49
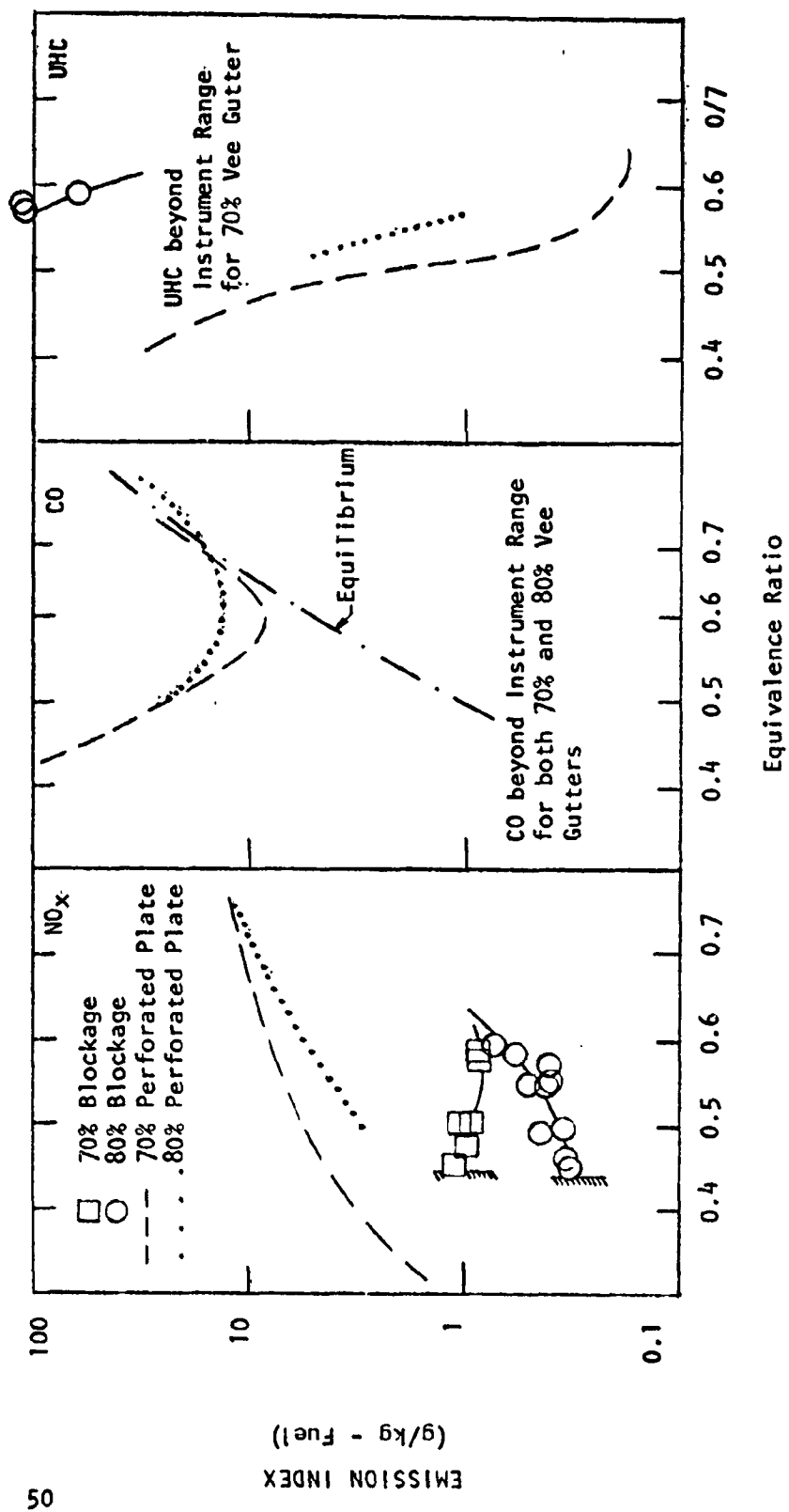
FIGURE 32. VEE GUTTER FLAMEHOLDER EMISSIONS (V_{ref} = 20 m/s; x = 10 cm)

EMISSION INDEX
(g/kg - Fuel)

50

level of NO_x sensitivity is not great. When the reference velocity is lowered to 25 m/s, the rather striking decrease in NO_x level noted at the higher velocity is substantially reduced while CO and UHC levels are still similar to those of the perforated plate. Again, CO and UHC emissions demonstrate considerably greater sensitivity to flameholder blockage than does NO_x with increased blockage producing substantial reductions in CO and UHC levels. Emissions measurements at the 10 cm combustor location indicate a very small degree of reaction with NO_x levels very low and CO and UHC emissions so high as to be beyond the range of the instruments. These results are indication that flame propagation has not been completed by the 10 cm station, a result which is not entirely surprising in light of the fact that the ignition width (see Table 1) of the vee gutter flameholder is three times larger than that of any other design.

The emissions measurements for the single cone flameholders are presented in Figures (33 through 36). At the 35 m/s reference velocity, NO_x levels are slightly higher than those observed for the perforated plate flameholder, while CO and UHC emissions are considerably increased. At the 25 m/s reference velocity, NO_x, CO and UHC emissions are all considerably reduced. Here, NO_x and CO emissions for the 70% single cone and 70% perforated plate are nearly identical, while UHC levels for the single cone are higher than those for the perforated plate. NO_x levels for the 80% blockage cone are lower than those observed for the perforated plate. At low equivalence ratio, CO and UHC emissions for the high blockage cone are somewhat higher than those of the perforated plate but these differences disappear as the equivalence ratio increases. At the 10 cm combustor location, measured levels of NO_x, CO and UHC species display greater sensitivity to blockage for the single cone than they do for the perforated plate. Of particular interest is that while both CO and UHC levels are considerably higher at the 10 cm position than they are at the 30 cm position, NO_x levels are nearly the same at the two locations. This is very likely the result of high NO_x levels in the large recirculation region and high CO and UHC levels in the outer flow close to the flameholder. NO_x and UHC levels measured at the 10 cm location at 25 m/s reference velocity both decrease as cone blockage increases from 70% to 80%. CO levels are higher for the higher blockage cone at low equivalence ratio but do not

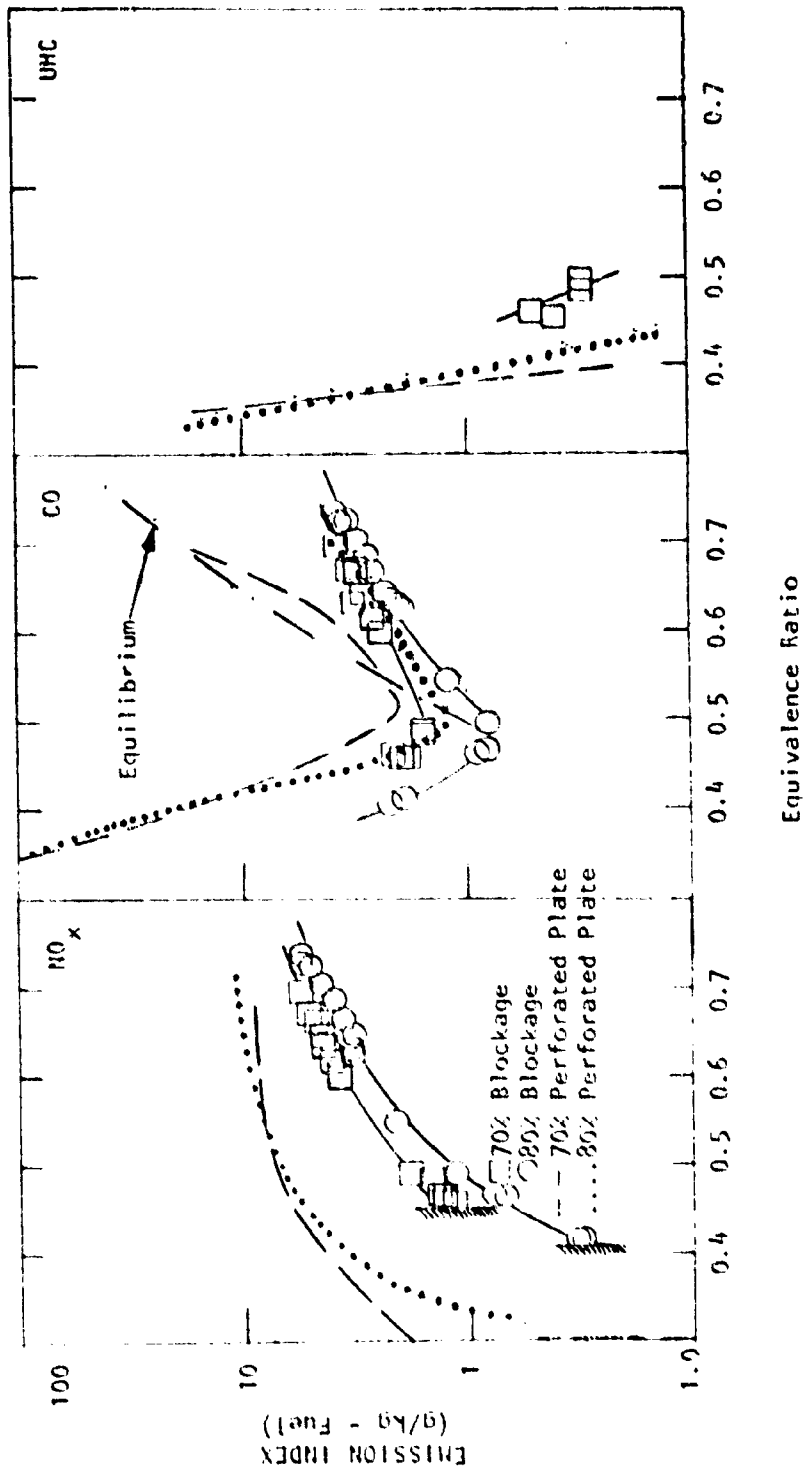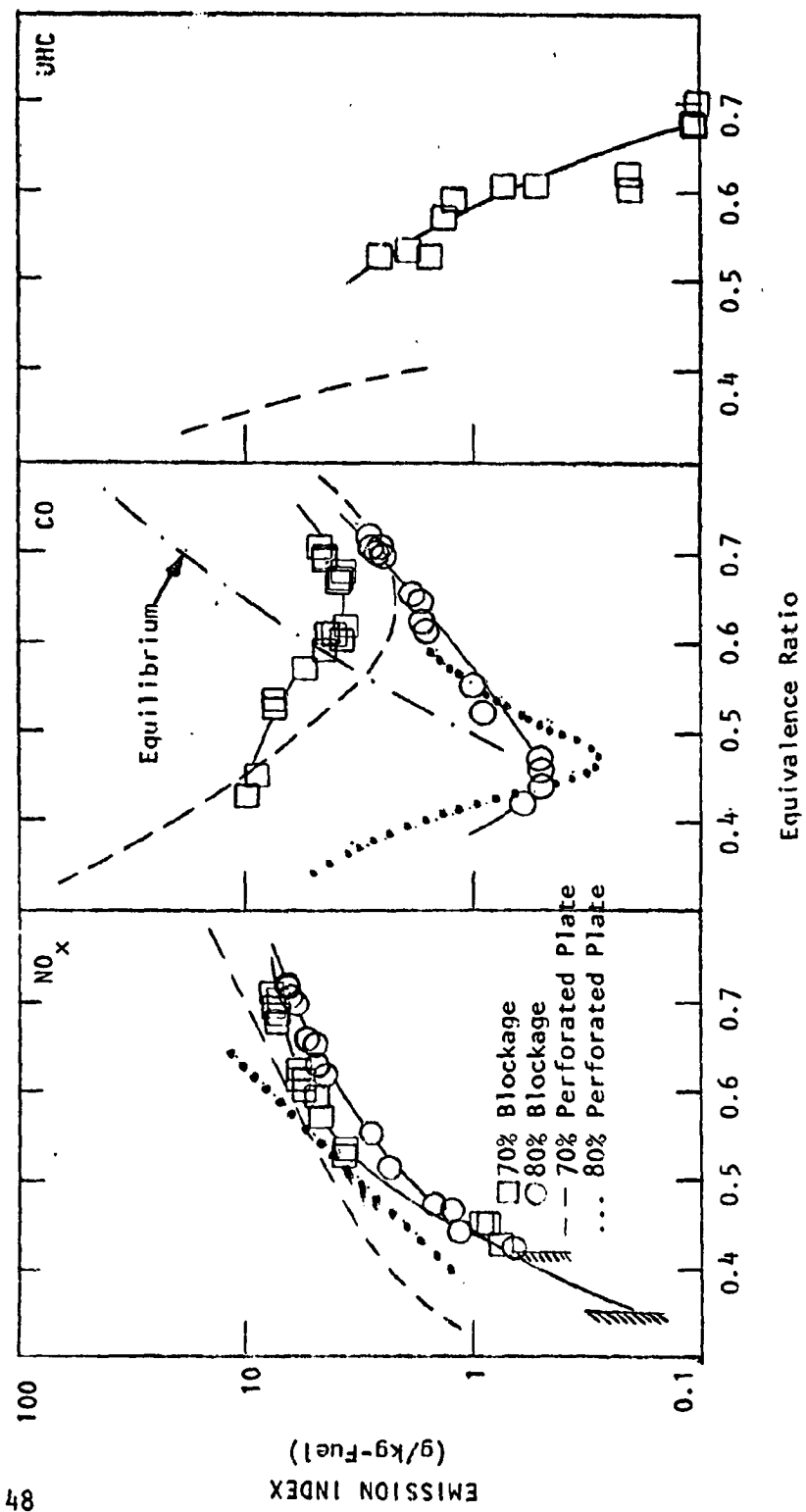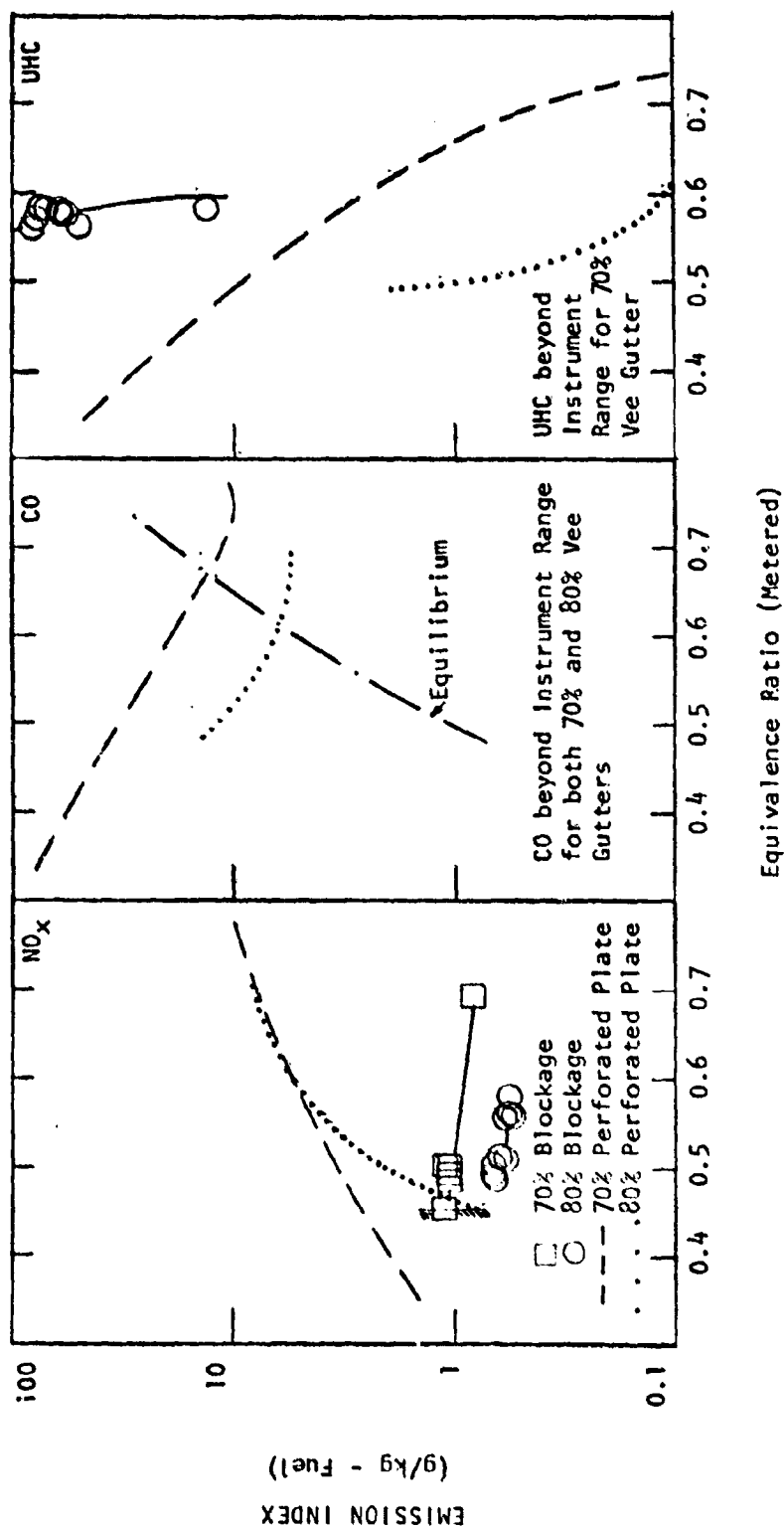FIGURE 33. SINGLE CONE FLAMEHOLDER EMISSIONS (V_{ref} = 35 m/s; x = 30 cm)

52
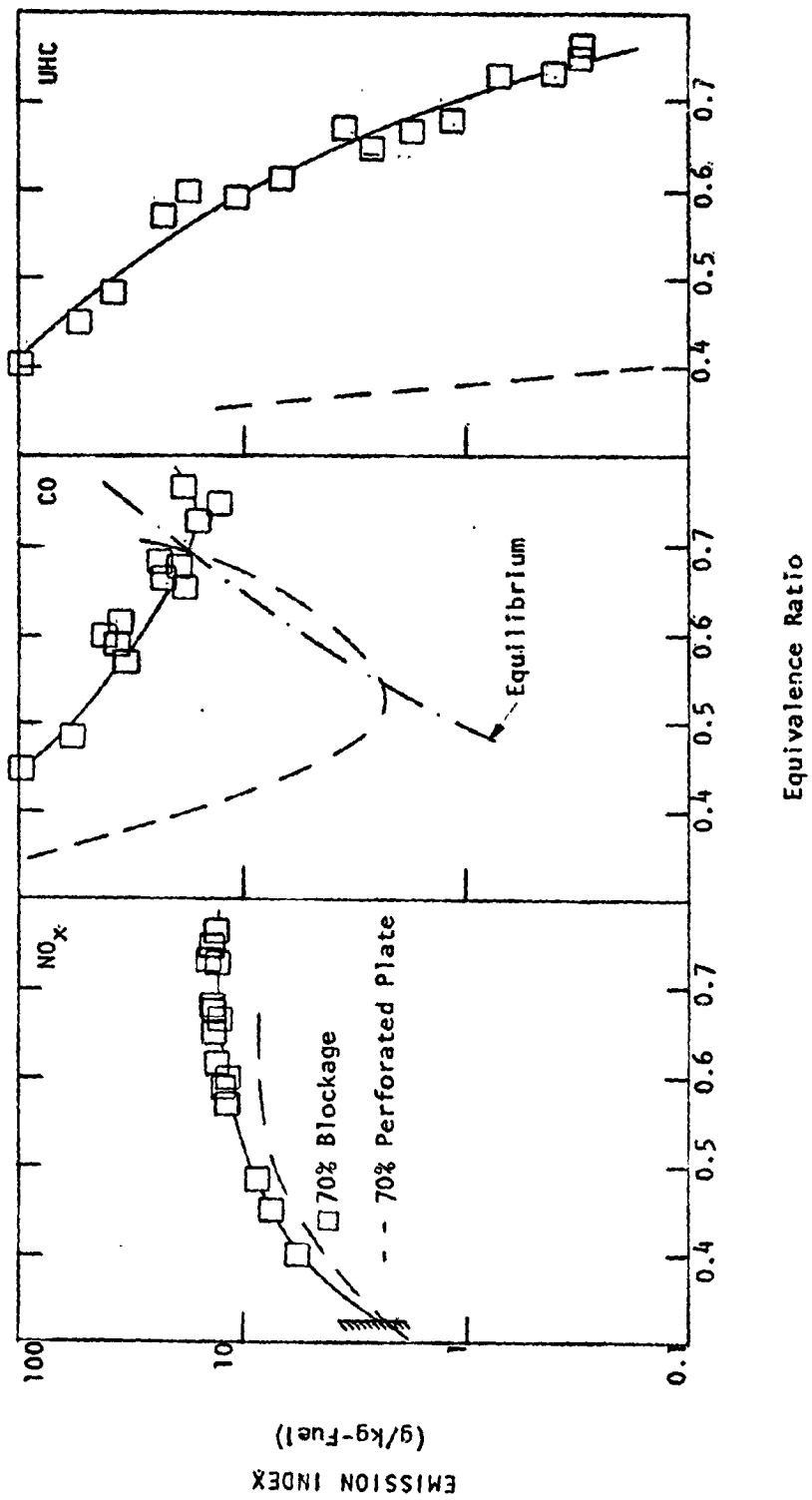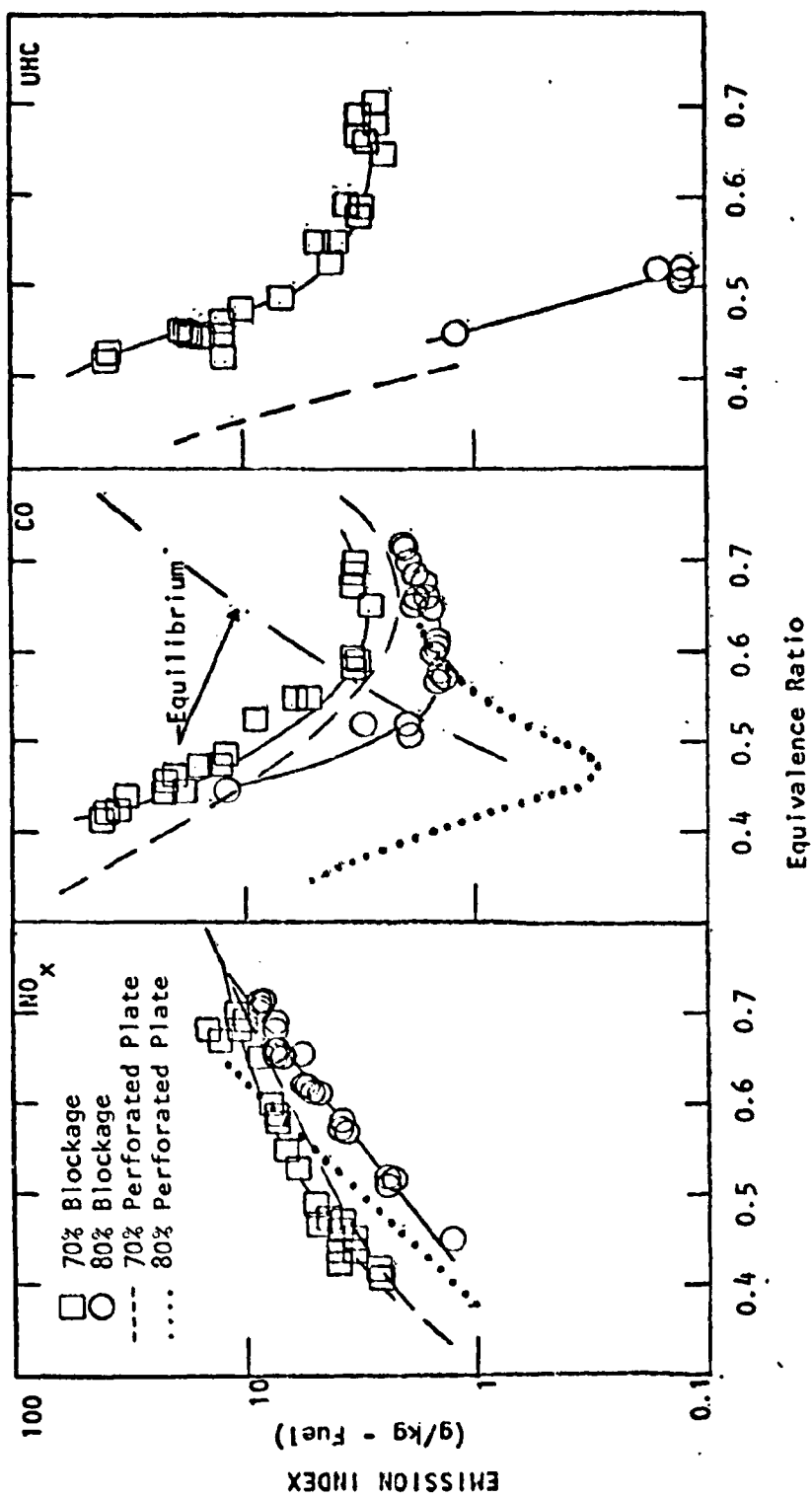
FIGURE 34. SINGLE CONE FLAMEHOLDER EMISSIONS (V_{ref} = 25 m/sec; x = 30 cm)

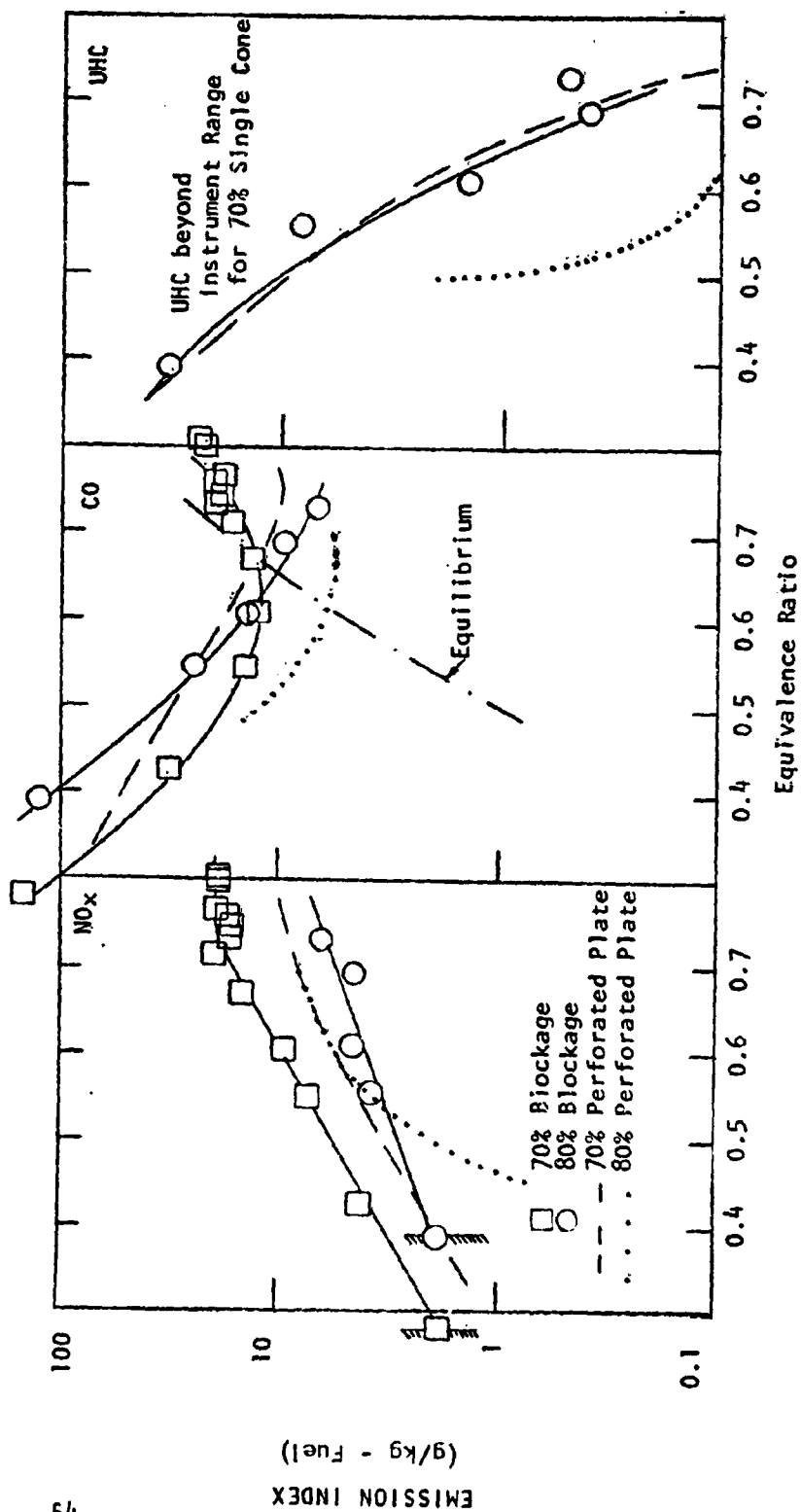FIGURE 35. SINGLE CONE FLAMEHOLDER EMISSIONS ($V_{ref} = 25$ m/s; $x = 10$ cm)
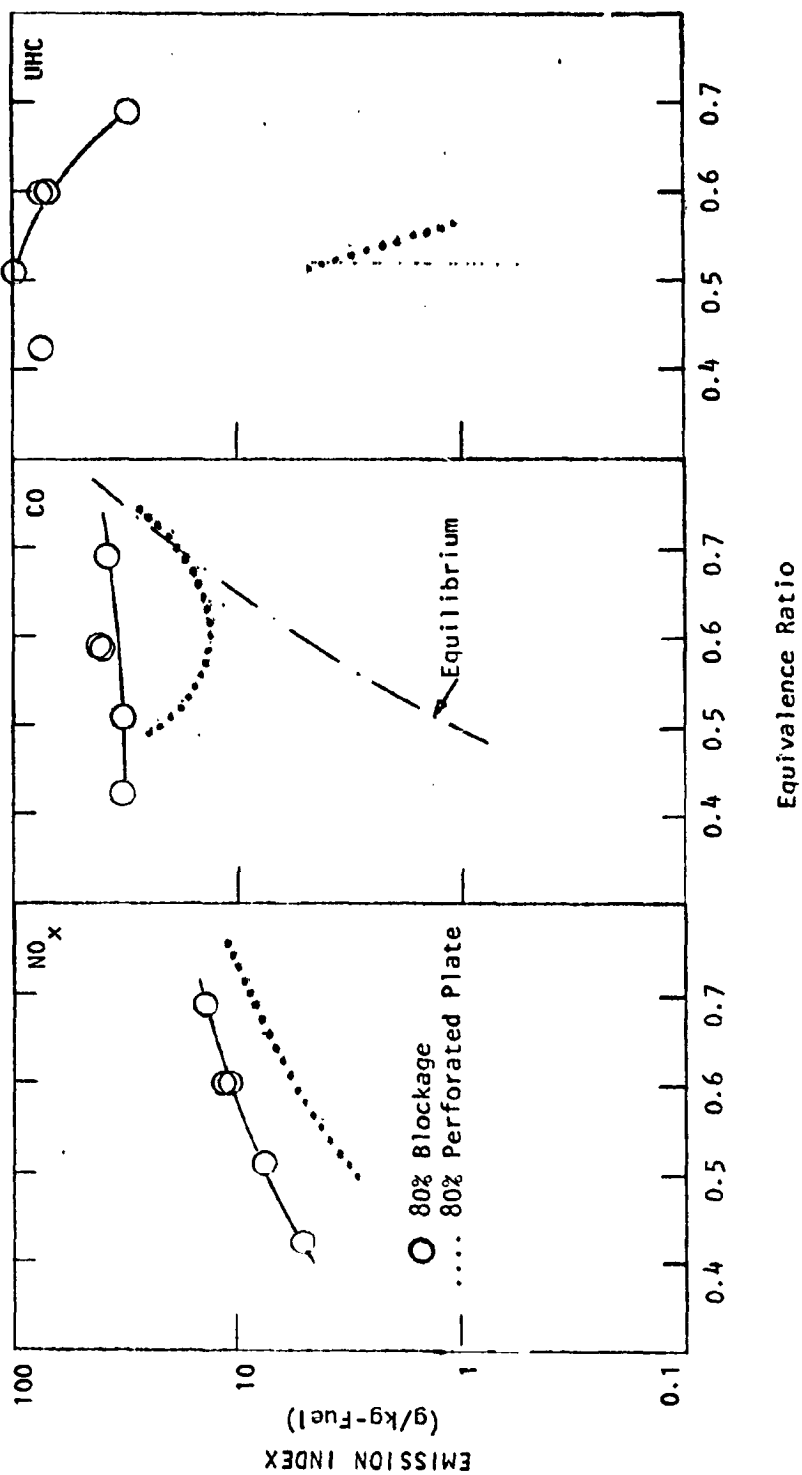
54

EMISSION INDEX
(g/kg - Fuel)

FIGURE 36.   SINGLE CONE FLAMEHOLDER EMISSIONS (V_{ref} = 20 m/s; x = 10 cm)

55

appear to approach equilibrium as rapidly at high equivalence ratio.

The emissions measurements for the swirl flameholders are presented in Figures (37 through 40). The results obtained at a reference velocity of 35 m/s with the 40° swirl flameholder (73% blockage) are particularly interesting in that NO_x levels are considerably lower than those obtained using any of the previous flameholder designs, displaying unusually low sensitivity to equivalence ratio at the low end of its operating range. It is significant that CO and UHC emissions for this design are also quite low, comparing favorably with those of the perforated plate. At low equivalence ratio, NO_x emission levels for the 50° swirl design are lower than those for the perforated plate. However, there is a corresponding increase in CO and UHC levels indicating that the lower NO_x emissions are simply reflecting lower combustion efficiency. At the 25 m/s reference velocity, the behavior of the 40° and 50° swirl flameholders are quite similar, producing higher levels of NO_x, CO and UHC than the perforated plate. The emissions measurements taken at the 10 cm combustor location using the swirl flameholders are interesting in that this sampling position undoubtedly encompasses a portion of the recirculating base flow. Here, although CO and UHC levels are considerably increased (as compared with the perforated plate), NO_x levels are generally comparable.

The emissions of the various flameholder designs are compared at the four combinations of operating condition/rake position in Figures (41 through 44), which summarize the results for the higher blockage series, and Figures (45 through 48), which summarize the results for the lower blockage series.

Lean Stability Limit

The lean stability limit observations for the twelve flameholders at reference velocities of 20, 25 and 35 m/s are summarized in Table IV. The lean limit phenomenon displayed a degree of intermittency with successive runs at nominally identical operating conditions often producing different blowout points. In most cases, the variation of blowout equivalence ratio

56
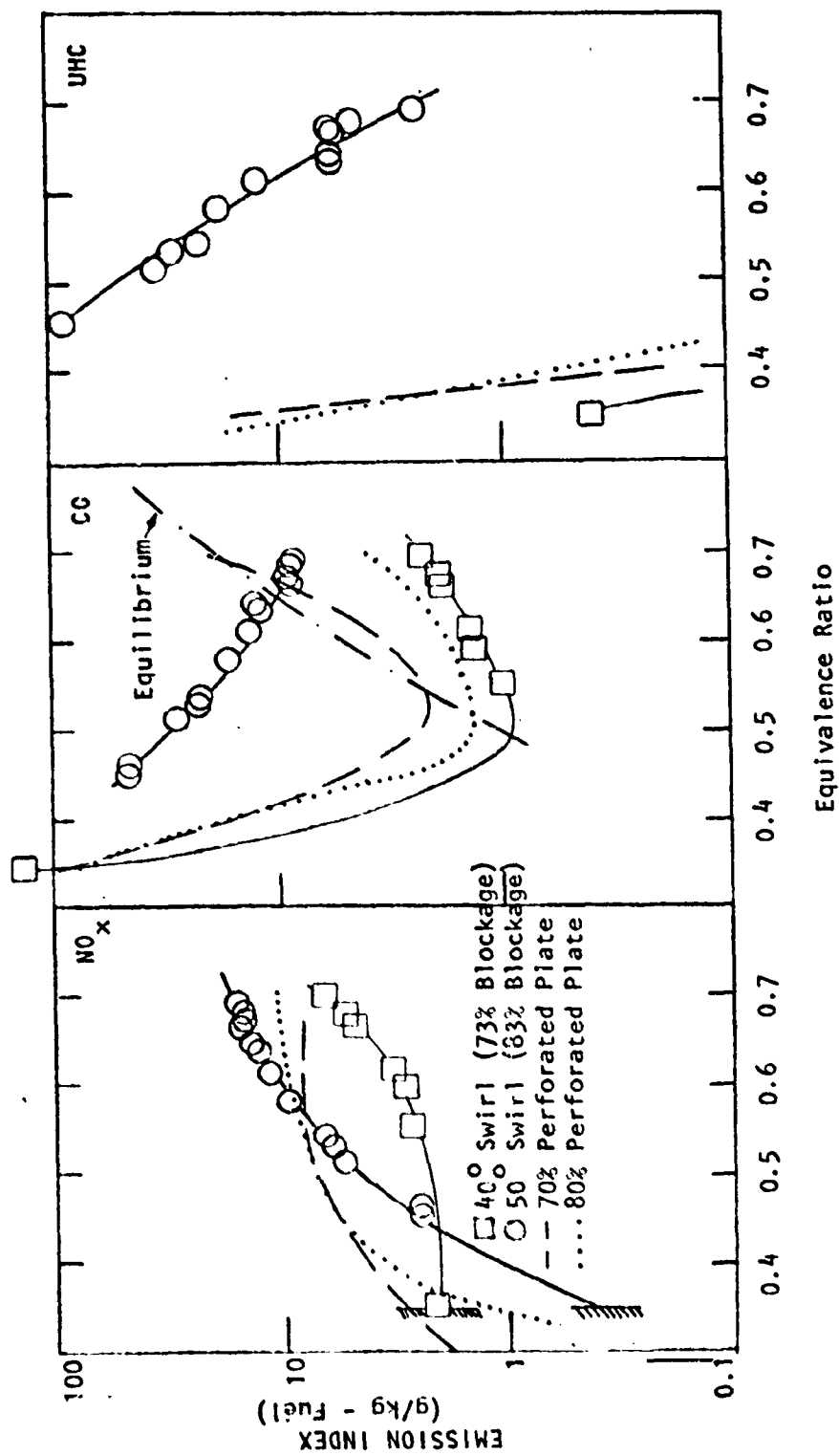
FIGURE 37. SWIRL FLAMEHOLDER EMISSIONS (V_{ref} = 35 m/s; x = 30 cm)
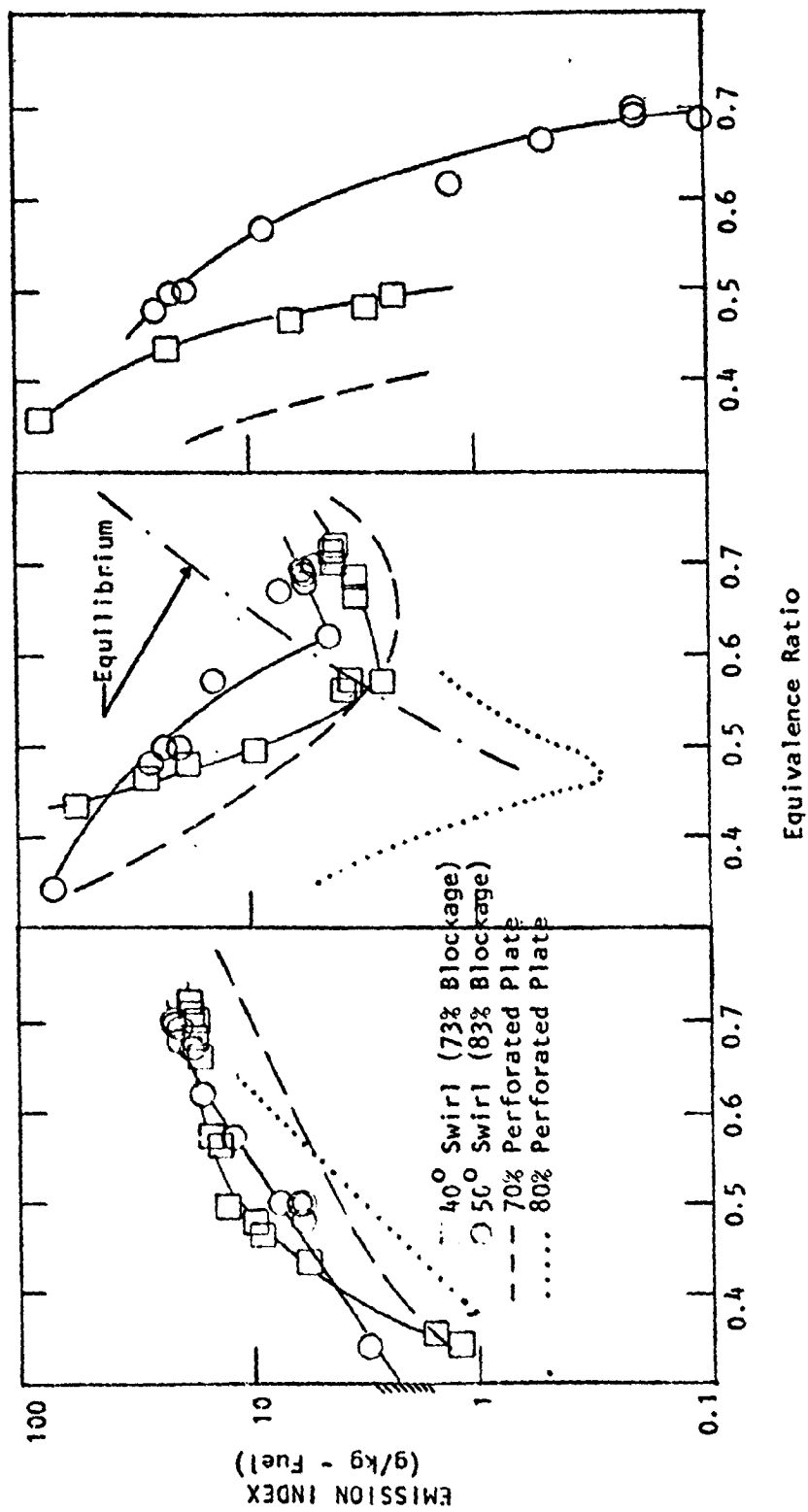
FIGURE 38. SWIRL FLAMEHOLDER EMISSIONS (V_{ref} = 25 m/s; x = 30 cm)

Legend:
— 40° Swirl (73% Blockage)
○ 50° Swirl (83% Blockage)
— — 70% Perforated Plate
······ 80% Perforated Plate

EMISSION INDEX (g/kg – Fuel)

Equivalence Ratio

Equilibrium

58
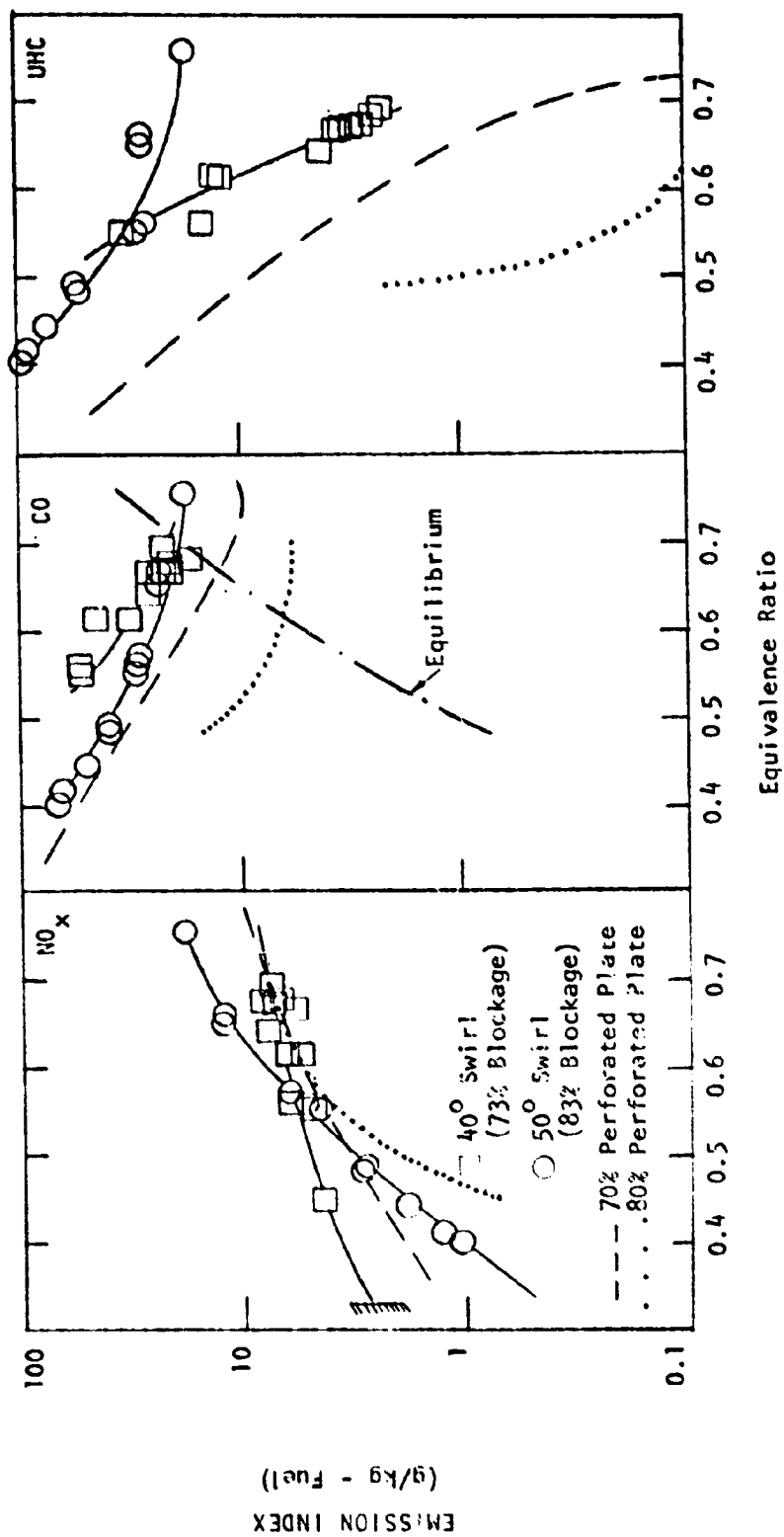
FIGURE 39. SWIRL CONE FLAMEHOLDER EMISSIONS (V_{ref} = 25 m/s; x = 10 cm)
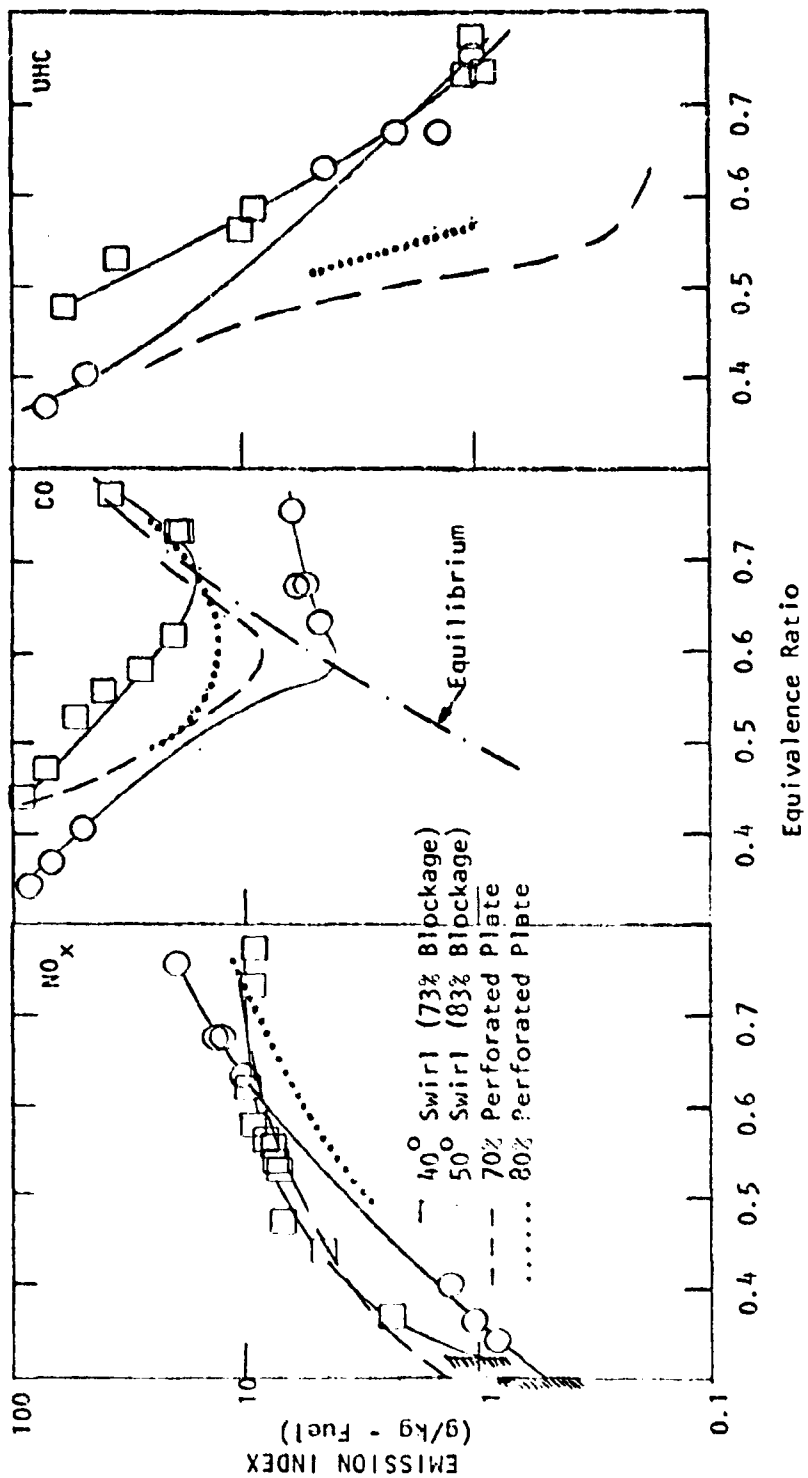
FIGURE 40. SWIRL FLAMEHOLDER EMISSIONS (V_{ref} = 20 m/s; x = 10 cm)

FIGURE 41. COMPARISON OF EMISSION LEVELS FOR HIGH BLOCKAGE FLAMEHOLDERS (V_{ref} = 35 m/s; x = 30 cm)

Legend:

WG - Wire Grid(73%)
VG - Vee Gutter (80%)
MC - Multiple Cone (80%)
SW - Swirl (50° Swirl; 83%)
PP - Perforated Plate (80%)

EMISSION INDEX
(g/kg-Fuel)

61

FIGURE 42. COMPARISON OF EMISSION LEVELS FOR HIGH BLOCKAGE FLAMEHOLDERS
(V_{ref} = 25 m/s; x = 30 cm)
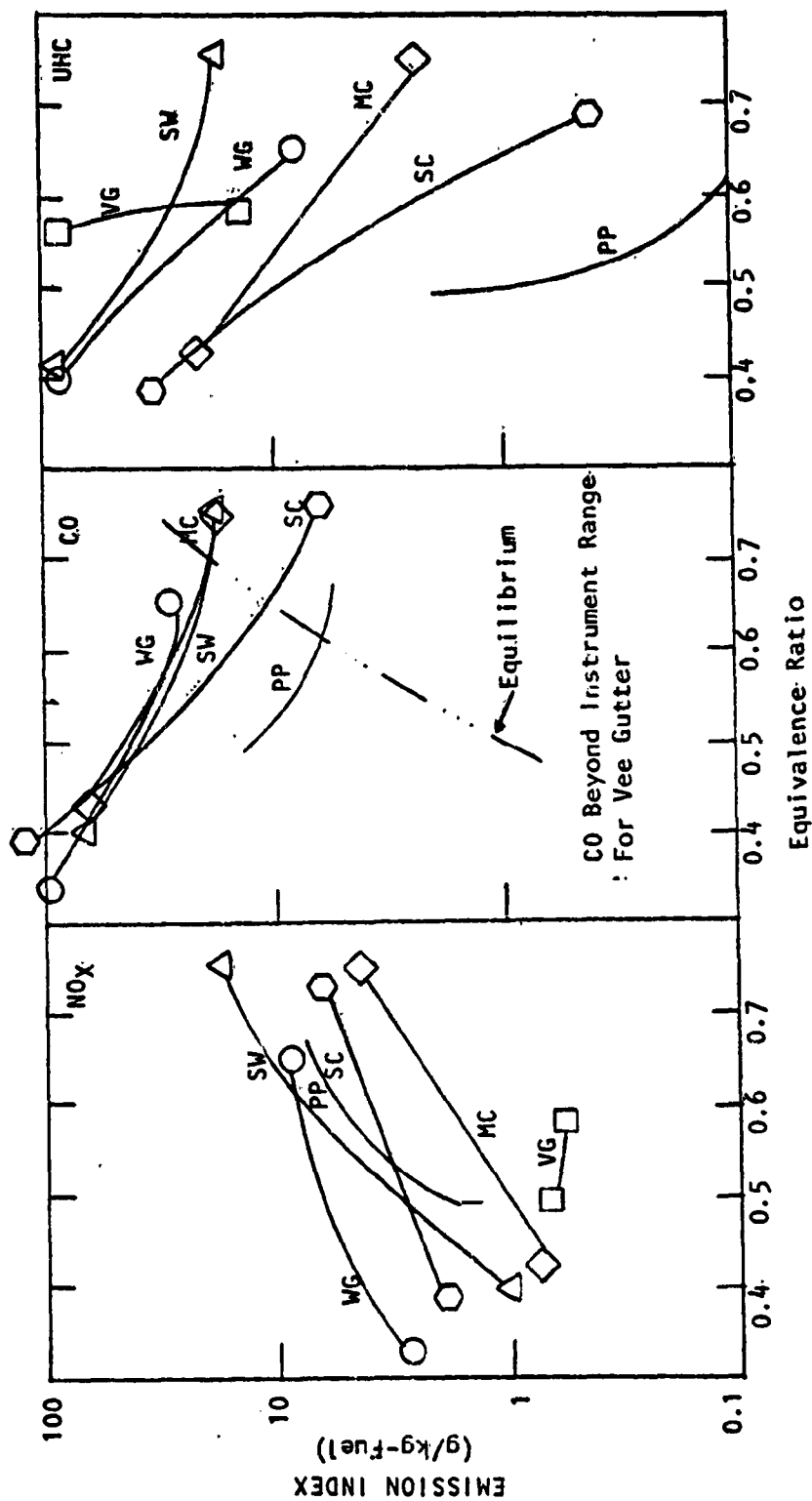
Legend:
WG – Wire Grid (73%)
VG – Vee Gutter (80%)
MC – Multiple Cone (80%)
SW – Swirl (50° Swirl, 83%)
SC – Single Cone (80%)
PP – Perforated Plate (80%)

FIGURE 43. COMPARISON OF EMISSION LEVELS FOR HIGH BLOCKAGE FLAMEHOLDER
(V_{ref}=25 m/s; x = 10 cm)

Legend:

WG. - Wire Grid (73%)
VG - Vee Gutter (80%)
MC - Multiple Cone (80%)
SW - Swirl (50° Swirl; 83%)
SC - Single Cone (80%)
PP - Perforated Plate (80%)

FIGURE 44. COMPARISON OF EMISSION LEVELS FOR HIGH BLOCKAGE FLAMEHOLDERS ($V_{ref} \approx 20$ m/s; $x = 10$ cm)

Legend:

WG – Wire Grid (73%)
VG – Vee Gutter (80%)
MC – Multiple Cone (80%)
SW – Swirl (50° Swirl; 83%)
SC – Single Cone (80%)
PP – Perforated Plate (80%)

64
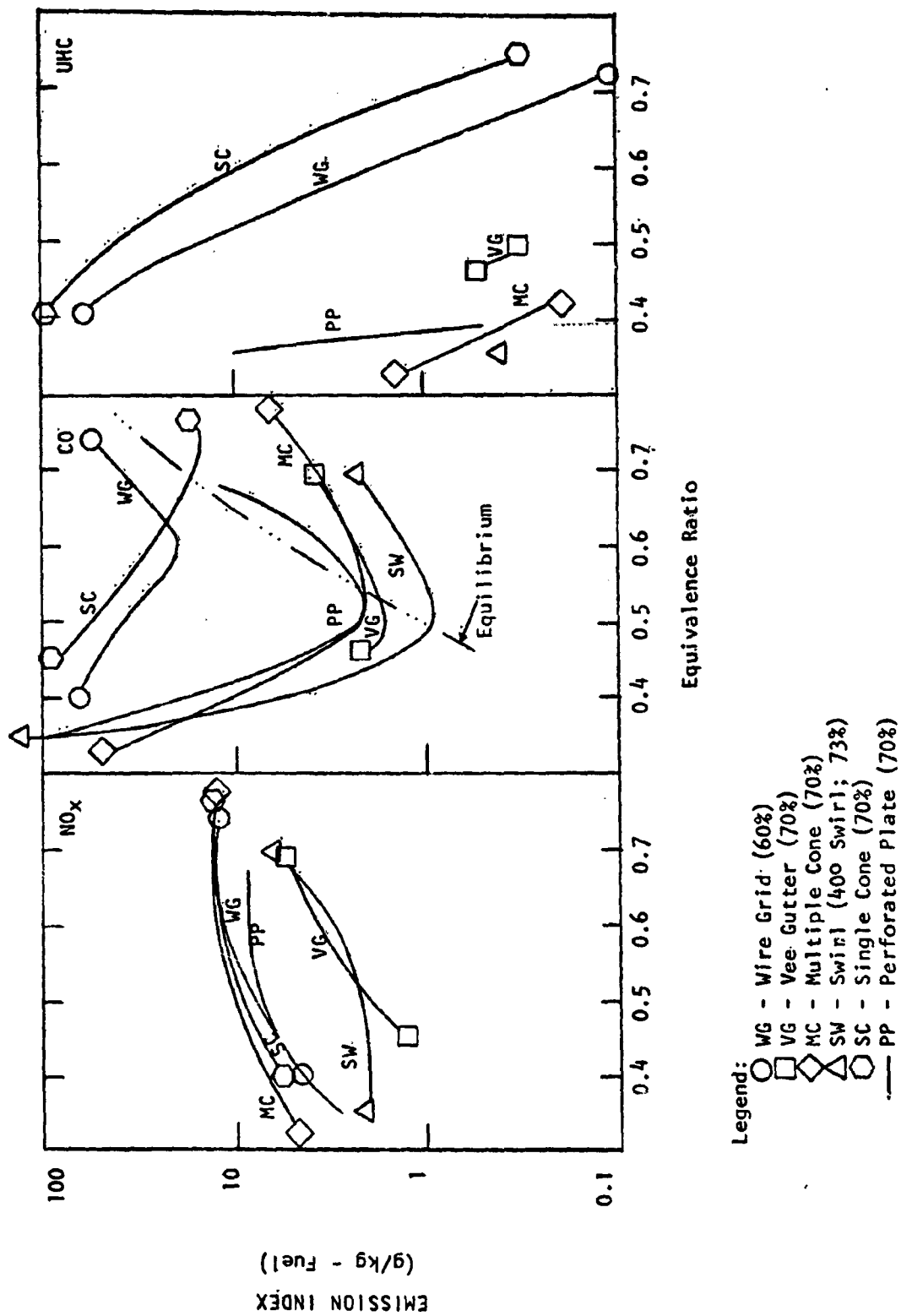
FIGURE 45. COMPARISON OF EMISSION LEVELS FOR LOW BLOCKAGE FLAMEHOLDER (V_{ref} = 35 m/s; x = 30 cm)

Legend:
WG - Wire Grid (60%)
VG - Vee Gutter (70%)
MC - Multiple Cone (70%)
SW - Swirl (40° Swirl; 73%)
SC - Single Cone (70%)
PP - Perforated Plate (70%)

EMISSION INDEX
(g/kg - Fuel)

Equivalence Ratio
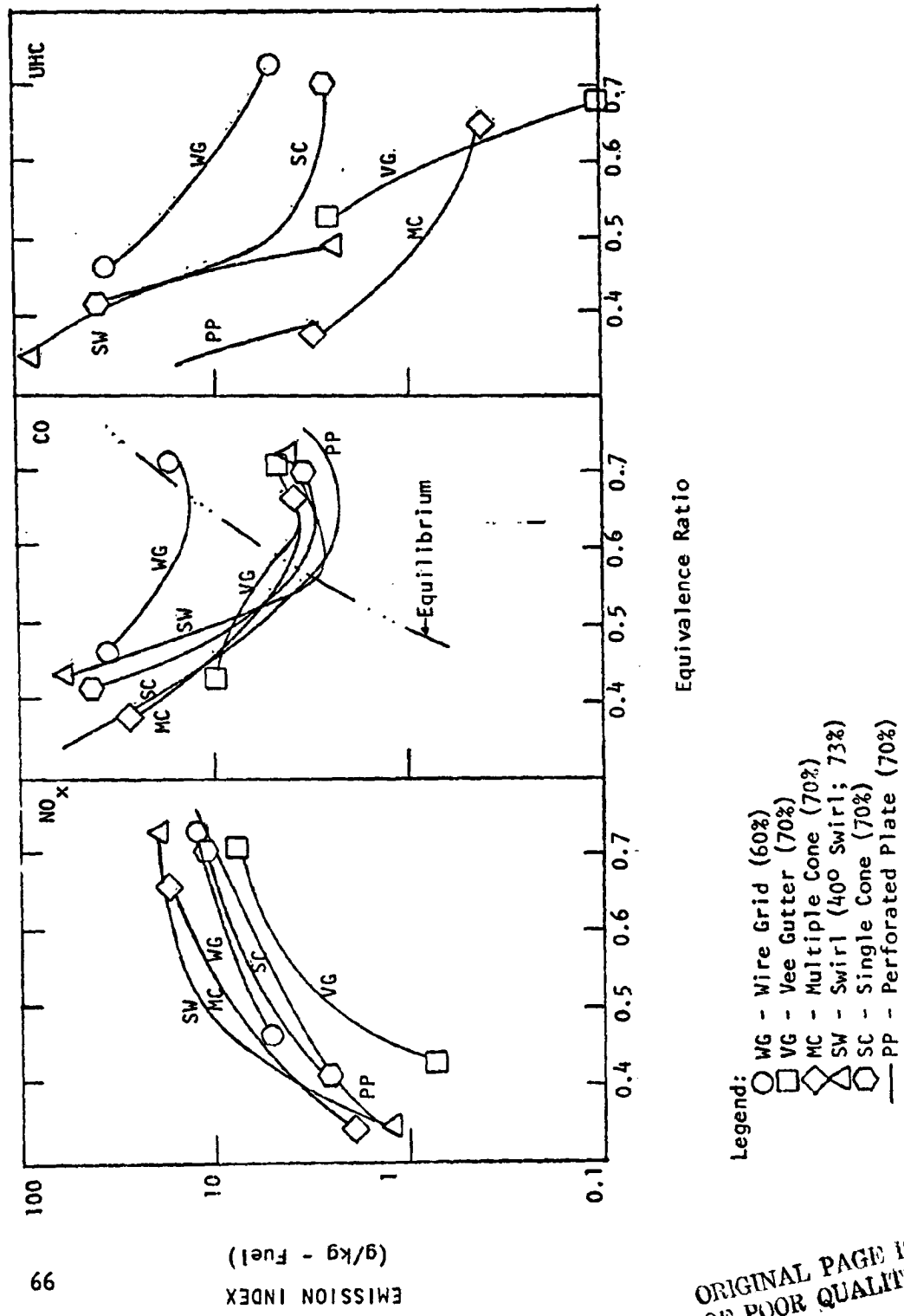
FIGURE 46. COMPARISON OF EMISSION LEVELS FOR LOW BLOCKAGE FLAMEHOLDERS (V_{ref} = 25 m/s; x = 30 cm)

Legend:
WG - Wire Grid (60%)
VG - Vee Gutter (70%)
MC - Multiple Cone (70%)
SW - Swirl (40° Swirl; 73%)
SC - Single Cone (70%)
PP - Perforated Plate (70%)

EMISSION INDEX
(g/kg - Fuel)

Equivalence Ratio

66
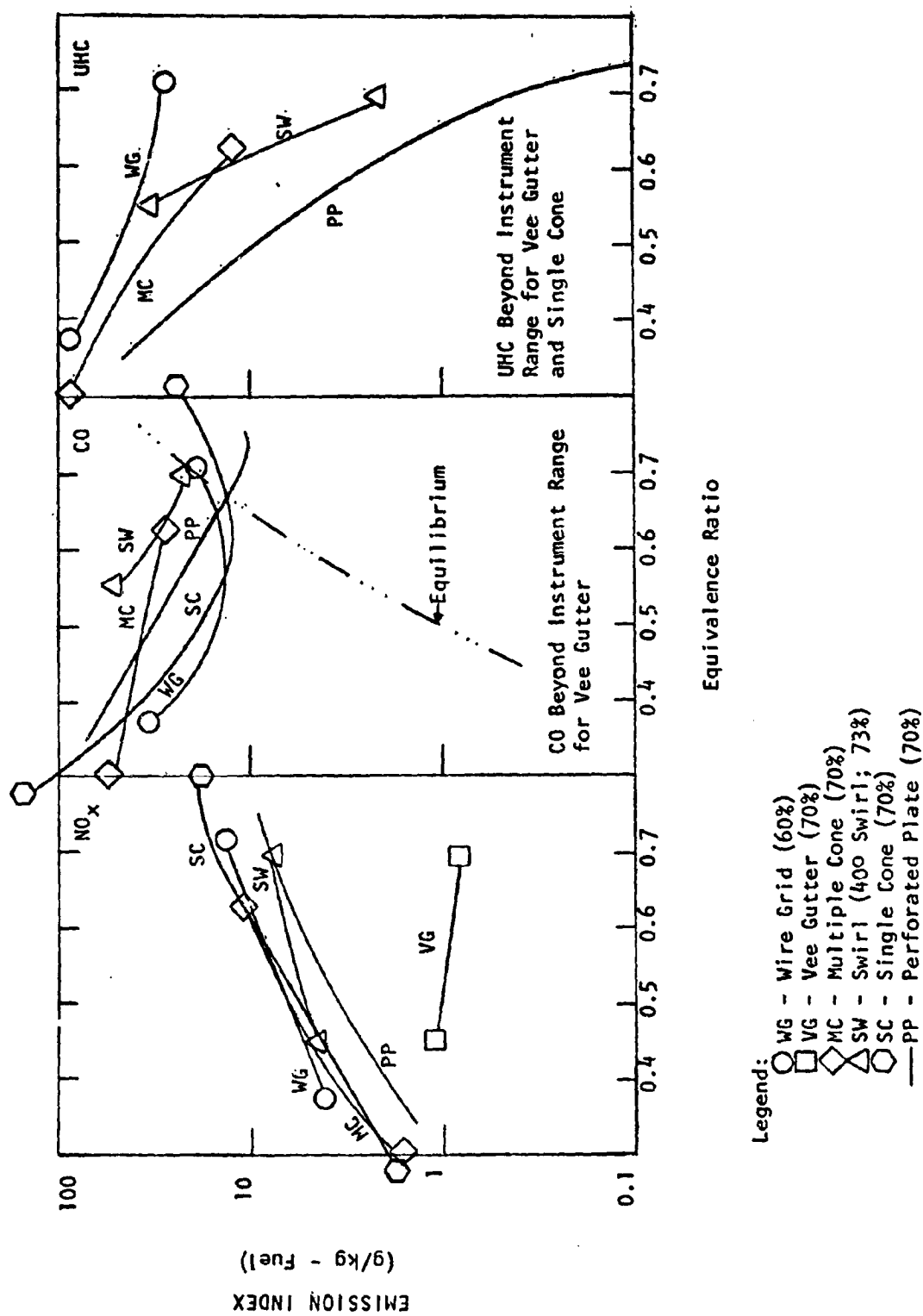
FIGURE 47. COMPARISON OF EMISSION LEVELS FOR LOW BLOCKAGE FLAMEHOLDERS (V_{ref} = 25 m/s; x = 10 cm)

Legend:
WG - Wire Grid (60%)
VG - Vee Gutter (70%)
MC - Multiple Cone (70%)
SW - Swirl (40° Swirl; 73%)
SC - Single Cone (70%)
PP - Perforated Plate (70%)

67
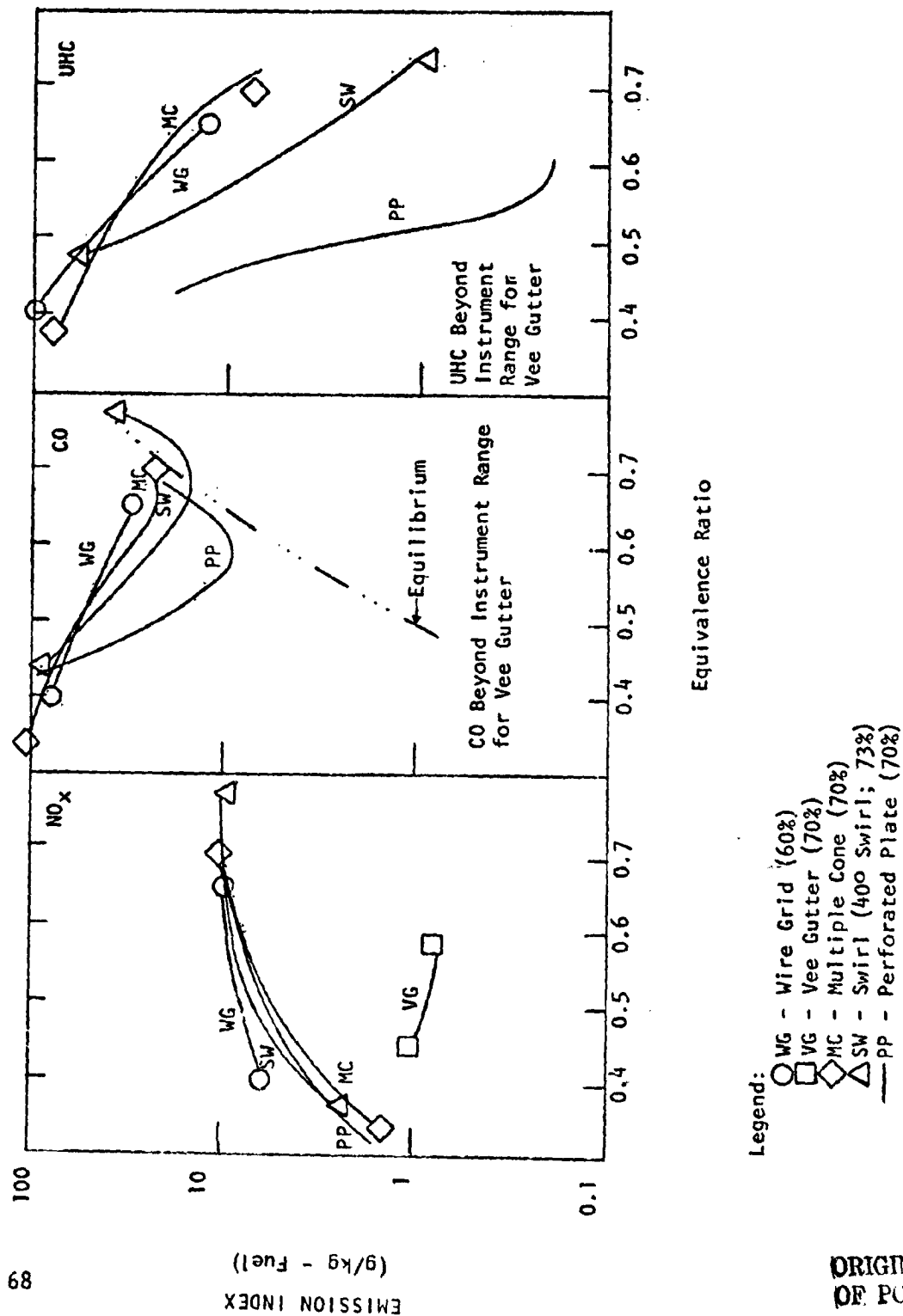
FIGURE 48. COMPARISON OF EMISSION LEVELS FOR LOW BLOCKAGE FLAMEHOLDERS (V_{ref} = 20 m/s; x = 10 cm)
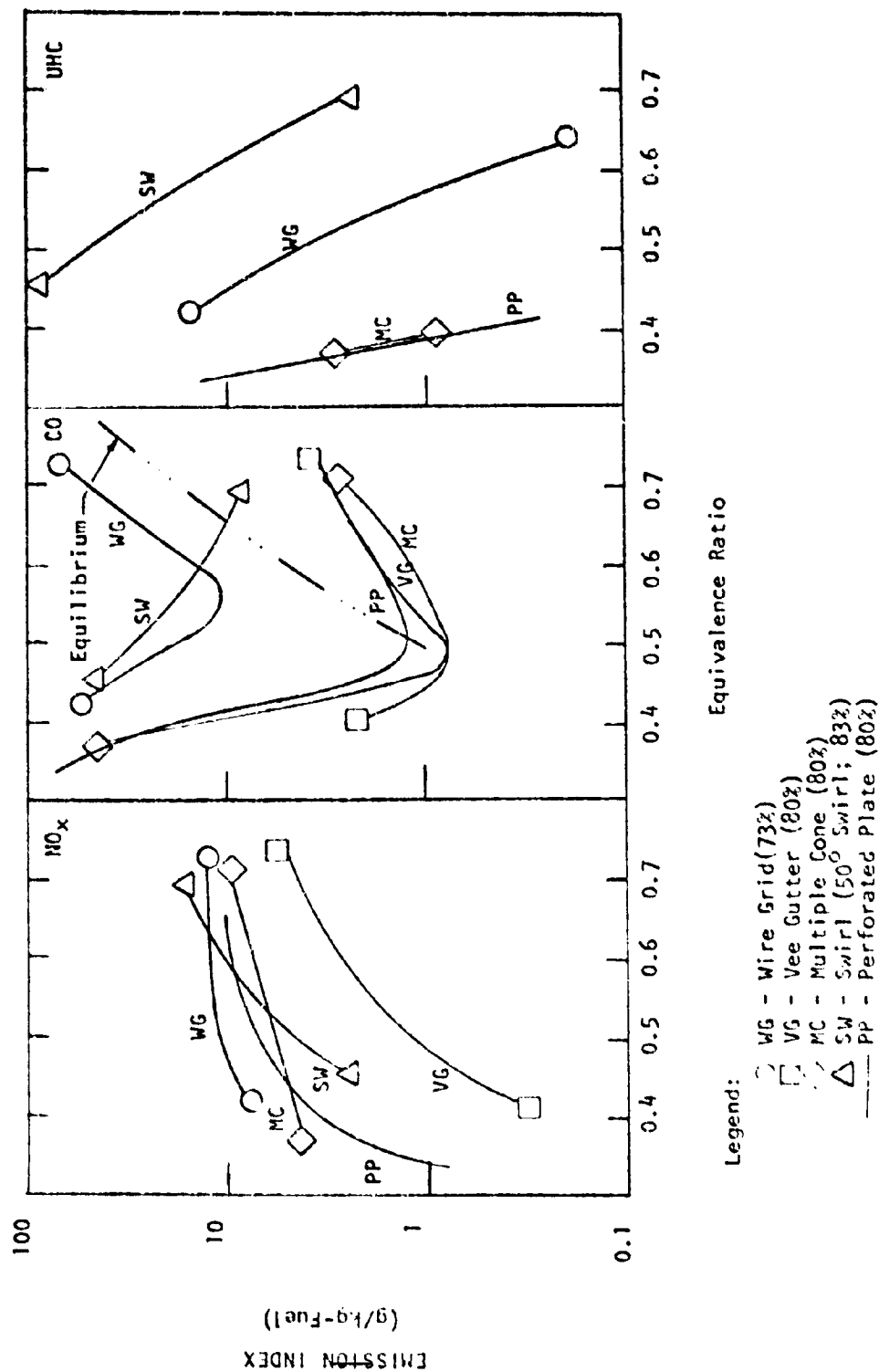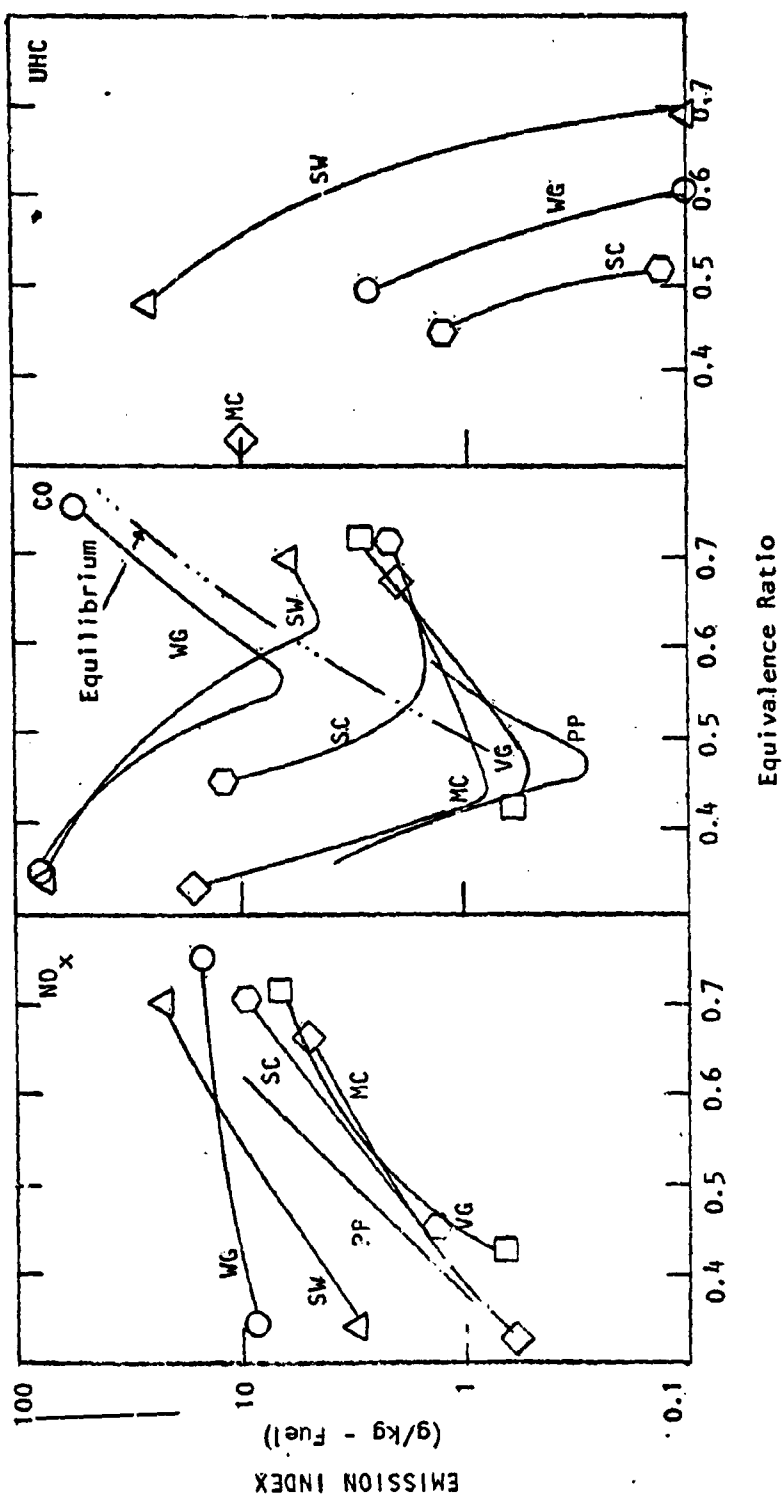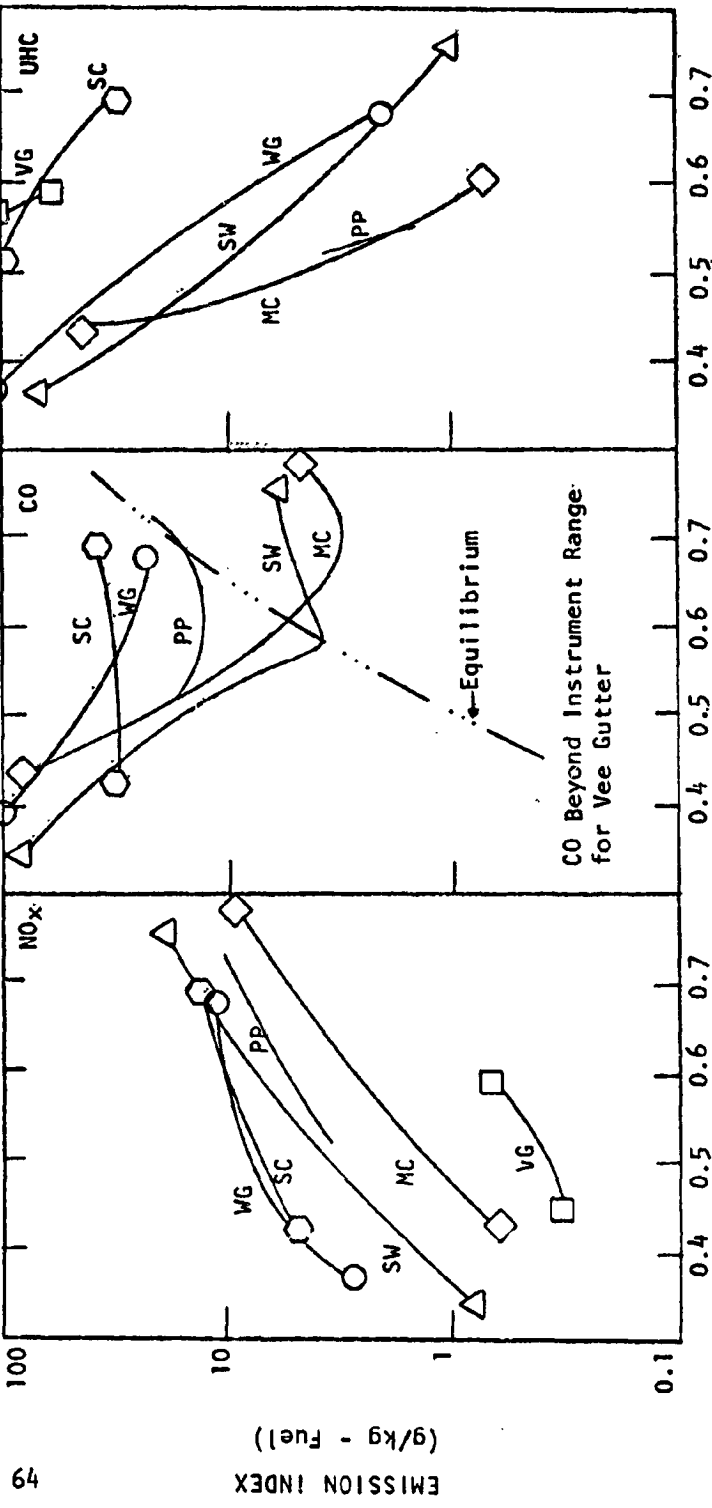
Legend:

○ WG - Wire Grid (60%)
□ VG - Vee Gutter (70%)
◇ MC - Multiple Cone (70%)
△ SW - Swirl (40° Swirl; 73%)
— PP - Perforated Plate (70%)

EMISSION INDEX
(g/kg - Fuel)

Equivalence Ratio

68

was less than 10% and an average value is used in the table. When a greater variation in lean stability limit was observed an appropriate notation has been included. In some cases, the experiment did not yield a clear blowout point. These instances were characterized by excessive emissions of CO and UHC species which saturated the analyzers before combustion actually ceased. Here, it would appear that the flame detached from the flameholder and anchored somewhere downstream, since the exit pressure did not indicate a sudden flameout.

The summary of lean stability limits presented in Table IV is particularly interesting in that, within the band of observations, there generally appears to be very little effect of flameholder configuration, blockage or reference velocity. The single exception to this appears to be the multiple cone flameholder, for which decreasing reference velocity appears to produce a somewhat destabilizing effect. It is also interesting to note that experiments conducted in the same combustion rig as that employed here using a water-cooled perforated plate flameholder with 80% blockage (Reference 5) produced a lean stability limit equivalence ratio of 0.44 at 25 m/s reference velocity, somewhat less stable than the uncooled designs tested here. The results reported in Reference (5) indicated that lean

stability limit was primarily a function of adiabatic flame temperature and was only weakly influenced by inlet temperature. Accordingly, it should be noted that the adiabatic flame temperature corresponding to the lean stability limit equivalence ratio (0.35) for the uncooled perforated plates is 1600K.

Flashback/Burnback

Reducing the mixer tube reference velocity was found to produce one of two modes of failure in the premixed combustion system, depending upon flameholder geometry. For some designs, the flame was observed to eventually jump sharply upstream, attaching itself to the fuel injection tubes in the premixing section. This mode of operating failure is defined as flashback. For the hollow-based single and multiple cone designs, decreasing the velocity eventually caused the flameholder to fail mechani-

TABLE IV

LEAN STABILITY LIMIT

GEOMETRY	BLOCKAGE (%)	V_r=20m/s LSL	V_r=25m/s LSL	V_r=35m/s LSL
Wire Grid	60	<.40	.35	<.42.
Wire Grid	73	<.37	.32	.38
Perforated Plate	70	.30	.35	<.30
Perforated Plate	80	<.48	.35*	.32
Multiple Cone	70	.32	.29	.24
Multiple Cone	80	.38	.32**	.30
Vee Gutter	70	.44	.42.	.44
Vee Gutter	80	.44.	.35	.41
Single Cone	70	--	.28	.32
Single Cone	80	<.42	.38	--
40° Swirl	73	.32	.32	.33
50° Swirl	83	.30	.30	.34

*On one test, 0.45
**On one test, 0.42

cally. In these instances, the flameholder apparently melted from the inside of the base cavity. This condition appears to have resulted from increased base region temperature and decreased external convective cooling at low reference velocity. This mode of failure is defined as burnback.

The observed flashback/burnback velocities are summarized in Table V. Two velocities are listed in the table to characterize the flashback or burnback condition: the reference velocity, defined as the combustor mass flow divided by entrance density and maximum combustor cross sectional area; and $V_{max-axial}$, defined as the maximum value of the axial component of velocity at the flameholder exit (combustor entrance) station. At conditions designated in the table as "No Failure" neither flashback nor burnback occurred at velocities down to the minimum level indicated. The properties of the control system were such that it was difficult to maintain constant equivalence ratio at reference velocities below 7-9 m/s and flashback/burnback could not be extended beyond this range. Both the single cone flameholders suffered burnback damage at the 20 m/s reference velocity during emissions testing. The onset velocity for this condition may be higher than 20 m/s but is certainly less than 25 m/s where operation produced no difficulty. The multiple cone flameholders suffered burnback damage at 18 m/s and 7 m/s for the 70% and 80% blockage designs, respectively.

The 60% wire grid flameholder allowed flashback at a reference ocity of 14 m/s. Lowering the reference velocity to 9 m/s did not ﹄ flashback for the 73% blockage wire grid, while the 40° and 50° sw ᴄone flameholders (73% and 83% blockage) and the 70% vee gutter allowed flashback at velocities between 9 m/s and 11 m/s.

TABLE V

FLAMEHOLDER FLASHBACK/BURNBACK SUMMARY

GEOMETRY	BLOCKAGE (%)	MODE	V_{ref} (m/s)	$V_{max-axial}$ (m/s)
Wire Grid	60	Flashback	14	35
	73	No Failure	<9	<33
Perforated Plate	70	No Failure	<7	<23
	80	No Failure	<8	<40
Vee Gutter	70	Flashback	9	30
	80	Not Tested		
40° Swirl	73	Flashback	11	31
50° Swirl	83	Flashback	10	38
Single Cone	70	Burnback	20	67
	80	Burnback	20	100
Multiple Cone	70	Burnback	18	60
	80	Burnback	7	35

DISCUSSION

Perhaps the most immediately striking feature of the emissions data
is that combinations of flameholder geometry and operating conditions
which produce low NO_x level also produce low levels of CO and unburned
hydrocarbons. From a purely one dimensional (time dependent chemistry)
point of view, one normally associates low NO_x with incomplete combustion
and would therefore expect that NO_x trends would be the reverse of those
for CO and UHC. And yet, for all but two of the test combinations (wire
grid flameholder, 35m/s and 25m/s, 30cm combustor station) parametric
changes which lowered NO_x also lowered CO and UHC.

For all but the swirl flameholders, increasing blockage decreases
emissions of NO_x, CO and UHC, an effect which is most pronounced at low
equivalence ratio. Reference (2) presents data which shows a substantial
increase in the intensity of turbulence downstream of a perforated plate
as plate blockage is increased and a corresponding increase in the rate
of oxidation of CO. NO_x levels in these experiments did not appear to be
sensitive to turbulence level although the fixed equivalence ratio (0.635)
at which tests were made was in the region where the data obtained here
also indicates little effect. An analysis of this data revealed that the
link between reaction rates and turbulence intensity was the mixing rates
which governed the transport of active species from the flame stabilizing
recirculation zones and the incoming jets of gas. Since swirl has been
shown (Reference 3) to inhibit mixing between a low density core flow and
a colder outer flow, the weak reversal of the emissions trend
exhibited by the swirl flameholders may be a simple reflection of that
phenomenon. Therefore, it appears that increasing the intensity of turbu-
lence in the reaction zone decreases the emissions of all species (NO_x, CO
and UHC). Turbulence level is increased by increasing pressure drop: for
a given geometric concept, pressure drop increases with increased blockage.

The general question of the effect of specific flameholder geometry
on the emissions of a lean premixed system can be addressed by examining
the comparative emission levels presented in Figures (41 through 48).
First, flameholder geometry is seen to be an important factor in determining

emission levels. At low equivalence ratios, changes in geometry produce order of magnitude changes in NO_x level: at high equivalence ratios, geometric changes alter NO_x by factors on the order of three. Hydrocarbon and CO emissions are even more sensitive.

Within this general framework of sensitivity to geometry lies the factor of turbulence intensity discussed earlier. In general, one sees that the arrangement of flameholder emission curves at any test condition follows the pattern of pressure drop. The vee gutter, which produces the highest pressure drop of the six concepts (resistance coefficient k of 2.2) also produces the least NO_x and CO and is among the lowest UHC emitters. The wire grid, producing the least pressure drop (k of 1.0) emits the most NO_x, CO and UHC. The distribution of emission curves between these two bounds follows this same pattern. Where minor discrepancies exist, the effects of other geometric properties are apparently becoming significant. (An example of this is the high CO and UHC levels which the vee gutter produces at the 10cm combustor station where the large ignition width of this design dominates the flame.) However, the influence of specific geometric properties such as ignition width and perimeter and characteristic recirculation zone size appears to be of little significance 30cm downstream of the flameholder.

Flameholder geometry appears to have a minimal effect on the equivalence ratio at which lean blowout occurs. Despite a sixtyfold increase in characteristic recirculation zone residence time, the 73% wire grid flameholder and 73% swirl flameholder have identical blowout points at 25m/s reference velocity and differ by only 15% at 35m/s. The lean stability limit, like most instability phenomena, displays a certain degree of intermittency and does not accurately reproduce from one test to another. Within the bounds of this intermittency, the 15% difference in stability limit between the grid and swirl flameholders is not significant.

The ability to withstand flashback appears to be a weak function of flameholder geometry. In reference (4), a premixed stream was burned at an inlet pressure of 0.56MPa and inlet temperatures of 610K and 700K in a sudden expansion (dump) combustor and measurements made of flashback velocity as a function of gas stream equivalence ratio (ϕ). Flashback

74

velocity was found to lie within a band which can be represented by the linear relation

$$V_{flashback} = 123 \ (\phi - 0.41) \ m/s$$

with a data spread of ±5m/s. At equivalence ratio 0.7, this data gives flashback velocities from 30m/s to 40m/s for a simple single entrance jet, 5.25cm in diameter. In order to compare the present data with that of Reference (4), we examine the maximum axial value of velocity at the combustor entrance (axial component of the velocity through the flameholder passages). Table V indicates that the maximum value of axial entrance velocity at which flashback occurred was 38m/s and occurred for the 50° swirl flameholder. The 60% wire grid produced flashback at an entrance velocity of 35m/s, the 40° swirler at 31m/s and the 70% vee gutter at 30m/s. Thus, all flashback incidents occurred with the 30m/s - 40m/s band predicted in Reference (4). With the single exception of the 70% perforated plate, tests which did not produce flashback did not extend to entrance velocities below 30m/s. The apparent ability of the perforated plate to operate at an entrance velocity below 30m/s bears further investigation.

SUMMARY OF RESULTS

Tests were conducted to determine the effect of flameholder geometry
on the emissions and performance of a lean premixed propane/air combustor.
Six flameholder concepts were evaluated; wire grid, perforated plate,
multiple cone, single cone, vee gutter and swirler. Two blockage values
were tested for each design concept. Emissions of NO_x, CO and unburned
hydrocarbons were measured at combustor entrance conditions of 800K/1Mpa
and reference velocities of 35 m/s, 25 m/s and 20 m/s. The lean stability
and flashback limits were also determined. The principal results of this
test program are summarized below.

1. Emissions measurements at a station 30 cm downstream from the
flameholder in an LPP combustor show flameholder pressure drop to be a
principal determinant of emissions performance. Increasing pressure
drop decreases emissions of NO_x, CO and unburned hydrocarbons. The de-
tails of flameholder geometry appear to be of second order importance
except for their effect on total pressure loss.

2. Sampling measurements at a station only 10 cm downstream from the
flameholder display greater sensitivity to the details of design geometry.
The vee gutter design,which produces one of the lowest CO and UHC charac-
teristics at the 30 cm station displays a large region of incomplete
combustion with excessive CO and UHC species at the 10 cm combustor station.

3. Flameholder pressure drop is a function of geometry and maximum
velocity at the flameholder exit station.

4. The lean stability limit was found to correspond to an equivalence
ratio of 0.4 for the 800K/1MPa entrance conditions of this experiment.
This condition corresponds to an adiabatic flame temperature of 1700K.
Lean stability limit did not vary significantly with flameholder geometry.

5. The single and multiple cone flameholder designs which were pro-
vided with hollow base cavities suffered burn damage to their downsteam
surfaces as reference velocity was reduced. This burnback damage occurred
without encountering flashback.

76

6. All incidents of flashback occurred at reference velocities producing maximum axial components of velocity at the flameholder exit station between 30 m/s and 40 m/s. The 70% and 80% blockage perforated plates and the 73% blockage wire grid flameholder did not produce flashback at the lowest velocities (7-9 m/s) at which tests could be conducted. (Flashback testing was carried out at equivalence ratio 0.7).

APPENDIX

DATA REDUCTION PROCEDURES

The gas analysis instrumentation provides raw data in the form of volume fractions of the particular gases being sampled. This raw data is converted into the more convenient form of emission index and equivalence ratio following the procedures detailed below.

Each of the gas analysis instruments must be calibrated in order to convert the instrument reading to the volume fraction of the particular gas being analyzed. This calibration is accomplished by passing prepared mixtures of calibration gas through the instruments and establishing calibration curves. The hydrocarbon analyzer was calibrated using gas standards containing 1040 ppm and 99 ppm propane in nitrogen. The instrument output is proportional to the number of carbon atoms with hydrogen bonds. Thus, pure hydrogen or pure carbon will produce no response and a given concentration of propane (C_3H_8) will produce three times the response of an equal concentration of methane (CH_4). The instrument responds to all C-H bonds. As a result, it measures the sum of both unoxidized hydrocarbon and partially oxidized hydrocarbon molecules. The instrument calibration curve is shown in Figure (49). The response is linear with hydrocarbon concentration, presented in units of ppmC, that is, the number of hydrogenated carbon atoms in parts per million.

Calibration of the Beckman Model 864 CO analyzer was accomplished using standard gases with 2530 ppm, 1550 ppm, 916 ppm, 608 ppm, 305 ppm and 64 ppm CO in nitrogen. The calibration curve is shown in Figure (49).

The gases used for calibration of the Beckman Model 864 CO_2 analyzer contained 15.3%, 10.0%, 4.72% and 2.0% CO_2 in nitrogen. The analyzer calibration curve is slightly nonlinear as shown in Figure (49). The Beckman Model 951 NO/NO_x analyzer was calibrated using standards containing 411 ppm, 197 ppm, 91 ppm and 52 ppm NO_x in nitrogen.

The gas analysis instruments were calibrated once each week using the entire set of standard gases. Zero gas and span gas were passed through all instruments immediately prior to each test and instrument output recorded on the same data roll which was used for the subsequent test run.
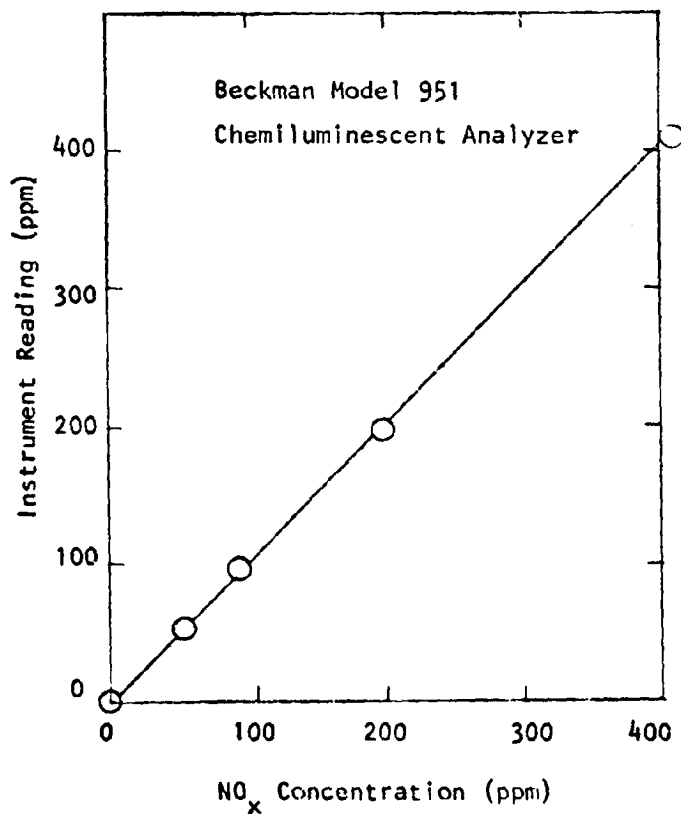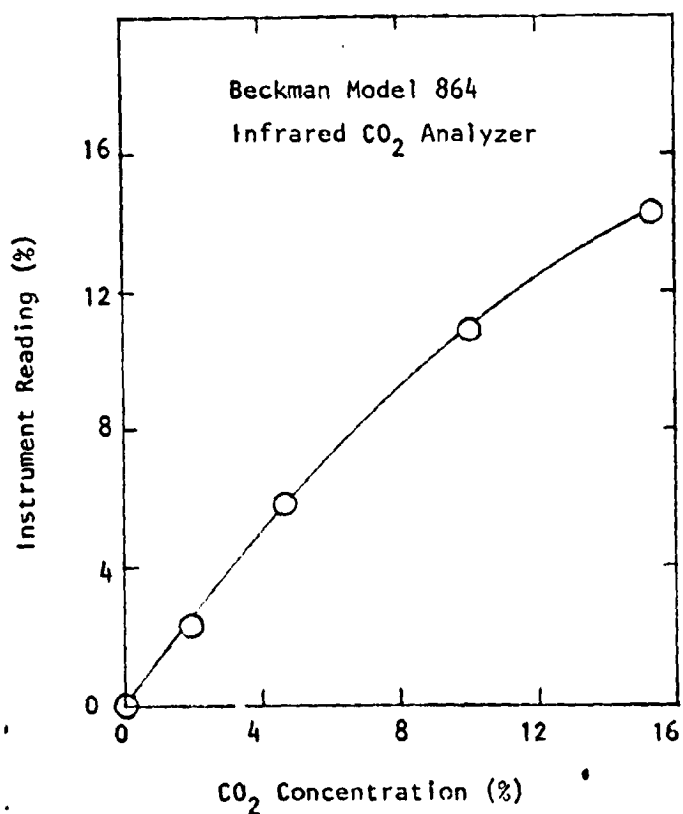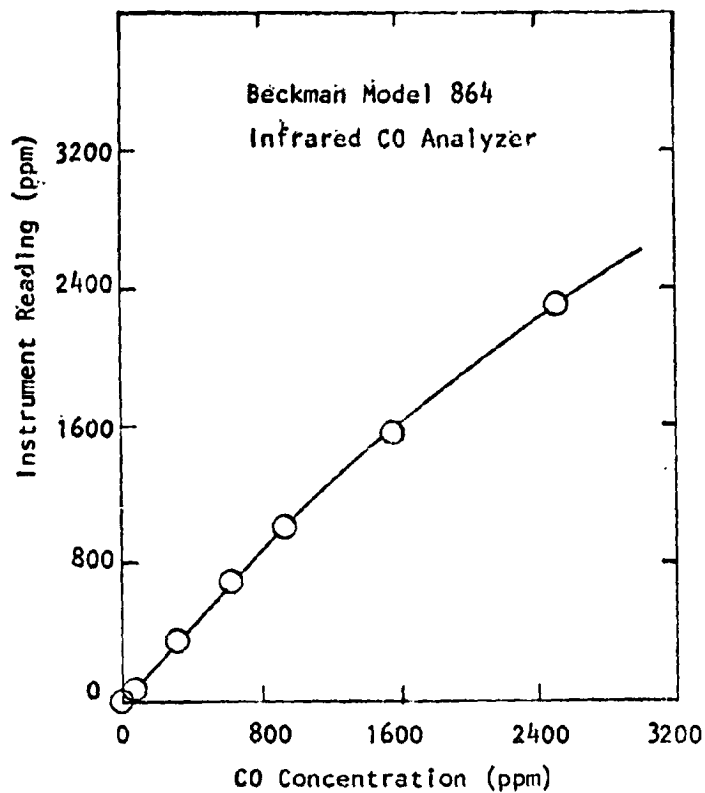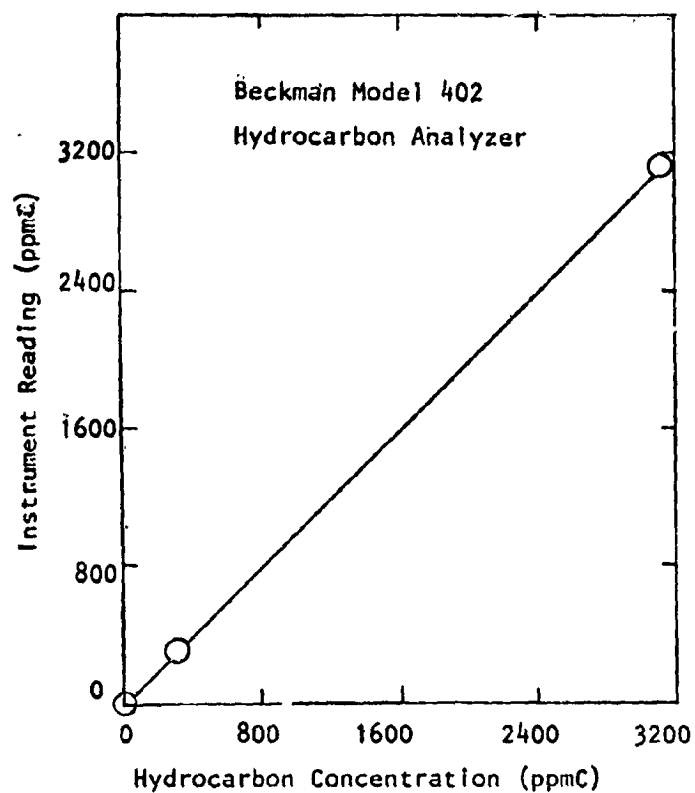
78

FIGURE 49. GAS ANALYSIS INSTRUMENT CALIBRATION CURVES

79

Conversion of the molar concentration (volume fractions) provided by the gas analysis instrumentation into the more convenient terms of emission index and equivalence ratio requires a knowledge of the ratio of carbon to hydrogen in the system. For propane the fuel/air ratio f/a is given by

$$f/a = \frac{CO \times 10^{-4} + CO_2 + HC \times 10^{-4}}{198 - 2.3 \times 10^{-4}\ CO - 1.32\ CO_2} \tag{1}$$

where CO and HC are the molar concentrations of carbon monoxide and unburned hydrocarbon in units of parts per million (ppm) and ppmC respectively and CO_2 is the volume percent of carbon dioxide expressed as a percentage of total gas volume.

The equivalence ratio, ϕ, is defined as the ratio of the actual fuel/air ratio to the stoichiometric fuel/air ratio. For pure propane,

$$\phi = 15.8\ (f/a) \tag{2}$$

The measured volume fractions expressed as ppm of CO, hydrocarbons and NO_x are converted into emission indices (grams of component per kilograms of fuel) using the following expressions:

$$E_{CO} = \frac{CO\ (1 + f/a)}{1034\ f/a} \tag{3}$$

$$E_{HC} = \frac{HC\ (1 + f/a)}{2069\ f/a} \tag{4}$$

$$E_{NO_x} = \frac{NO_x\ (1 + f/a)}{630\ f/a} \tag{5}$$

80

REFERENCES

1. Beer, J. M. and Chigier, N. A., _Combustion Aerodynamics_, Halstead Press Div., John Wiley & Sons, Inc., New York, 1972.

2. Robinson, G. F. and Kovitz, A. A., "The Effect of Turbulence on Pollutant Formation in a Tubular Burner," AIAA Paper 75-166, AIAA 13th Aerospace Sciences Meeting, 1975.

3. Rubel, A., "Swirling Jet Turbulent Mixing and Combustion Computations," ATL TR 180, 1972.

4 Marek, C. J. and Papathakos, L. C., "Preliminary Studies of Auto-ignition and Flashback in a Premixing Prevaporizing Flame Tube Using Jet-A Fuel at Lean Equivalence Ratios," NASA TMX -3526, 1977.

5. Roffe, G. and Venkataramani, K. S., "Experimental Study of the Effects of Cycle Pressure on Lean Combustion Emissions," GASL TR 248, General Applied Science Laboratories, Inc., Final Report Prepared for NASA Lewis Center, (1977).